A distributed transmission line model for the base transit time of a nonuniformly doped bipolar junction transistor

by

Farseem Mannan Mohammedy

A thesis submitted to the Department of Electrical and Electronic Engineering

of

Bangladesh University of Engineering and Technology

in partial fulfillment of the requirement for the degree of

MASTER OF SCIENCE IN ELECTRICAL AND ELECTRONIC ENGINEERING

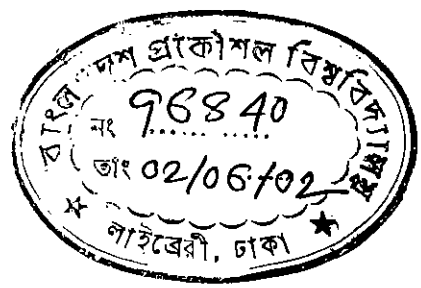

DEPARTMENT OF ELECTRICAL AND ELECTRONIC ENGINEERING

BANGLADESH UNIVERSITY OF ENGINEERING AND TECHNOLOGY

2002

The thesis titled "**A distributed transmission line model for the base transit time of a nonuniformly doped bipolar junction transistor**" submitted by Farseem Mannan Mohammedy, Roll No.: 040006218P, Session: April 2000, has been accepted as satisfactory in partial fulfillment of the requirement for the degree of MASTER OF SCIENCE IN ELECTRICAL AND ELECTRONIC ENGINEERING on 1st June, 2002.

BOARD OF EXAMINERS

1. _____
Dr. M. M. Shahidul Hassan — **Chairman**
Professor — (Supervisor)
Department of Electrical and Electronic Engineering
BUET, Dhaka-1000, Bangladesh.

2. _____
Dr. M. Rezwan Khan — **Member**
Professor
Department of Electrical and Electronic Engineering
BUET, Dhaka-1000, Bangladesh.

3. _____ 01.06.02
Dr. Jahangir Alam — **Member**
Assistant Professor
Department of Electrical and Electronic Engineering
BUET, Dhaka-1000, Bangladesh.

4. _____
Dr. M. M. Shahidul Hassan — **Member**
Professor and Head — (Ex-officio)
Department of Electrical and Electronic Engineering
BUET, Dhaka-1000, Bangladesh.

5. _____
Dr. M. Ali Asgar — **Member**
Professor — (External)
Dept. of Physics
BUET, Dhaka-1000, Bangladesh.

DECLARATION

I hereby declare that this thesis or any part of it has not been submitted elsewhere for the award of any degree or diploma.

Signature of the candidate

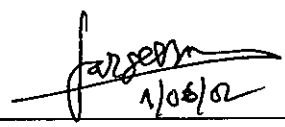

(Farseem Mannan Mohammedy)

DEDICATION

To

Prof. M. M. Shahidul Hasan
Prof. Rezwan Khan

- two of the most humane teachers I have ever seen

TABLE OF CONTENTS

LIST OF FIGURES

LIST OF SYMBOLS

Symbols	Description
C	Capacitance of transmission line
C_n, C_p	Capture coefficient for electron and hole in base
D_n, D_P	Diffusion coefficient for electron and hole in base
$E(x)$	Built in electric field
f_{max}	Maximum frequency of operation
f_T	Cut-off frequency
F_n	Normalization factor
G	Conductance of a transmission line
G', G_n	Normalized conductance of TL model
$G(u, x)$	Conductance of TL model
$I(x)$	Current distribution in transmission line
$J(x)$	Total current density in base
J_n, J_P	Current density for electron and hole in base
L	Inductance of transmission line
L_n	Diffusion length for electron in base
k_B	Boltzmann constant
m	Mass of electron
m^*	Effective mass of electron
$n(x)$	Electron concentration in base
n_{ie}	Intrinsic carrier concentration
$p(x)$	Hole concentration in the base

$N_A(0)$	Peak doping concentration in the base
$N_A(x)$	Acceptor doping concentration
q	Charge of electron
Q_n	Stored charge density in base
R	Resistance of transmission line
R', R_n	Normalized resistance of TL model
$R(u, x)$	Resistance of the TL model
T	Absolute temperature
v_s	Saturation velocity
v_{th}	Thermal velocity
V_{be}	Base-emitter voltage
V_g	9 mV
V_T	Thermal voltage
$V(x)$	Voltage distribution in transmission line
w, W_b	Base width
$u(x)$	Excess electron concentration
Z_0	Characteristic impedance
Z_{in}	Input impedance
Z_L	Load impedance
$\mathcal{R}(u, x)$	Shockley-Hall-Read and Auger recombination
γ	Propagation constant of transmission line
η	Slope of base-doping
μ_n, μ_p	Electron and hole mobility
μ_{min}	Minimum electron mobility in the base
μ_{max}	Maximum electron mobility in the base
τ_B	Base transit time
τ_{n0}, τ_{p0}	Electron and hole lifetime

ACKNOWLEDGEMENT

Over the past few months the person who had been constantly knocking me to start my MSc thesis is my mother. This thesis owes all the credit to her. Besides her, I wish to convey my heartiest gratitude to my supervisor, the real brain behind this thesis, Dr. M. M. Shahidul Hassan, Professor & Head, Department of Electrical and Electronic Engineering (EEE), Bangladesh University of Engineering and Technology (BUET), Bangladesh, for his continuous guidance, suggestions and wholehearted supervision. I am grateful to him for acquainting me with the world of advanced research. In cases of real needs he extended his helpful hands even at the expense of his normal office hours.

Lest I forget, thanks are also due to my dear friend Ziaur Rahman Khan who clarified many theoretical concepts. And also my friend Mohammad Yunus, whose meticulous training on mathematical softwares helped me build up required software algorithms. I also thank all the personnel at the departmental office and library, BUET reference library and xerox section for providing me with the valuable journals and thesis papers to complete this work. Finally the honorable Vice Chancellor waived many official formalities for the timely submission of this thesis.

I am grateful to Almighty Allah for giving me the strength and courage to complete this thesis.

ABSTRACT

Transit time of a Bipolar Junction Transistor (BJT) is an important parameter. It is required in determining different performance figures of a BJT. In the present work the current-continuity equations for electrons and holes; expressions for Shockley-Reed-Hall and Auger recombination are used in obtaining first order differential equations for voltage and current. These two equations are rearranged in a form that is analogous to the well-known time-independent Telegraphers' equation of transmission line analysis. In this thesis transmission line methods have been employed to construct an iterative procedure to find minority carrier distribution for a particular electron current density. Integration of this distribution over the base width will give the total electron charge for a given electron current density. The ratio of electron charge to current density gives the base transit time. Doping dependence of mobility, velocity saturation effect and bandgap narrowing effect within the base are also incorporated in the analysis. The present approach is easier and conceptually straightforward, in that this work did not lump the R/G's of the transmission line (base). Instead the base is segmented and classical TL analysis has been followed for each segment considering R/G's as strictly distributed element. Thus transmission line model has been employed in a more fundamental way and this is for the first time minority carrier distribution and base transit time of BJT's have been computed. Here both uniform and nonuniform base doping have been considered. Finally many other useful profiles, such as base transit time with base-emitter voltage (for both uniform and nonuniform doping), electron charge with current density and base-emitter voltage etc are obtained. It is observed that base transit time increases strongly with base width, but moderately with peak base-doping. It decreases with increasing slope of base-doping.

বাংলা একাডেমী গ্রন্থাগার
96840
তাং 02/06/02
লাইব্রেরী, ঢাকা

CHAPTER 1

INTRODUCTION

1.1 INTRODUCTION

The purpose of this thesis is to introduce a semi-numerical procedure to obtain minority carrier concentration from which base transit time of a bipolar transistor can be calculated. The basic process behind the numerical work is the transmission line (TL) model. In this introductory chapter, bipolar junction transistor, base transit time, discussions on classical transmission line analysis and review of the published works are discussed. Objective of the present thesis and a summary have also been discussed.

1.2 BIPOLAR JUNCTION TRANSISTOR

The revolution in solid-state electronics occured in 1948 by the invention of the bipolar junction transistor (BJT) by a research team of the Bell Telephone Laboratories. This device along with its field-effect counterpart has an enormous impact on virtually every area of modern life. The action of both electrons and holes are important in BJT, so it is called a bipolar transistor. After the invention of BJT, the transistor theory has been extended to include frequency, high power and switching behaviors. Transistors are now key elements in high-speed computers, space vehicles, satellites and all modern communication and power systems.

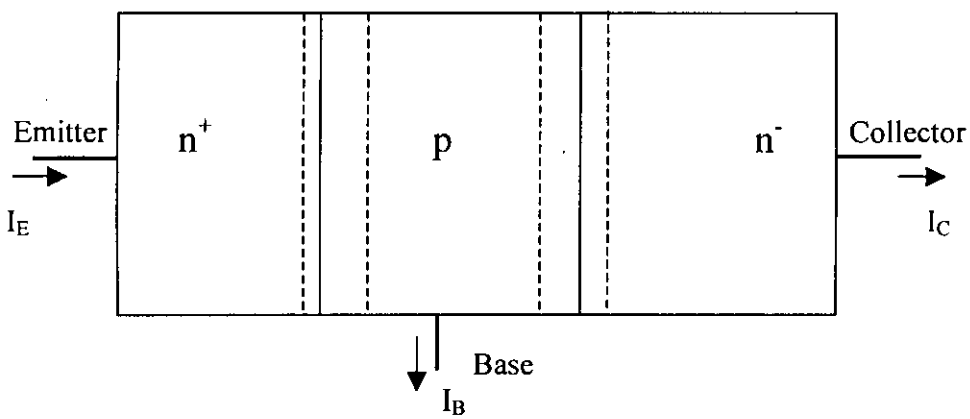

Figure1.1: An n^+pn^- transistor

The cross sectional view of an *npn* bipolar junction transistor is shown in fig. 1.1. The operation of bipolar junction transistors relies on the coupling between two *pn* diodes, which share a common *n* or *p*-type region called the base. This coupling is due to minority carriers injected across one of the *pn* junctions. The minority carrier then travels through this base and contribute to the current in the other *pn* diode. The practical mode of operation, called the active forward mode, is obtained when the *pn* diode, which injects minority carriers into the base region, is forward biased. The other diode is reverse biased so that the current through that diode is primarily due to the minority carriers, which were injected from the other diode. So the first *pn* diode controls the current through both, while the current supplied through the base contact is small. This causes both voltage and current gain in the device when applying a signal to the base contact. There are other possible modes of operation, but they are not used in practice. For example, in saturation mode, both the diodes are forward biased. So no control of current can be achieved. Again in reverse active mode, the first diode in reverse biased and the second one is forward biased. This gives very small amplification and is also impractical. Finally in the cutoff mode, both the diodes are reverse biased and the transistor doesn't conduct.

The complete expressions of different currents for bipolar junction transistor can be derived subject to the following assumptions:

- Low level injection.
- The electric field intensity in the bulk region outside the depletion region is so small that the drift current of minority carriers is negligible.
- No recombination and generation in the depletion region.
- The widths of the emitter and collector regions are greater than the diffusion length of the minority carriers so that the minority carrier densities have their equilibrium values at the contacts.
- The collector area is much larger than the emitter area so as to collect all electrons crossing the collector junction.
- Each of the three bulk regions is assumed to be uniformly doped and both junctions are considered to be step junctions so that the change in impurity density, from one region to another, is abrupt.
- The emitter current is made up entirely of electrons; the emitter injection efficiency is one.
- The active part of the base and two junctions are of uniform cross sectional area; current flow in the base is essentially one-directional from emitter to collector.

The expression for emitter, collector and base currents can be written as:

$$I_E = qA\frac{D_n}{L_n}\left(\Delta n_E ctnh\left(\frac{W_b}{L_n}\right) - \Delta n_C csc\,h\left(\frac{W_b}{L_n}\right)\right) \tag{1.2.1a}$$

$$I_C = qA\frac{D_n}{L_n}\left(\Delta n_E csc\,h\left(\frac{W_b}{L_n}\right) - \Delta n_C ctnh\left(\frac{W_b}{L_n}\right)\right) \tag{1.2.1b}$$

$$I_B = I_E - I_C = qA\frac{D_n}{L_n}\left[(\Delta n_E + \Delta n_C)tanh\left(\frac{W_b}{2L_n}\right)\right] \tag{1.2.1c}$$

where, D_n is the diffusion co-efficient for electron, L_n is diffusion length for electron, q is the charge of electron, W_B is base width, A is the cross sectional area in the perpendicular direction of current flow, Δn_E and Δn_C are the minority carrier concentrations at the base side of base-emitter and base-collector junction respectively.

1.3 BASE TRANSIT TIME

In an active npn transistor minority carrier electrons are injected into the base from emitter. These injected electrons travel towards the collector through the base. The average time taken by minority carriers to diffuse across the quasi-neutral base or the average time that an excess electron spends in the base is called the base transit time (τ_B).

The total charge storage of the injected carriers $n(x)$ in the base per unit area can be written as [1]

$$Q_n = q\int_0^{W_B} n(x)dx \tag{1.3.1}$$

Base transit time (τ_B) is given by [2],

$$\tau_B = \frac{Q_n}{J_n} = \frac{q}{J_n}\int_0^{W_B} n(x)dx \tag{1.3.2}$$

where J_n is the current density.

The eqn (1.3.2) can be analytically solved for two region of operation of the transistor. The regions are: low injection region and high injection region.

The low injection region is the region where the concentration of the injected carrier is far less than the base doping concentration, i.e. $n(x) << N_A(x)$. The high injection region is the region where the concentration of the injected carrier is greater than the base doping concentration, i.e. $n(x) >> N_A(x)$.

For uniform base doping and low injection eqn (1.3.2) is reduced to [2]:

$$\tau_B = \frac{W_B^2}{2 D_n} \tag{1.3.3}$$

For uniform base doping and high injection eqn (1.3.2) is reduced to [2]:

$$\tau_B = \frac{W_B^2}{4 D_n} \tag{1.3.4}$$

This base transit time is very important in determining different performance parameters like the maximum frequency of operation (f_{max}), cut-off frequency (f_T) and the noise figure of a bipolar transistor.

The base transit time depends upon many factors such as

(i) Base width.
(ii) Base sheet resistance.
(iii) Various concentration profiles in the base region (uniform, linear, exponential & complementary error function).
(iv) Velocity saturation effect
(v) Collector current density
(vi) Quasi-saturation
(vii) Built-in electric field in the base region
(viii) Mobility
(ix) Band gap narrowing.

1.4 ESSENTIALS OF CLASSICAL TL ANALYSIS

In this section, the fundamental equations of classical transmission line are described. They will be frequently referred to in constructing the TL model of a quasi-neutral base. As shown in figure1.2a, the TL is often schematically represented as a two-wire line, since TL's (for TEM wave propagation) always have at least two conductors. The short piece of line of length Δx of fig.1.1a can be modeled as a lumped-element circuit, as shown in fig.1.2b, where R, L, G, C, are per unit length quantities defined as:

R= series resistance per unit length in Ω/m.
L= series inductance per unit length in H/m.
G= shunt conductance per unit length in S/m.
C= shunt capacitance per unit length in F/m.

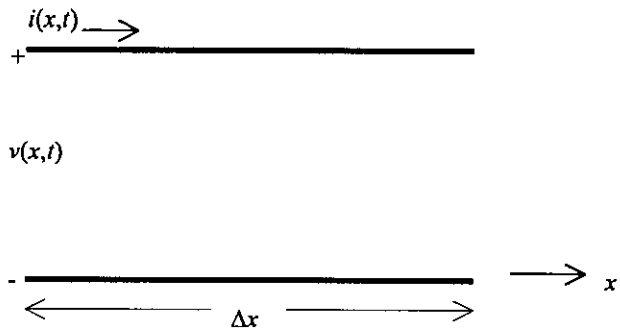

(a)

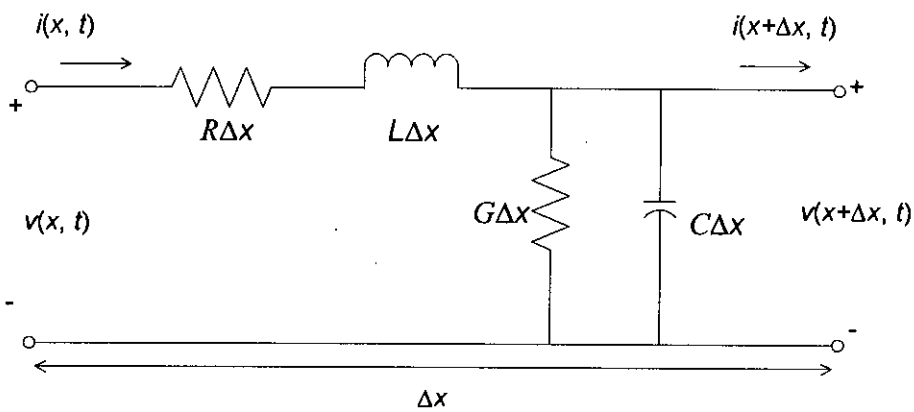

(b)

Figure 1.2 Voltage and current definitions and equivalent circuit for an incremental length of transmission line. (a) Voltage and current definitions, (b) lumped-element equivalent circuit.

The series inductance L represents the total self-inductance of the two conductors, and the shunt capacitance C is due to the close proximity of the two conductors. The series resistance R represents the resistance due to the finite conductivity of the conductors, and the shunt conductance G is due to dielectric loss in the material between the conductors. R and G, therefore, represent loss. A finite length of TL can be viewed as a cascade of sections of the form of fig.1.2b. From the circuit of fig.1.2b, KVL gives:

$$v(x,t) - R\Delta x i(x,t) - L\Delta x \frac{\partial i(x,t)}{\partial t} - v(x+\Delta x,t) = 0. \qquad (1.4.1a)$$

Again applying KCL to circuit of fig.1.2b gives:

$$i(x,t) - G\Delta x v(x+\Delta x,t) - C\Delta x \frac{\partial v(x+\Delta x,t)}{\partial t} - i(x+\Delta x,t) = 0. \qquad (1.4.1b)$$

Dividing equations (1.4.1a) and (1.4.1b) by Δx and taking the limit as $\Delta x \to 0$ gives the following system of differential equations:

$$\frac{\partial v(x,t)}{\partial x} = -Ri(x,t) - L\frac{\partial i(x,t)}{\partial t}, \qquad (1.4.2a)$$

$$\frac{\partial i(x,t)}{\partial x} = -Gv(x,t) - C\frac{\partial v(x,t)}{\partial t}. \qquad (1.4.2b)$$

These equations are the time-domain form of the TL. These are known as the **Telegraphers' Equations**.

For the sinusoidal steady-state condition, with cosine-based phasors, equations (1.4.2) simplify to (putting $j\omega t$ in place of $\partial/\partial t$):

$$\frac{dV(x)}{dx} = -(R + j\omega L)I(x), \qquad (1.4.3a)$$

$$\frac{dI(x)}{dx} = -(G + j\omega C)V(x). \qquad (1.4.3b)$$

These two equations (1.4.3) can be solved simultaneously to give wave equations for $V(x)$ and $I(x)$:

$$\frac{d^2V(x)}{dx^2} - \gamma^2 V(x) = 0, \qquad (1.4.4a)$$

$$\frac{d^2 I(x)}{dx^2} - \gamma^2 I(x) = 0, \tag{1.4.4b}$$

where $\gamma = \alpha + j\beta = \sqrt{(R + j\omega L)(G + j\omega C)}$ (1.4.5)

is the propagation constant, which is a function of frequency.

Travelling wave solutions to equations (1.4.4) are:

$$V(x) = V_0^+ \exp(-\gamma x) + V_0^- \exp(\gamma x), \tag{1.4.6a}$$

$$I(x) = I_0^+ \exp(-\gamma x) + I_0^- \exp(\gamma x), \tag{1.4.6b}$$

here the exponential term ($\exp(-\gamma x)$) represent wave propagation in the $+x$ direction and $\exp(\gamma x)$ term represent propagation in the $-x$ direction. Putting the value of eqn.(1.4.6a) into eqn.(1.4.3a) gives the current on the line:

$$I(x) = \frac{\gamma}{R + j\omega L}\left[V_0^+ \exp(-\gamma x) - V_0^- \exp(\gamma x)\right]. \tag{1.4.7}$$

Comparison with eqn.(1.4.6b) gives the definition of characteristic impedance, Z_0:

$$Z_0 = \frac{R + j\omega L}{\gamma} = \sqrt{\frac{R + j\omega L}{G + j\omega C}}. \tag{1.4.8}$$

The voltage and current on the line are also related:

$$\frac{V_0^+}{I_0^+} = Z_0 = \frac{-V_0^-}{I_0^-}. \tag{1.4.9}$$

Using eqn.(1.4.9), eqn.(1.4.7) can be rewritten as:

$$I(x) = \frac{V_0^+}{Z_0}\exp(-\gamma x) - \frac{V_0^-}{Z_0}\exp(\gamma x). \tag{1.4.10}$$

These solutions are for a general TL, including loss effects, and it is seen that the propagation constant and characteristic impedance are, in general, complex quantities. In case of a lossless line, R=G=0 and eqn.(1.4.5) gives:

$$\gamma = \alpha + j\beta = j\omega\sqrt{LC}\,, \tag{1.4.11}$$

so $\beta = \omega\sqrt{LC}$ and $\alpha = 0$.

The characteristic impedance (eqn.1.4.8), in lossless case, is:

$$Z_0 = \sqrt{\frac{L}{C}}, \tag{1.4.12}$$

which is now a real number. So the general solutions for voltage and current in a lossless line are (equations 1.4.6):

$$V(x) = V_0^{+}\exp(-j\beta x) + V_0^{-}\exp(j\beta x), \tag{1.4.13a}$$

$$I(x) = I_0^{+}\exp(-j\beta x) + I_0^{-}\exp(j\beta x), \tag{1.4.13b}$$

remembering: $I_0^{+} = \frac{V_0^{+}}{Z_0}$ and $I_0^{-} = -\frac{V_0^{-}}{Z_0}$.

Assume now that the above lossless TL is terminated (at x=0) by an arbitrary load impedance Z_L. The need to introduce this problem is that this will illustrate a unique property of the TL's, namely the property of wave reflection. As shown in Fig.1.3 below, an incident wave (of the form $V_0^{+}\exp(-j\beta x)$) is generated from a source at x<0.

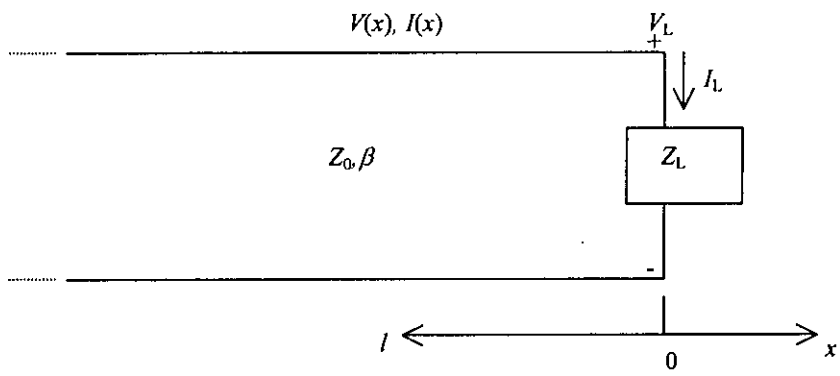

Figure 1.3 A lossless TL terminated in a load-impedance Z_L.

As the line is terminated in an arbitrary load, the ratio of voltage to current at the load must be Z_L (not Z_0). Thus a reflected wave must be excited with the appropriate amplitude to satisfy this condition. Summing up the incident and reflected voltage will give the total voltage on the line (eqn.1.4.13a). Similarly the total current on the line is given by eqn.(1.4.13b).

The total voltage and current at the load is related to load impedance, so at x=0, Z_L is given by:

$$Z_L = \frac{V(0)}{I(0)} = \frac{V_0^+ + V_0^-}{V_0^+ - V_0^-} Z_0, \tag{1.4.14}$$

and V_0^- is given by:

$$V_0^- = \frac{Z_L - Z_0}{Z_L + Z_0} V_0^+. \tag{1.4.15}$$

The amplitude of the reflected voltage wave normalized to the amplitude of the incident voltage wave is known as the voltage reflection coefficient, or simply the reflection coefficient, ρ:

$$\rho = \frac{V_0^-}{V_0^+} = \frac{Z_L - Z_0}{Z_L + Z_0}. \tag{1.4.16}$$

There is also a term known as current reflection coefficient (ratio of reflected current wave to incident current wave), but this is just the negative of voltage reflection coefficient. However the equations (1.4.13) can be rewritten in terms of reflection coefficient (eqn.1.4.16) as:

$$V(x) = V_0^+ [\exp(-\mathrm{j}\beta x) + \rho \exp(\mathrm{j}\beta x)], \tag{1.4.17a}$$

$$I(x) = \frac{V_0^+}{Z_0} [\exp(-\mathrm{j}\beta x) - \rho \exp(\mathrm{j}\beta x)]. \tag{1.4.17b}$$

The reflection coefficient, expressed in eqn.(1.4.16) at l=0, can be generalized to any point l on the line. From eqn.(1.4.13a), with x=-l, the ratio of the reflected to the incident wave gives:

$$\rho(l) = \frac{V_0^- \exp(-\mathrm{j}\beta l)}{V_0^+ \exp(\mathrm{j}\beta l)} = \rho(0) \exp(-2\mathrm{j}\beta l), \tag{1.4.18}$$

here $\rho(0)$ is the reflection coefficient at x=0 as given by eqn.(1.4.16). The above form is useful when transforming the effect of a load mismatch down the line. Also the input impedance at a distance l (= -x) from the load looking toward the load is given by either:

$$Z_{in} = \frac{V(-l)}{I(-l)} = \frac{1+\rho\exp(-2\mathrm{j}\beta l)}{1-\rho\exp(-2\mathrm{j}\beta l)} Z_0, \qquad (1.4.19a)$$

or:

$$Z_{in} = Z_0 \frac{Z_L + \mathrm{j}Z_0 \tan \beta l}{Z_0 + \mathrm{j}Z_L \tan \beta l}. \qquad (1.4.19b)$$

The above analysis however holds for a lossless line. In practice, all TL's have loss due to finite conductivity and/or lossy dielectric. For much of practical cases, these losses can be neglected. But in the case of quasi-neutral base, the system of TL equations (2.3.3a,b) suggest a lossy line. So a terminated lossy line is considered next.

Fig.1.4 below shows a length l of a lossy TL terminated in a load impedance Z_L. Propagation constant will then be complex ($\gamma = \alpha + \mathrm{j}\beta$).

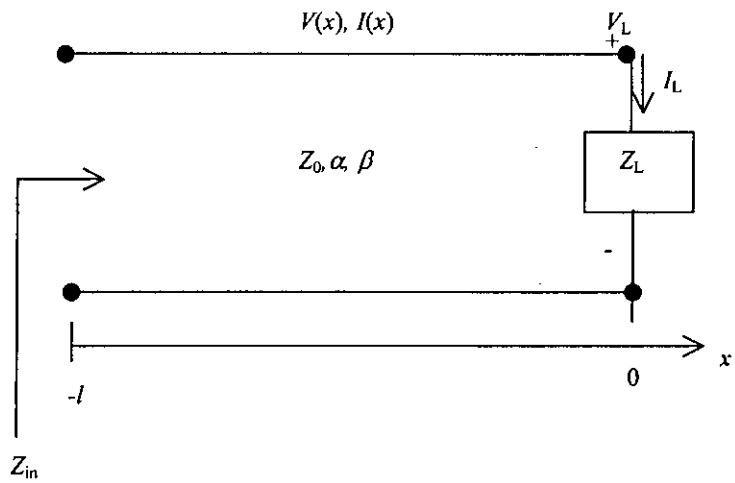

Figure 1.4: A lossy TL terminated in a load-impedance Z_L.

The expressions for voltage and current in a lossy transmission line, therefore, are:

$$V(x) = V_0^+ \left[\exp(-\gamma x) + \rho \exp(\gamma x)\right], \tag{1.4.20a}$$

$$I(x) = \frac{V_0^+}{Z_0}\left[\exp(-\gamma x) - \rho \exp(\gamma x)\right], \tag{1.4.20b}$$

here ρ is the reflection coefficient of the load and V_0^+ is the incident voltage amplitude at x=0. The reflection coefficient at a distance l from the load is:

$$\rho(l) = \rho e^{-2j\beta l} e^{-2\alpha l} = \rho e^{-2\gamma l}, \tag{1.4.21}$$

the input impedance at a distance l from the load, therefore, is given by:

$$Z_{in} = \frac{V(-l)}{I(-l)} = Z_0 \frac{Z_L + Z_0 \tanh \gamma l}{Z_0 + Z_L \tanh \gamma l}. \tag{1.4.22}$$

The profiles of the voltage and current waves within a typical lossy transmission line are shown below in figure 1.5.

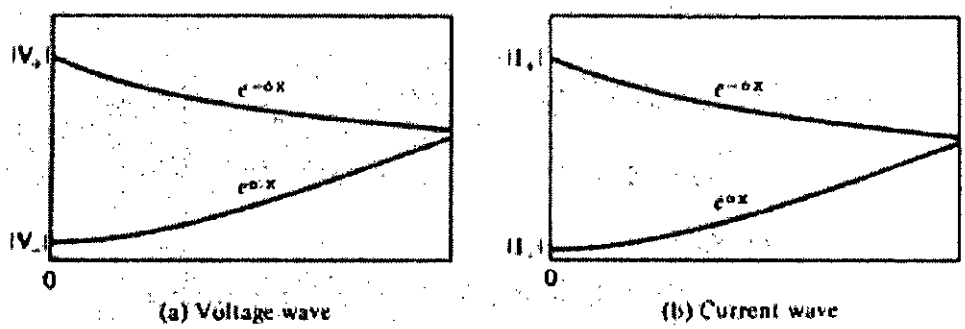

Figure:1.5 Voltage and current profile in a lossy TL.

This ends the brief digression into classical transmission line analysis.

1.5 REVIEW OF RECENT LITERATURE

There has been a considerable number of papers on different aspects of base transit time over the past few decades. Specific interest has been focused on estimating base transit time using analytical and numerical methods.

In Van den Biesen [3] a regional analysis to study the transit time of the BJT as a function of base-emitter bias was used. He subdivided the total transit time from emitter to collector contact into five components. But no closed form solution in [3] was obtained. J. S. Yuan [4] studied the effect of the base profile on the base transit time of the bipolar transistor for all levels of injection. He proposed equation for the minority carrier distribution within the base for different types of base doping. Using boundary conditions and the proposed equation he numerically evaluated the base transit time. Suzuki [5] proposed electron current density J_n and base transit time (τ_B) models of uniformly doped bipolar transistor for high level of injection. He also considered the electron velocity saturation effect in the collector-base depletion region. Ma *et al* in [1] improved their earlier work [6] considering the velocity saturation of the electron in the depletion region of base-collector and the electrical field dependence on the minority carrier mobility. This method is based on iteration techniques. Shahidul Hassan and A. H. Khandoker [2] developed a mathematical expression for J_n and τ_B for uniform base doping density for all levels of injection ignoring the velocity saturation of electron at base-collector depletion region. Rosenfeld [7] derived an analytical formula of base transit time through a dopant-graded base considering the dependence of mobility on the doping level valid for low level of injection only and ignoring the bandgap narrowing effect. Among many other analytical works important for the present work are [8-10]. Marshak [8] presented a review on general transport equations describing electron and hole motion and densities. As a special case minority carrier flow in quasi-neutral material is derived and discussed. Chyan *et al* [9] developed a complete analytical model of the electron and hole current density, current gain and forward transit time under high injection before the onset of the Kirk effect, for heavily doped base and emitter with nonuniform band structures. Ziaur Rahman Khan [10] studied base transit time of BJT with nonuniformly doped base. An analytical expression for the base transit time for low and high levels of injection are obtained incorporating exponentially doped base, doping dependence of mobility, bandgap narrowing, electric field developed due to high injection, nonuniform doping and velocity saturation effects at the collector-base junction. Base transit time was calculated and it was found that low-injection base transit time is smaller than that of high-injection. The results of the present work are in good agreement with [1].

For numerical work on base transit time there are a host of papers appeared in the literature. Among them emphasis is given on those models that considered transmission line (TL) model. The transmission line equivalent circuit (TLEC) model for solving general drift-diffusion equations had been first introduced by Sah [11]. This procedure was followed in [12] and [13]. Karamarković *et al* [14] solved one-dimensional time-

dependent, isothermal, minority carrier transport equations for an arbitrarily doped quasi-neutral base under periodical steady-state voltage excitation of the emitter-base junction using the now-familiar TL method assuming a lossy transmission line. The novelty of the method lies in the ability to exploit periodical steady-state frequency-domain analysis where the momentum relaxation-time effect is easily included as the TL inductivity. Again Karamarković *et al* [15] developed a novel TLEC for minority carrier transport through arbitrarily doped quasi-neutral silicon regions. This particular model (compared to that of [11]) has two advantages:

1. The novel TLEC deals with normalized minority carrier excess concentration as a TL voltage. This approach is employed in the present work also.

2. The novel TLEC model incorporates inductance.

Anyway the virtue of this paper lies in its elaboration on the normalization procedure of spatially and temperature-dependent TL parameters. In [16] Janković *et al* showed that it is possible to model minority carrier transport through quasi-neutral base region at all injection levels using a nonlinear inhomogeneous lossy TL. This model also includes Kirk effect. This particular paper is a very important guide to the present work. In a very recent paper Karamarković *et al* [17] worked on an analytical approach to model Kirk effect. Here an analytical expression is derived which enables the calculation of minimum carrier velocity in high-injection regime.

In the present model, a novel iterative procedure is employed using the nonlinear, inhomogeneous, lossy TL model to determine minority carrier distribution $n(x)$ for a given current density J_n. An integration of $n(x)$ over the base width W_B gives the total electron charge Q_n. The ratio of Q_n to J_n gives the base transit time. Uniformly and nonuniformly doped base along with bandgap narrowing effects and velocity saturation at the base-collector junction are duely considered.

1.6 OBJECTIVE OF THE PRESENT THESIS

A considerable number of analytical modeling has been done to determine base transit time. These procedures involve many assumptions. So here a semi-numerical procedure has been developed to present a clear picture of the actual physical events that occur within the base. Numerical procedures are easier to handle and take less computational time compared to analytical models. The electrical characteristics of bipolar devices are determined by the minority carrier transport through arbitrarily doped quasi-neutral regions. This transport is described by a complex set of partial differential equations with space-dependent coefficients. However in quasi-neutral regions, the drift-diffusion (DD) model is enough to describe carrier transport. These transport equations can be

successfully modeled by TLEC procedure. It is a demonstrated fact that an all injection level TL model of carrier transport through the base of silicon BJT is also possible. The normalized excess minority carrier concentration acts as 'voltage' and the current density constitutes the 'current' in the novel TL model. As the resulting TL base-model is nonlinear, an efficient iterative method is devised to calculate minority carrier distribution throughout the base. The space and temperature-dependent TL parameters are normalized. The advantage of the TL model is that it can be used in frequency and/or time domain analysis. As the excess minority carriers are normalized, so the same TL can be used for both small and large signal analysis. The objective of the present thesis is to employ the above novel TL approach to calculate minority carrier distribution throughout base and thereby to determine numerically the base transit time. Other important profiles (such as transit time versus base-emitter voltage and injection ratio for uniformly and nonuniformly doped bases, electric field distribution within the base etc.) are also obtained. This is for the first time that TL model has been employed to obtain base transit time and other important parameters involving base transit time.

1.7 SUMMARY OF THE THESIS

In this work, the base transit time of a BJT is evaluated by employing a novel iterative method, i.e. the TL method. In chapter 1, the defining equations of base transit time are discussed. Also basics of classical transmission line are discussed for future reference. Recent works (both analytical and numerical) on base transit time have also been reviewed, emphasis is given on TL models. In chapter 2 mathematical background on TL model has been provided. It has been shown how the transport equations (drift-diffusion and continuity equations) reduce to a set of equations analogous to TL equations. The proper normalization procedure and its necessity are also discussed. Also the algorithm generating the minority carrier profile by using the TL model equations is discussed. The results obtained are discussed in chapter 3 and the dependence of base transit time on different transistor parameters are studied. The relevant graphs are included there. Chapter 4 ends with suggestions for future work.

CHAPTER 2

MATHEMATICAL ANALYSIS

2.1 INTRODUCTION

Base transit time is an important parameter for bipolar junction transistors (BJT). This transit time can be reduced by creating a quasi-electric field in the base. It has been established that quasi-electric field can be established by grading the dopant density in the base. In this chapter drift-diffusion (DD) and transport equations are described for a dopant-graded base in order to derive the transmission line (TL) model equations. The analytical analogy between transport equations (DD and continuity equations for electrons and holes) and classical transmission line equations (*Telegraphers' equation*) are fully derived. A new TL method has been introduced to compute minority carrier distribution within base. Cosequently an algorithm is also constructed, based on the present novel TL model, to compute the base transit time.

2.2 TRANSPORT EQUATIONS

The electron current density J_n, and hole current density J_p with arbitrary base doping concentration $N_A(x)$ are given by [4,9]:

$$J_n(x) = q\,D_n(x)\frac{dn(x)}{dx} + q\,\mu_n(x)n(x)E(x), \qquad (2.2.1a)$$

$$J_p(x) = q\,\mu_p(x)p(x)E(x) - q\,D_p(x)\frac{dp(x)}{dx}, \qquad (2.2.1b)$$

where, x is the distance of a point in the base from the base-emitter junction, $D_n(x)$ and $D_p(x)$ are the diffusion coefficients for electrons and holes, $\mu_n(x)$ and $\mu_p(x)$ are the electron and hole mobilities, $n(x)$ and $p(x)$ are electron and hole concentration respectively, q is the charge of electron and $E(x)$ is the electric field at a point x in the base.

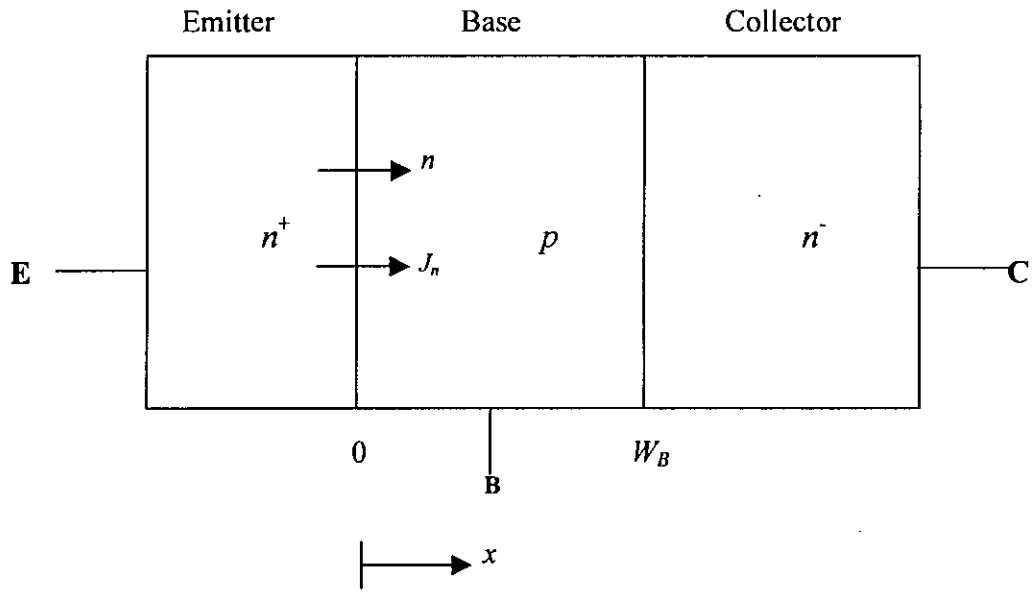

Fig. 2.1. One-dimensional structure of an n^+pn^- Si bipolar transistor

The total current density, which is constant, is the sum of the contribution due to electrons and holes:

$$J\ (x) = J_n(x) + J_p(x)\,. \tag{2.2.2}$$

The base width of a modern bipolar transistor is very thin. So the carrier recombination within the base can safely be neglected [4]. Neglecting J_p, and considering the conventional direction of current (opposite to electron flow) eqn.(2.2.2) becomes:

$$J\ (x) \approx -J_n(x)\,. \tag{2.2.3}$$

In the absence of recombination, the collector current density J_n becomes constant [7]. Using $J_p(x)$=0 and band gap narrowing effect, it can be shown that the electric field in the base is [4]:

$$E(x) = \frac{k_B T}{q}\left[\frac{1}{p}\frac{dp}{dx} - \frac{1}{n_{ie}^2(x)}\frac{d\,n_{ie}^2(x)}{dx}\right], \tag{2.2.4}$$

where k_B is Boltzmann constant, T is temperature and $n_{ie}(x)$ is the effective intrinsic carrier concentration in the base.

The first term in eqn.(2.2.4) represents electric field due to concentration gradient and the second term in eqn.(2.2.4) represents the quasi-fields due to nonuniform band gap narrowing.

The intrinsic carrier concentration n_{ie} is given by:

$$n_{ie}^2(x) = n_{io}^2\left(\frac{N_A(x)}{N_r}\right)^{\frac{2V_g}{V_T}}, \tag{2.2.5}$$

where N_r=1×10^{17} cm^{-3}, V_g is 9mV and V_T is thermal voltage.

The electron mobility in the base is given by [4]:

$$\mu_n(x) = \mu_{\min} + \frac{\mu_{\max} - \mu_{\min}}{1+\left(\frac{N_A(x)}{N_{ref}}\right)^{\gamma}}, \tag{2.2.6}$$

where, μ_{min}=92 cm^{2}V^{-1}s^{-1}, μ_{max}=1360 cm^{2}V^{-1}s^{-1}, N_{ref}=1.3×10^{17} cm^{-3} and γ= 0.91.

From eqn.(2.2.6), $D(x)$ can be determined using the Einstein's relation:

$$\frac{D(x)}{\mu(x)} = \frac{k_B T}{q}. \tag{2.2.7}$$

In this work, a non-uniform doped base is considered. For practical devices, it follows exponential distribution and is given by [4]:

$$N_A(x) = N_A(0)exp\left(\frac{-\eta x}{W_B}\right), \tag{2.2.8}$$

where η is the slope of the base doping and is written as:

$$\eta = ln\left(\frac{N_A(0)}{N_A(W_B)}\right), \tag{2.2.9}$$

As a standard choice for practical devices, most often η=3, whereas η=0 represents uniform doping.

Employing basic definitions of differential calculus, the terms of $E(x)$, as shown in eqn.(2.2.4), can be rearranged in a compact form [9]:

$$E(x) = \frac{k_B T}{q} \frac{d}{dx} \ln\left[\frac{p(x)}{n_{ie}^{\ 2}(x)}\right]. \qquad (2.2.10)$$

Substituting eqn.(2.2.10) into eqn.(2.2.1a) gives:

$$J_n = k_B T \mu_n(x) \left\{ n(x) \frac{d}{dx} \ln\left[\frac{p(x)}{n_{ie}^{\ 2}(x)}\right] + \frac{dn(x)}{dx} \right\} \qquad (2.2.11)$$

Using the Einstein relation (eqn.2.2.7), eqn.(2.2.11) gives:

$$J_n = qD_n(x) \left\{ n(x) \frac{d}{dx} \ln\left[\frac{p(x)}{n_{ie}^{\ 2}(x)}\right] + \frac{dn(x)}{dx} \right\} \qquad (2.2.12)$$

So after some mathematical manipulation, eqn.(2.2.12) can be written in the following way:

$$\frac{J_n p(x)}{k_B T \mu_n(x) n_{ie}^{\ 2}(x)} = \frac{d}{dx}\left[\frac{p(x)n(x)}{n_{ie}^{\ 2}(x)}\right]. \qquad (2.2.13)$$

The electron diffusion length in crystalline silicon is about 3.8 μm (even at doping concentration of 10^{19}cm^{-3}). Base width of high-speed transistors is less than 100 nm (so $L_n >> W_B$). Therefore, the carrier recombination in crystalline silicon region is negligible [9]. This results in a constant J_n (in eqn.2.2.3).

Now a new novel term, the *normalized excess electron concentration,* is introduced which acts as 'voltage' in TL model. The definition of normalized excess electron concentration is:

$$u(x) = \frac{p(x)n(x)}{n_{ie}^{\ 2}(x)} - 1. \qquad (2.2.14)$$

Note that, according to eqn.(2.2.14):

$$\frac{du(x)}{dx} = \frac{d}{dx}\left[\frac{p(x)n(x)}{n_{ie}^{\ 2}(x)} - 1\right] \approx \frac{d}{dx}\left[\frac{p(x)n(x)}{n_{ie}^{\ 2}(x)}\right]. \qquad (2.2.15)$$

Substituting eqn.(2.2.15) into eqn.(2.2.13), the first of the transport equations applicable to a *p*-type quasi-neutral base takes the form of:

$$\frac{J_n p(x)}{k_B T \mu_n(x) n_{ie}^{\ 2}(x)} = \frac{d}{dx}\left[\frac{p(x)n(x)}{n_{ie}^{\ 2}(x)} - 1\right] = \frac{du(x)}{dx}. \qquad (2.2.16)$$

Again using eqn.(2.2.3), that $J(x) = -J_n(x)$, and recalling eqn.(2.2.7), eqn.(2.2.16) reduces to:

$$\boxed{\frac{du(x)}{dx} = -\frac{p(x)}{qD_n(x)n_{ie}^{\ 2}(x)}J(x)} \qquad (2.2.17)$$

Now the continuity equation has to be used to obtain the other one of the transport equations.

A uniform semiconductor sample in zero electric field must be neutral:

$$N_D^{\ +} - N_A^{\ -} - n + p = 0, \qquad (2.2.18)$$

here $N_D^{\ +}$ and $N_A^{\ -}$ are the concentrations of ionized donors and acceptors respectively. This is known as the *charge neutrality condition*. However semiconductor devices are rarely uniform and usually operate under nonequilibrium condition. A photon absorbed in the semiconductor may promote an electron from the valence band into the conduction band, thus creating both an electron in the conduction band and a hole in the valence band. This process is known as electron-hole pair (EHP) generation or generally 'Generation'. *Generation rate*, G is the equal to the concentration of EHP's produced in one second. On the other hand, an electron from the conduction band may fall into a vacant space in valence band. This process is known as 'Recombination'. So *recombination rate* R gives the concentration of EHP's recombining in one second. In a uniform semiconductor:

$$\frac{dp}{dt} = \frac{dn}{dt} = G - R. \qquad (2.2.19)$$

In steady-state: $G = R$.

For a nonuniform semiconductor, equation (2.2.19) has to be modified in order to account for changes in the current densities. For an incremental volume such changes in the current is proportional to $\nabla \cdot J$ and equation (2.2.19) has to be duely changed [19]:

$$\frac{\partial n}{\partial t} = \frac{1}{q}\nabla \cdot \mathrm{J_n} + G_n - R_n, \tag{2.2.20a}$$

$$\frac{\partial p}{\partial t} = \frac{1}{q}\nabla \cdot \mathrm{J_p} + G_p - R_p. \tag{2.2.20b}$$

These equations are known as Continuity equations, where n and p in the subscripts of G, R refer to generation/recombination rates of electrons and holes respectively.

When electrons and holes are generated in pairs (EHP's) in a uniform semiconductor, the semiconductor sample remains neutral or nearly neutral. This situation arises when, for example, light generates extra carriers in a piece of n-type semiconductor. This situation is known as Quasi-neutrality. The assumption that a semiconductor piece is quasi-neutral means that:

$$n - n_0 \approx p - p_0, \tag{2.2.21}$$

n_0 and p_0 are equilibrium electron and hole densities.

In a p-type quasi-neutral base, the total carrier recombination is the sum of Shockley-Hall-Read (SHR) and Auger recombination [16]:

$$\Re(u,x) = \frac{p(x)n(x) - n_{ie}^{\ 2}(x)}{\tau_{p_0}(n(x) + n_{ie}(x)) + \tau_{n_0}(p(x) + n_{ie}(x))} + C_n n(x) + C_p p(x), \tag{2.2.22}$$

where τ_{n0} and τ_{p0} are electron are hole lifetimes ($\cong 10^{-7}$s) [20], C_n and C_p are capture coefficients (for silicon, $\cong 3\times10^{-31}\mathrm{cm^6s^{-1}}$) [21].

Noting that, for one dimensional time-independent analysis, $\nabla \cdot \mathrm{J_n}$ reduces to $dJ_n(x)/dx$, continuity equation (2.2.20a) gives [16]:

$$\boxed{\frac{dJ(x)}{dx} = -q\Re(u,x)} \tag{2.2.23}$$

Therefore, equations (2.2.17) and (2.2.23) constitute the "general 1D drift-diffusion isothermal minority carrier transport equations at all injection levels."

2.3 TL MODEL

By assuming normalized excess electron concentration as 'voltage' and electron current density as 'current', the system of differential equations, (2.2.17) and (2.2.23), can be made analogous to well-known Telegraphers' equation. This requires only a few minor algebraic manipulation of equations (2.2.17) and (2.2.23). For example, eqn.(2.2.17) can be made to look as a TL equation if all the terms of the right side of eqn.(2.2.17), except $J(x)$, is grouped under a single term. From now on, this term will act as 'resistance' of the transmission line (base). So,

$$R(u,x) = \frac{p(x)}{qD_n(x)n_{ie}^{\ 2}(x)}. \tag{2.3.1}$$

In a similar fashion, eqn.(2.2.23) lacks the term $u(x)$ explicitly. But this term can be made to appear explicitly in the equation by rearranging the recombination term (eqn.2.2.22). Thus:

$$q\Re(u,x) = q\left[p(x)n(x) - n_{ie}^{\ 2}(x)\right]\left\{C_n n(x) + C_p p(x) + \frac{1}{\tau_{p_0}(n(x)+n_{ie}(x)) + \tau_{n_0}(p(x)+n_{ie}(x))}\right\}$$

$$= u(x)\left[qn_{ie}^{\ 2}(x)\left\{C_n n(x) + C_p p(x) + \frac{1}{\tau_{p_0}(n(x)+n_{ie}(x)) + \tau_{n_0}(p(x)+n_{ie}(x))}\right\}\right]$$

here use has been made of the definition of $u(x)$ (eqn.2.2.14). According to this manipulation, the "voltage" $u(x)$ is singled out from the expression of recombination and the terms under the third bracket of the right side of the above equation are grouped into a single term, which will henceforth be known as the 'conductance' $G(u,x)$ of the transmission line. So,

$$G(u,x) = qn_{ie}^{\ 2}(x)\left\{C_n n(x) + C_p p(x) + \frac{1}{\tau_{p_0}(n(x)+n_{ie}(x)) + \tau_{n_0}(p(x)+n_{ie}(x))}\right\}. \tag{2.3.2}$$

Then using the new definitions of $R(u,x)$ and $G(u,x)$ (i.e. combining equations 2.3.1 and 2.3.2), the transport equations (2.2.17) and (2.2.23) can be rewritten as:

$$\frac{du(x)}{dx} = -R(u,x)J(x), \tag{2.3.3a}$$

$$\frac{dJ(x)}{dx} = -G(u,x)u(x). \tag{2.3.3b}$$

Equations (2.3.3) are analogous to the time-independent transmission line equations. In the classical TL analysis, if the line inductances and capacitances (L and C) are omitted (i.e. if the equations are made time-independent so that time derivatives vanish), the same equations are obtained (consider equations 1.4.2a,b). Also notable is the fact that equations (2.3.3) represent lossy TL. Furthermore, the set of equations (2.3.3) are inhomogeneous, because R and G are functions of both $u(x)$ and x through $n(u,x)$ and $p(u,x)$. The TL model thus completes with the formulation of equations (2.3.3).

For an *npn* transistor, the *pn*-product at the base edge is given by [9]:

$$p(0)n(0) = [n(0) + N_A(0)]n(0) = nie^2(0)\exp\left(\frac{E_{fn} - E_{fp}}{k_B T}\right) \cong n_{ie}^2(x)\exp\left(\frac{qV_{be}}{k_B T}\right),$$

here $n_{ie}(0)$ is the effective intrinsic carrier concentration and V_{be} is the base-emitter voltage. The above expression reduces to (using eqn.2.2.14):

$$\begin{aligned} u(0) &= \exp\left(\frac{qV_{be}}{k_B T}\right) - 1 \\ &\approx \exp\left(\frac{qV_{be}}{k_B T}\right) \end{aligned} \qquad (2.3.4)$$

It is also assumed that the electron velocity at the base-collector junction is saturated and so the electron current density is given by [9]:

$$J_n = -qv_s n(W_B), \qquad (2.3.5)$$

here v_s is minority carrier velocity at the collector end (i.e. $x=w$) of quasi-neutral base. Typical value of v_s is 10^7 cm^{-1}s [22]. Then using eqn.(2.2.3), eqn. (2.3.5) gives:

$$J(w) = qv_s n(w), \qquad (2.3.6)$$

here w is the base width W_B.

Equations (2.3.4) and (2.3.6) constitute the *Boundary conditions* for the system of equations (2.3.3).

The load-impedance at the collector-base junction (x=w) is:

$$Z_L(w) = \frac{u(w)}{J(w)} = \frac{p(w)}{qn_{ie}^{\ 2}(w)v_s} \tag{2.3.7}$$

For a p-type base, the quasi-neutrality condition (2.2.21) can be rewritten as:

$$p(u,x) = n(u,x) + N_A(x). \tag{2.3.8}$$

2.3.1 Normalization process

In eqn.(2.2.14), a normalized $u(x)$ has been defined. In all other equations in this section, this $u(x)$ is used as it is in eqn. (2.2.14). One problem that immediately arises is that in the TL model, so far discussed, the 'voltage' is normalized but the 'current' is not. So there is a need to devise a procedure to normalize the current also. Besides TL parameters are extremely temperature-dependent. Consequently, a straightforward implementation of TL equations along with its parameters (equations 2.3.1, 2.3.2, 2.3.3a,b) to solve the voltage and current distribution along inhomogeneous TL is difficult. The normalization scheme that is being followed here makes the parameters stable against temperature variation, besides being able to normalize the current also.

According to this normalization scheme [15], the current density J_n is redifined as:

$$J_n = F_n J^*, \tag{2.3.9}$$

where:

$$F_n = q\frac{n_{ie}^{\ 2}(w)}{N_A(w)}v_{th}. \tag{2.3.10}$$

the thermal velocity v_{th} is defined as:

$$v_{th} = \left(3k_BT/m^*\right)^{\frac{1}{2}}, \tag{2.3.11}$$

here m^* is the effective mass and for silicon it is $1.1m$, m being the mass of electron.

So the normalized resistance of the TL model are as follows:

$$R_n = RF_n, \tag{2.3.12a}$$

and normalized conductance becomes:

$$G_n = \frac{G}{F_n}, \tag{2.3.12b}$$

where R and G are originally defined as in equations (2.3.1 & 2).

Owing to the opposite influence of F_n on G_n and R_n, the normalized parameter values approach those of the typical TL if the micrometer is used as the unit of length (as suggested by [15]). This is in accordance with the micrometer order of length of quasi-neutral regions. After normalization (with F_n expressed in A/μm^2), $u(x)$ and $J(x)$ become dimensionless. But R_n and G_n are expressed in 1/μm. The temperature dependence of F_n enables the excessive temperature variation of TL parameters to be substantially reduced after normalization. The doping dependence of TL parameters are not affected by the normalization scheme.

Finally, the normalized loading impedance Z_L (eqn. 2.3.7) becomes:

$$Z_L(w) = \frac{u(w)}{J(w)} = \frac{u(w)}{F_n J^*(w)} = \frac{p(w)}{q n_{ie}^{\ 2}(w) v_s}.$$

Therefore, substituting eqn.(2.3.10) in the above expression and assuming $p(w) \approx N_A(w)$, the load-impedance (eqn.2.3.7) becomes simply the ratio of thermal and the effective recombination velocity of minority carriers at the end of the quasi-neutral region:

$$Z_L(w) = \frac{u(w)}{J^*(w)} \approx \frac{v_{th}}{v_s}. \tag{2.3.13}$$

2.4 FORMULATION OF THE PRESENT TL MODEL

The inhomogeneous lossy TL, discussed in sections 2.2 and 2.3, can be represented as a series of n homogeneous segments of uniform length. As per the boundary conditions (equations 2.3.4 and 2.3.6), only the voltage at the base-emitter junction

(V_{be}=u(0)=exp(V_{be}/V_T)) and the current at the collector-base end ($J(w)=qv_sn(w)$) are known. The complete transmission line (base) can be represented as in figure 2.2.

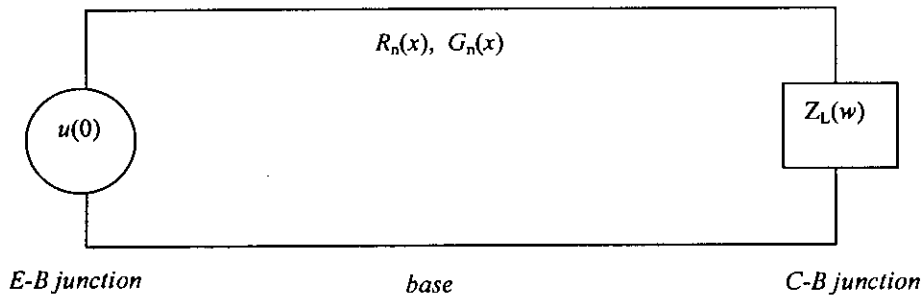

Figure:2.2 The base transmisision line.

In the present work, at the collector-base junction, $J(w)$ is assumed. Then $n(w)$ is known (from eqn.2.3.6) and hence $p(w)$ can be calculated (eqn.2.3.8 at x=w). Then $R_n(w)$ and $G_n(w)$ can be calculated from $n(w)$ and $p(w)$ (using equations 2.3.1 & 2 and then using the normalization process as in equations 2.3.12). The load impedance at x=w is given by eqn.(2.3.13).The propagation constant, reflection coefficient and characteristic impedance are then obtained from equations 1.4.5, 1.4.16 and 1.4.8 respectively. The voltage and current at the end of the (n-1)th segment (i.e. the beginning of the nth segment) is calculated using transmission line equations (1.4.20a,b). The base is then fragmented into n segments of uniform length (Δx=w/n). All the calculations mentioned above are for the load-end, i.e. at the end of the nth segment. Now these parameters can be used to determine the minority carrier distribution at the receiving-end, i.e. to the end of the (n-1)th segment (or the beginning of the nth segment). As $n(x)$ at the end of (n-1)th segment is known, then again $p(w)$, $R_n(w)$, $G_n(w)$, reflection coefficient, propagation constant, characteristic impedance etc. are calculated using the same equations as above. But the load-impedance is determined from the ratio of $u(w-\Delta x)$ to $J^*(w-\Delta x)$. Then again all the other parameters are calculated using the same old equations successively. Repeating this process ultimately ends in reflecting the voltage and current to the beginning of the 1st segment (i.e. at x=0). Then at x=0, V_{be} is obtained from eqn.(2.3.4). This is, in brief, the present TL model, which will be elaborated below.

In the following figure 2.3, the transmission line (base) is thought to be composed of an array of n homogeneous segments of uniform length Δx ($=w/n$). Then the following analysis is carried on:

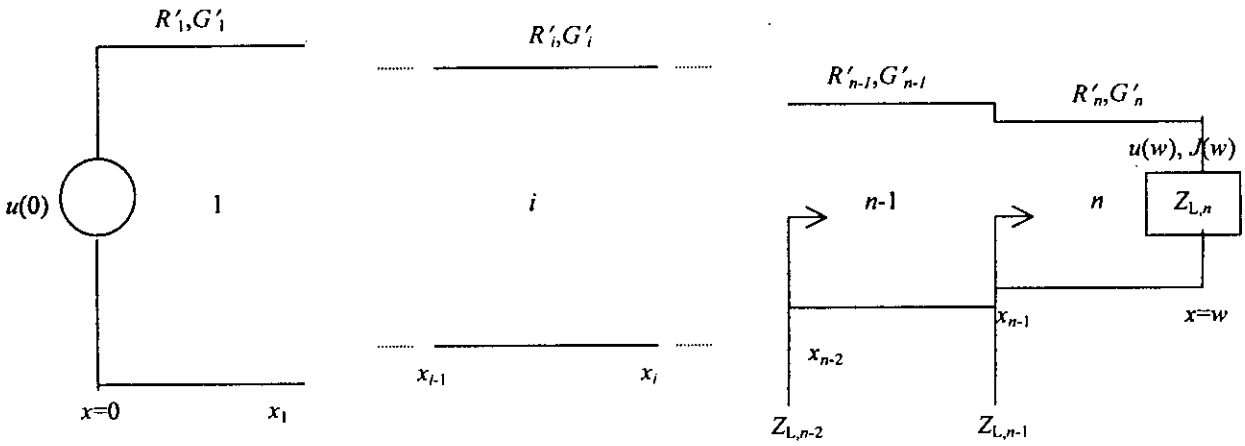

Figure:2.3 The base TL divided into n segments of equal length.

a) For the nth segment, at $x=w$ or W_B, a particular value of $J(w)$ is assumed.

b) $n(w)$ is then calculated using eqn.(2.3.6), again repeating here for convenience:

$$J(w) = qv_s n(w), \tag{2.4.1}$$

here q, v_s and $J(w)$ is known.

c) Using quasi-neutrality condition (eqn.2.3.8) $p(w)$ is calculated:

$$p(w) = n(w) + N_A(w), \tag{2.4.2}$$

here again $n(w)$ is known from eqn.(2.4.1) and a particular form of $N_A(x)$ is assumed in eqn.(2.2.8), repeated again:

$$N_A(x) = N_{A0}\exp\left(\frac{-\eta x}{w}\right). \qquad (2.4.3)$$

d) Using $n(w)$ and $p(w)$ from equations (2.4.1 & 2) the voltage at $x=w$ is calculated from eqn.(2.2.14):

$$u(w) = \frac{p(w)n(w)}{n_{ie}^{\ 2}(w)} - 1. \qquad (2.4.4)$$

the effective intrinsic concentration is given by eqn.(2.2.5):

$$n_{ie}^{\ 2}(x) = n_{io}^{\ 2}\left(\frac{N_A(x)}{N_r}\right)^{\frac{2V_g}{V_t}}, \qquad (2.4.5)$$

here the values of N_r, V_g and V_T are constant.

e) And load-impedance at $x=w$ is given by eqn.(2.3.13):

$$Z_L(w) = \frac{v_{th}}{v_s}. \qquad (2.4.6)$$

f) Resistance for the nth segment is calculated using eqn.(2.3.1):

$$R(w) = \frac{p(w)}{qD_n(w)n_{ie}^{\ 2}(w)}. \qquad (2.4.7)$$

g) Conductance for the nth segment is calculated using eqn.(2.3.2):

$$G(w) = qn_{ie}^{\ 2}(w)\left\{C_n n(w) + C_p p(w) + \frac{1}{\tau_{p_0}(n(w)+n_{ie}(w)) + \tau_{n_0}(p(w)+n_{ie}(w))}\right\} \qquad (2.4.8)$$

h) Resistance and conductance of the TL are then normalized by a constant F given by equations (2.3.12):

$$R' = RF, \qquad (2.4.9a)$$

$$G' = \frac{G}{F}, \qquad (2.4.9b)$$

where the normalizing factor is given by eqn.(2.3.10):

$$F = q\frac{n_{ie}^{\ 2}(w)}{N_A(w)}v_{th}. \qquad (2.4.10)$$

i) Characteristic impedance $Z_{0,n}$ for the nth segment is given by eqn.(1.4.8). In that equation putting L=C=0:

$$Z_{0,n} = \sqrt{\frac{R'}{G'}}. \qquad (2.4.11)$$

here the normalized values of resistance and conductance are used (equations 2.4.9).

j) Putting L=C=0 in eqn.(1.4.5), the propagation constant is obtained:

$$\gamma_n = \sqrt{R'G'}. \qquad (2.4.12)$$

k) Reflection coefficient is given by eqn.(1.4.10). Into that equation putting the values of equations (2.4.6 and 2.4.10) gives:

$$\rho(w) = \frac{Z_L(w) - Z_{0,n}}{Z_L(w) + Z_{0,n}} \qquad (2.4.13)$$

l) At this point, all parameters of the TL are at hand. Now the voltage and current at x=w are to be reflected to the generating end (at the end of (n-1)th segment or the beginning of the nth segment, i.e. at x=x_{n-1}==w-Δx). For a lossy TL, the voltage and current at the generating end is given in terms of those at the load/receiving end by equations (1.4.20a,b). Since those equations were deduced for a TL where the x-coordinate runs from left to right, the sign of x in the exponential terms for the present case will be simply reversed. Because in the present case x-coordinate runs in the opposite sense (see figure 2.4 below). So the voltage and current in the TL at distance Δx from the load (i.e. at x= x_{n-1} =w-Δx) is given by:

$$u(x_{n-1}) = u_{0,n}^{\ +}\left[exp(\gamma_n \Delta x) + \rho\, exp(-\gamma_n \Delta x)\right], \qquad (2.4.14a)$$

$$J^*(x_{n-1}) = \frac{u_{0,n}^{\ +}}{Z_{0,n}}\left[exp(\gamma_n \Delta x) - \rho\, exp(-\gamma_n \Delta x)\right], \qquad (2.4.14b)$$

here the current is dimensionless, as all terms in eqn.(2.4.14b) are normalized according to the normalization procedure mentioned in section 2.4.

The incident voltage at load $u_{0,n}^{+}$ is given by [23]:

$$u_{0,n}^{+} = \frac{u(w)}{1+\rho(w)}. \qquad (2.4.15)$$

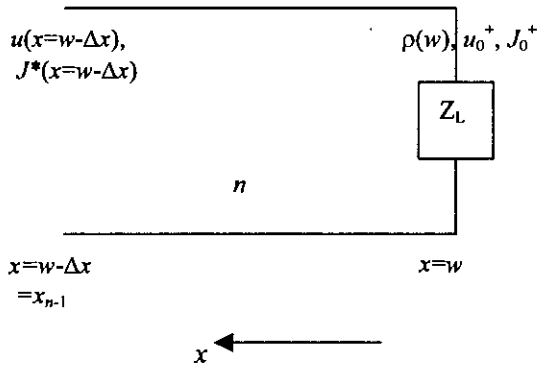

Figure: 2.4 The nth segment of base.

m) For the (n-1)th segment, $n(x_{n-1})$ at the end of the (n-1)th segment or the beginning of the nth segment (i.e. at $x=x_{n-1}=w-\Delta x$) is unknown there and it is not possible to calculate it from eqn.(2.4.1). Therefore, substituting eqn.(2.4.2) into eqn.(2.4.4) and solving the resulting quadratic equation for $n(x)$ gives:

$$n(x_{n-1}) = \frac{1}{2}\left(-N_A(x_{n-1}) + \sqrt{N_A^{\,2}(x_{n-1}) + 4n_{ie}^{\,2}(x_{n-1})(1+u((x_{n-1})))}\right), \qquad (2.4.16)$$

here the negative solution is disregarded.

n) Then $p(x_{n-1})$ is calculated from eqn.(2.4.2). Here $x= x_{n-1}=w-\Delta x$.

o) Therefore, as above, R, G, γ_{n-1}, $\rho(x_{n-1})$, $Z_{0,n-1}$ are calculated using equations (2.4.4-13). The load impedance in these cases are given by eqn.(2.4.17) below. Here x_{n-1} stands for $w-\Delta x$.

p) $Z_L(x_{n-1})$ is given by:

$$Z_L(x_{n-1}) = \frac{u(x_{n-1})}{J^*(x_{n-1})}. \qquad (2.4.17)$$

q) The above parameters are calculated for $x=w-\Delta x$, i.e. at the end of the $(n-1)$th segment. So using equations (2.4.14a,b) the voltage and current at the beginning of $(n-1)$th segment or at the end of the $(n-2)$th segment (i.e. at $x=w-2\Delta x$) can be obtained:

$$u(w-2\Delta x) = u_{0,n-1}^{+}\left[\exp(\gamma_{n-1}\Delta x) + \rho\exp(-\gamma_{n-1}\Delta x)\right], \qquad (2.4.18a)$$

$$J^*(w-2\Delta x) = \frac{u_{0,n-1}^{+}}{Z_{0,n-1}}\left[\exp(\gamma_{n-1}\Delta x) - \rho\exp(-\gamma_{n-1}\Delta x)\right], \qquad (2.4.18b)$$

where $u_{0,n-1}^{+}$ is the incident voltage at x_{n-1} and is obtained from eqn.(2.4.15) by substituting x_{n-1} for w.

r) The above procedure (equations 2.4.1-18) is repeated until $x=0$ is reached. The voltage $u(0)$ at that end is also calculated from eqn.(2.4.18a). This is the generating end of the TL base or the base-emitter junction of the BJT.

s) The base-emitter voltage V_{be} is obtained from eqn.(2.3.4) as follows:

$$V_{be} = V_T \ln u(0), \qquad (2.4.19)$$

V_T is the thermal voltage.

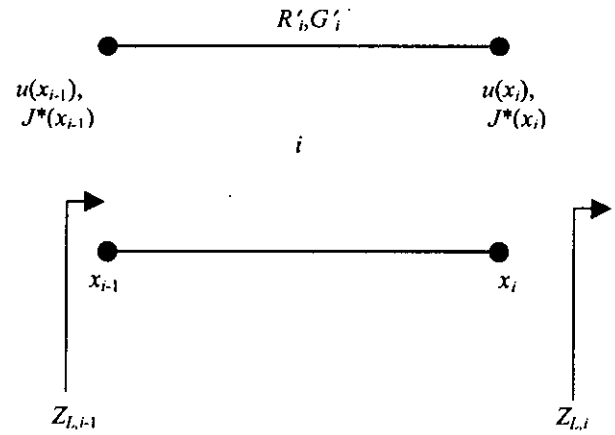

Figure2.5: The i-th segment of the base TL. Note that $x_i=w-(n-i)\Delta x$, with $x_0=0$ for $i=1$ and $x_n=w$ for $i=n$.

2.5 ALGORITHM BASED ON THE PROPOSED TL MODEL

The proposed TL model in section 2.4, therefore, can be used to calculate base transit time and other related profiles, which are very important for study of BJT characteristics. This TL model is then used to obtain the minority carrier distribution $n(x)$ through the base. Once $n(x)$ is known, eqn.(1.3.1) readily gives the stored electron charge within the base. Then eqn.(1.3.2) can be used to calculate the base transit time.

The procedure of the proposed TL model is in brief: for a given $J(w)$, $n(w)$ can be calculated. Hence $p(w)$ can also be calculated. Then voltage $u(w)$ is calculated. Once these are known, R and G are calculated and then normalized accordingly. Therefore, characteristic impedance, load-impedance, propagation constant and reflection coefficient are also calculated. Up to this, the calculation are done for the last of the base segments (i.e. the nth segment, particularly at $x=w$ or W_B). Now the voltage and current at $x=w$ are then reflected along the base TL (using reflection coefficient, characteristic impedance, load-impedance and using well-known transmission line equations) toward the generating end (i.e. at $x=w-\Delta x=x_{n-1}$). When at $x=x_{n-1}$, a new $n(w)$ is calculated using a new relation (eqn.2.4.16). Again $p(x_{n-1})$, $Z_L(x_{n-1})$, R and G and their normalized values, reflection coefficient and characteristic impedance are calculated.

These calculations are for the (n-1)th segment and for $x=x_{n-1}$. So the voltage and current at $x=x_{n-2}$ are calculated using the previously calculated voltage and current at $x=x_{n-1}$. This process is repeated successively until x=0, i.e. the base-emitter junction, is reached. Then the base-emitter voltage V_{be} is calculated (eqn.2.4.19). The $n(x)$ for each point in the base TL are then calculated, so these values of $n(x)$ can be integrated numerically over the base width W_B. This gives the stored electron charge. Dividing this by the base current gives the base transit time (eqn. 1.3.2).

Now there is a problem of selecting a suitable length for each segment of the base TL. There is an analytical formula defining a critical width w_c ($\Delta x<w_c$), which the width of each segment must not exceed. The following formula for w_c is derived in [15]:

$$w_c = 2\sqrt{\frac{2}{3}}v_{th}\tau\,, \qquad (2.5.1)$$

here τ is the relaxation time ($\cong 10^{-13}$s). Also a table is given in [15] showing estimated values of w_c for different doping concentrations and temperatures. It is shown that w_c decreases with increasing doping concentration but never drops below 10nm even for the highest doping (5×10^{19}cm^{-3}). So a standard choice for the number of segments of base TL can be n=100.

The value of $J(w)$, assumed in eqn.(2.4.1), is restrained by a maximum value determined by $N_A(w)$:

$$J(w) = qv_s N_A(w)\,. \qquad (2.5.2)$$

The following figure gives the algorithm that has been followed in constructing a program (written in MATLAB) to compute minority carrier distribution within base and other useful parameters using the present TL model.

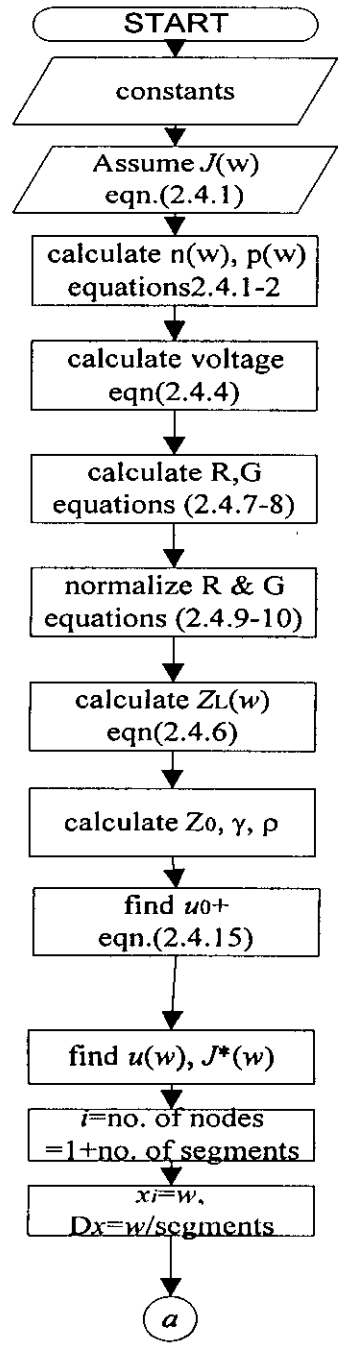

Figure 2.6: Flowchart of the TL model (continued to next page).

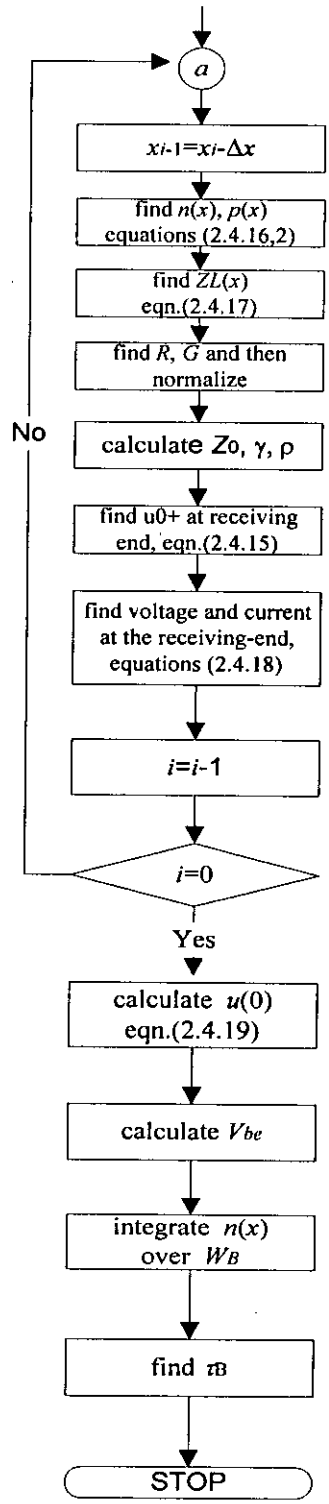

Figure: 2.6 (cont.): Flowchart of the TL model.

The above algorithm is used to calculate the minority carrier distribution within the base for an assumed $J(w)$. For each segment $n(x)$ is determined and it is possible to compute stored electron charge Q_n by integrating $n(x)$ over base width numerically. For numerical integration, trapezoidal method can be followed as is available in any numerical software packages, such as MATLAB. Then the ratio of Q_n to $J(w)$ gives base transit time τ_B. Again a series of $J(w)$ can be generated for which the above algorithm could be run for each $J(w)$ and thus V_{be} and base transit time (τ_B) are calculated in each case. Then V_{be} is plotted against τ_B. In this process other plots (for example, electric field distribution within the base) could also be obtained. In the present case the above algorithm was run in MATLAB software.

CHAPTER 3

RESULTS AND DISCUSSION

3.1 INTRODUCTION

The novel transmission line approach has been developed in chapter 2. The procedure and a relevant algorithm are developed there. In this chapter that novel model is used to calculate minority carrier distribution within the base. With this minority carrier profile, the electric field distribution within the base, the electron charge variation with current density and base-emitter voltage have been calculated. Finally, base transit time is calculated for different values of peak base-doping, slope of base-doping and base width. Results obtained are then plotted and discussed in this chapter.

3.2 DISTRIBUTION OF MINORITY CARRIER WITHIN BASE

The distribution of minority carrier within the base is plotted in Figure 3.1. The figures are for three different values of slope of base-doping η (for definition of η, see eqn 2.2.9). Two sets of curves for two voltages (one for low voltage (0.7V) and the other for high voltage (0.82V)) are also drawn. As seen from the curve minority carrier distribution decreases from its peak value at x=0 (base-emitter junction) as distance from the base-emitter junction increases. This is due to diffusion of carriers within base. Also as the base-emitter voltage increases, more carriers are injected into the base region across the base-emitter junction. So carrier profiles for high voltage are always higher than those of low voltage. Again minority carrier distribution decreases with increase of η. This is because as electric field increases, drift velocity also increases. So a high electric field doesn't allow the charges to accumulate within base. Hence $n(x)$ decreases with increase of η. But at the collector-base junction the trend is opposite. Because in that region electron velocity is saturated. So as electric field increases, current density increases, hence $n(x)$ also increases (eqn 2.3.6).

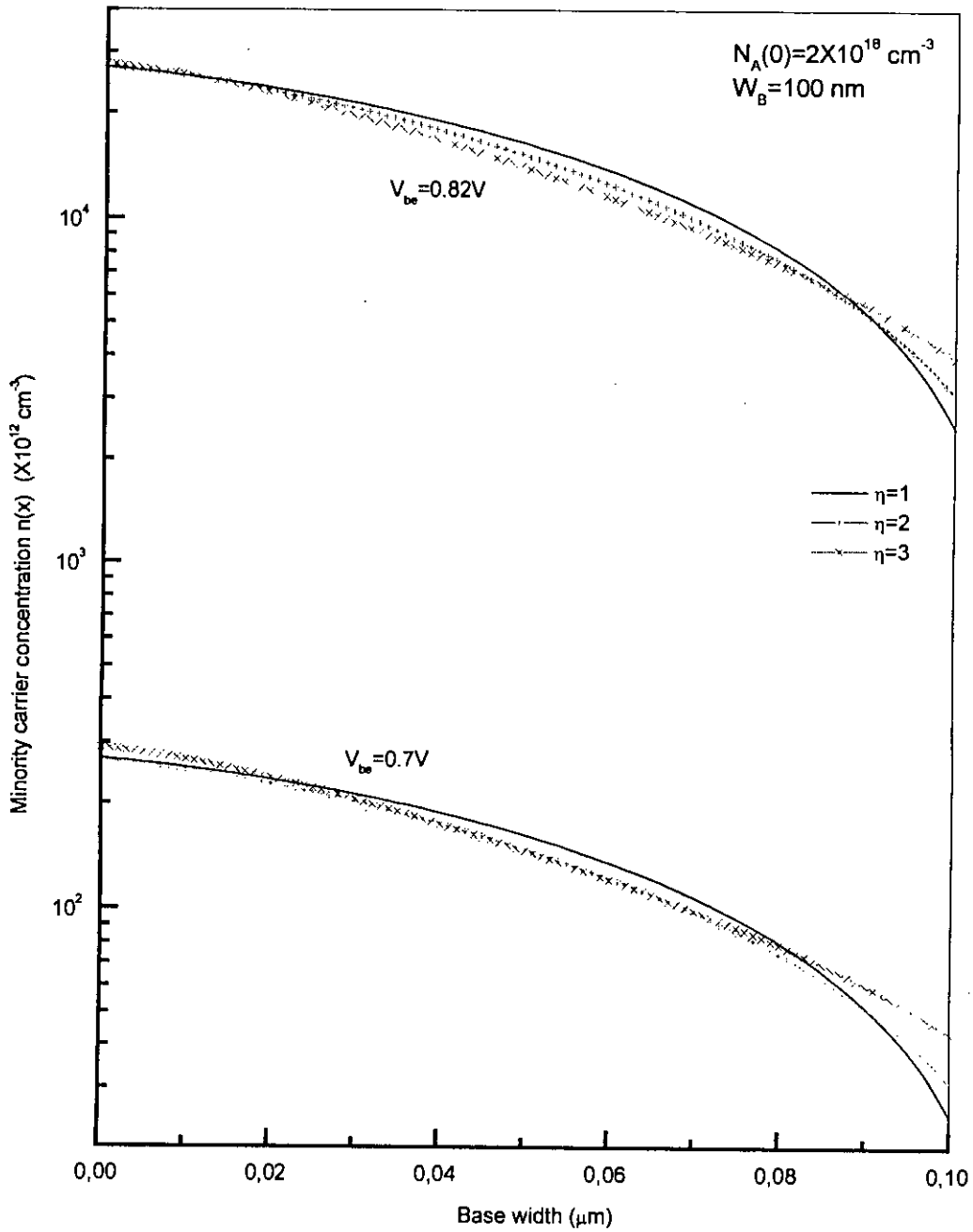

Figure 3.1: Minority carrier distribution within base for two base-emitter voltages and for three values of slope of base-doping.

3.3 ELECTRIC FIELD DISTRIBUTION WITHIN BASE

The distribution of electric field $E(x)$ within the base for different base-emitter voltage is shown in figures 3.2 (a), (b) and (c). The curves show that, when base-emitter voltage is small, the slope of field distribution within the base is very small. But for high base-emitter voltage it is a decreasing function of distance. From equation (2.2.4), we see that electric field depends upon the hole concentration and effective carrier concentration. The quasi-field due to nonuniform bandgap narrowing (i.e. the second part of the equation) is $\frac{-2k_BT\eta V_g}{qW_BV_t}$. This part of the electric field is independent of distance from the base-emitter junction. So the variation of electric field with distance is due to the first part of the electric field only. When base emitter voltage is low (i.e. for low injection) $p(x) \approx N_A(x)$. So the concentration gradient part of the electric field (i.e. the first part of the equation) becomes $-\frac{k_BT\eta}{qW_B}$, which is also independent of distance. So for low voltage the electric field is constant. In this region the electric field acts in a direction that assists the flow of electron within the base. For high voltage (or high injection level), $p(x) \approx n(x)$. The change in the aiding field in the base is due to the modulation of electron concentration as well as electron concentration gradient at high voltage. From fig.3.2 we find that the electric field for high voltage region opposes the flow of minority carrier when the distance is small, but when the distance increases its direction also changes.

In figures 3.2 (a), (b) and (c), the electric field distributions within the base for different slopes of base-doping are also shown. It can be seen that, for low voltage, as the slope of base-doping increases, the aiding electric field distributions within the base increases. This is because, the first part of the electric filed in eqn (2.2.4) is directly proportional to the slope of base doping for low voltage. For high voltage when slope of base doping increases, the distance at which the electric field for low and high injection are equal move towards the collector-base junction.

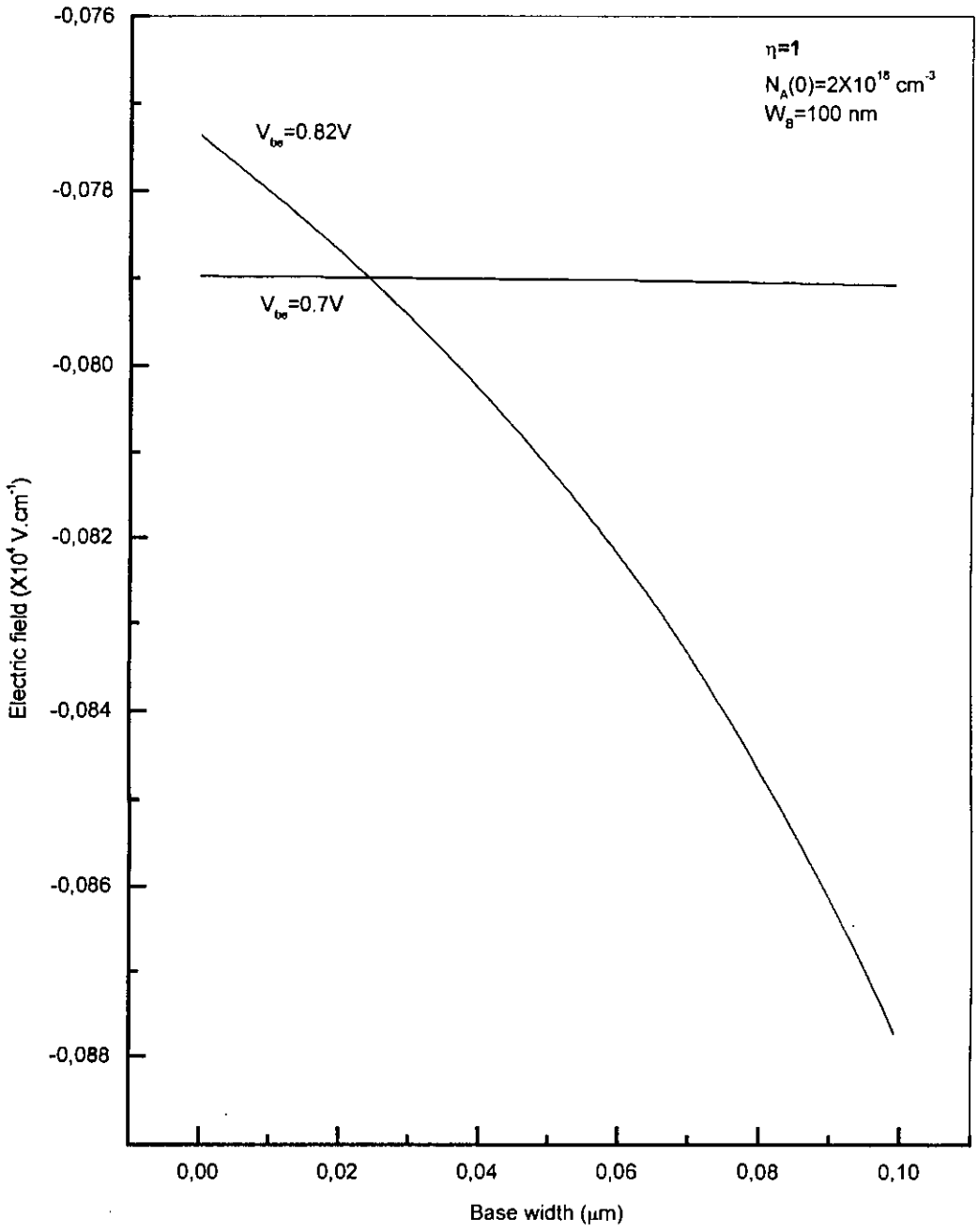

Figure 3.2(a): Variation of electric field within base for $\eta = 1$ and for low and high

voltages.

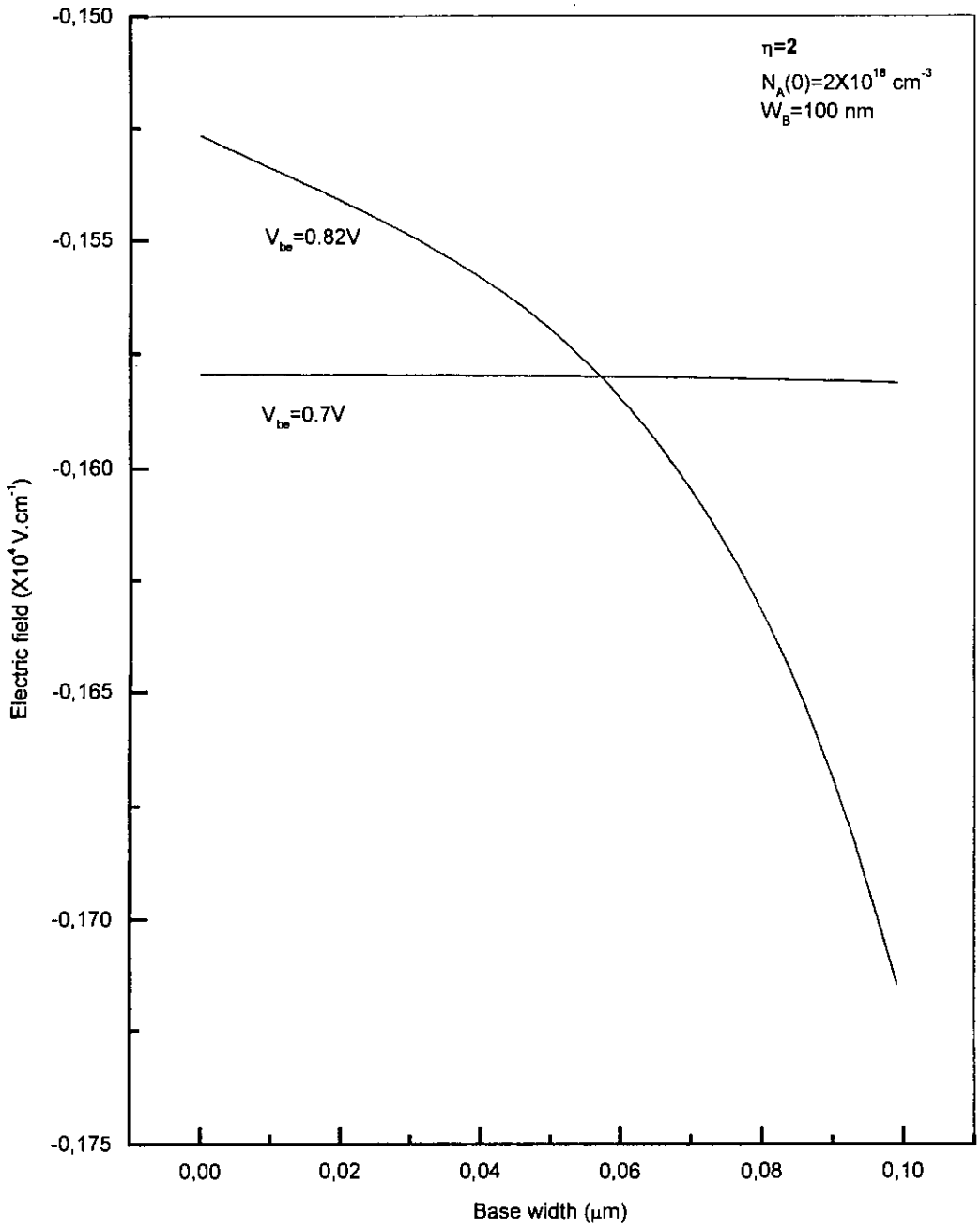

Figure 3.2(b): Variation of electric field within base for η=2 and for low and high voltages.

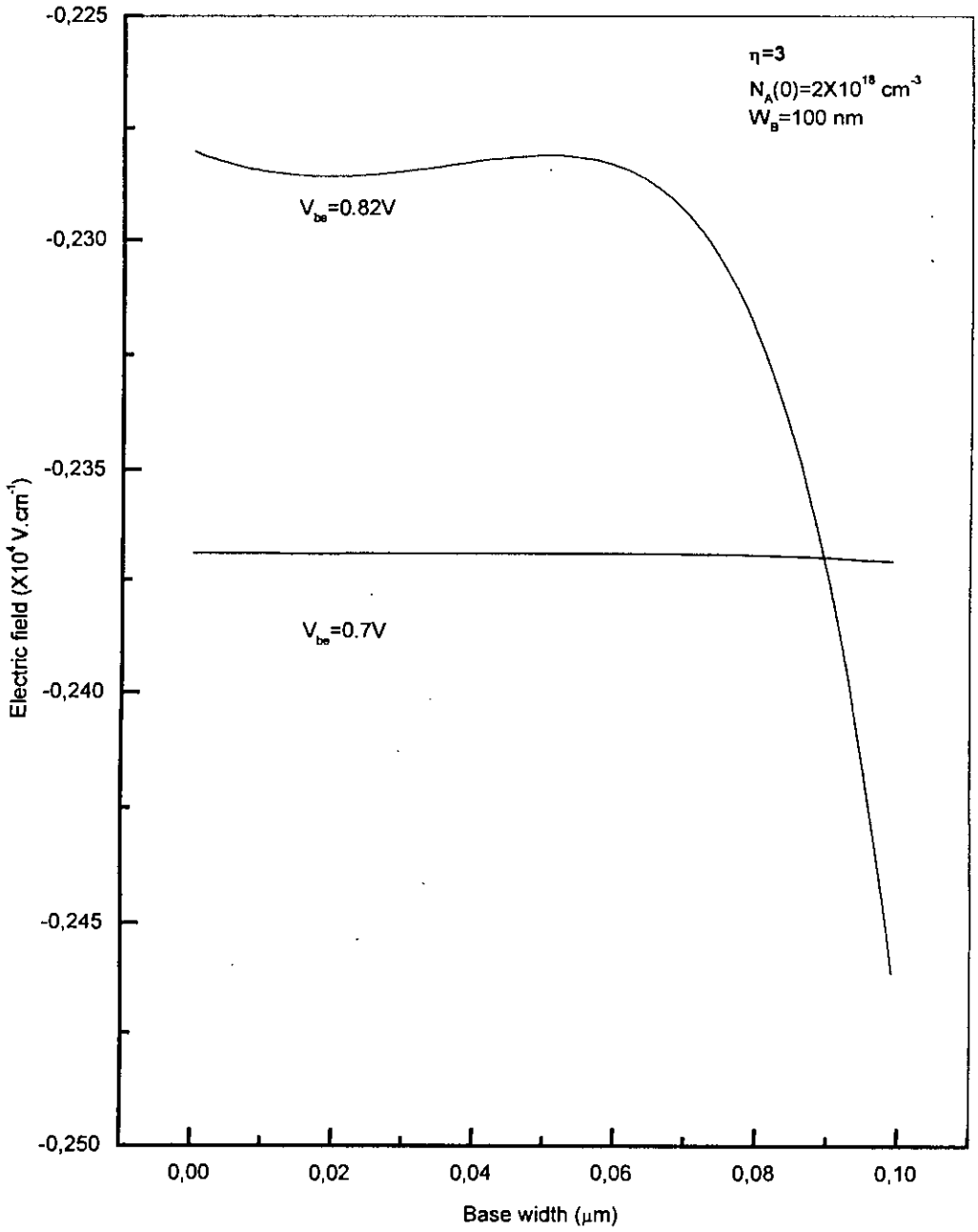

Figure 3.2(c): Variation of electric field within base for η =3 and for low and high voltages.

3.4 VARIATION OF ELECTRON CHARGE WITH BASE-EMITTER VOLTAGE AND CURRENT DENSITY

In figures 3.3 (a) and (b), variation of stored electron charge Q_n with current density J_n and base-emitter voltage V_{be} are plotted. The variation of electron charge with base-emitter voltage are plotted in figures 3.3 (a) ; and the variation of electron charge with current density are plotted in figures 3.3 (b). These are plotted for three different values of slope of base-doping (η = 1, 2, 3). As can be seen from figure 3.3 (a), electron charge increases with increasing base-emitter voltage in an exponential manner. This is expected: as the voltage level increases more charges are accumulated in the base region. The process is cumulative. Hence is the exponential change. The distribution of electric field within the base also affects the accumulation of charges as is explained in the subsection 3.3. On the other hand the variation of electron charge with current density is seen to be linear from figure 3.3 (b). As more currents flow, more is the electron charge stored. Besides, for a given current density stored electron charges decrease with increasing η (η =1, 2, 3) . This correspondingly reduces base transit time for increasing η =1, 2, 3 (this is also evident from figures 3.5(a), 3.6(a) and 3.7(a) and other such curves. Furthermore, as can be seen from figures 3.3, as the variation of electron charge with base-emitter voltage is exponential and that with current density is linear, so it can be logically inferred that the variation of current density with base-emitter voltage will also be exponential. So no extra curves are plotted for this purpose.

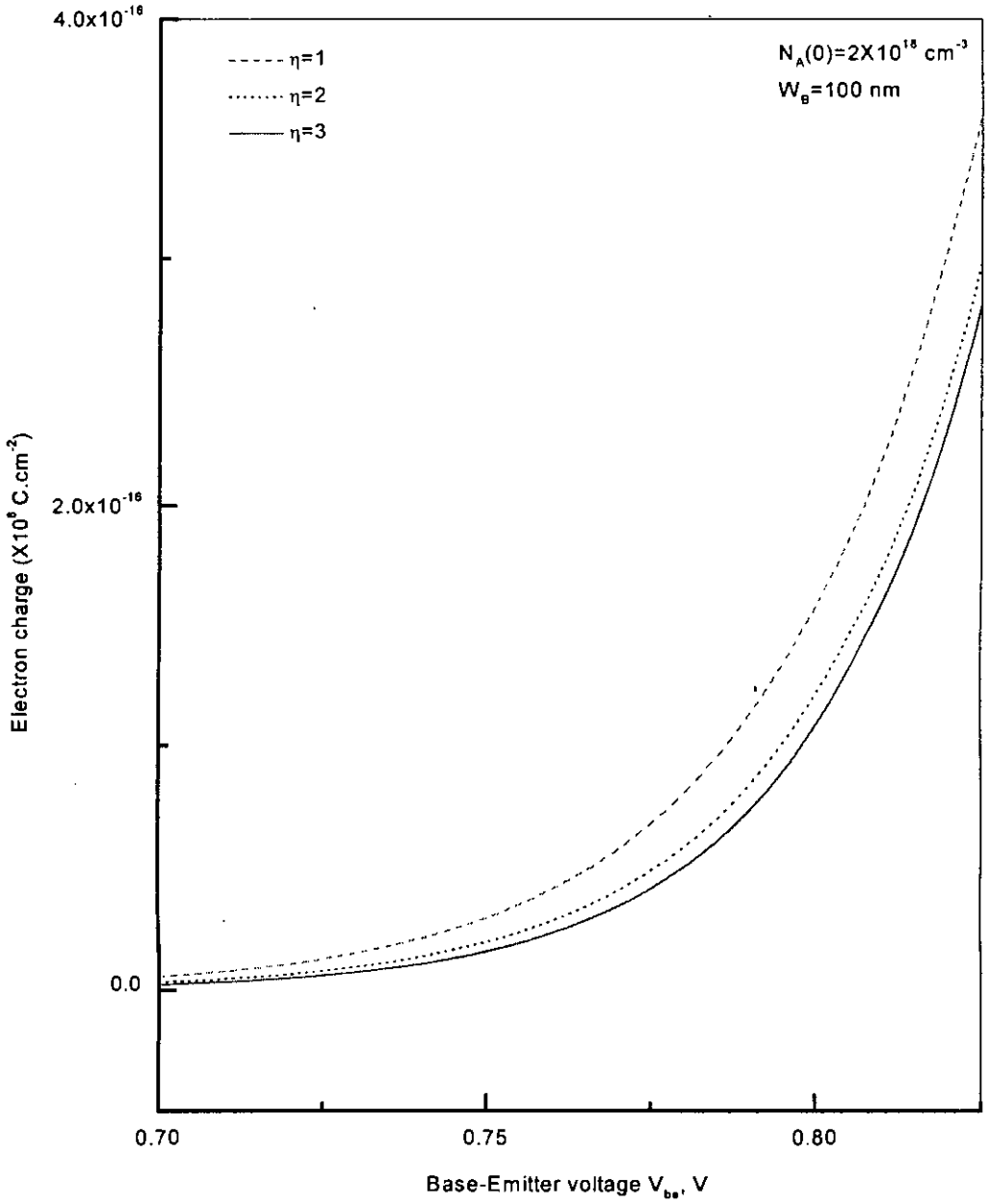

Figure 3.3(a): Variation of electron charge with base-emitter voltage for different slopes of base-doping.

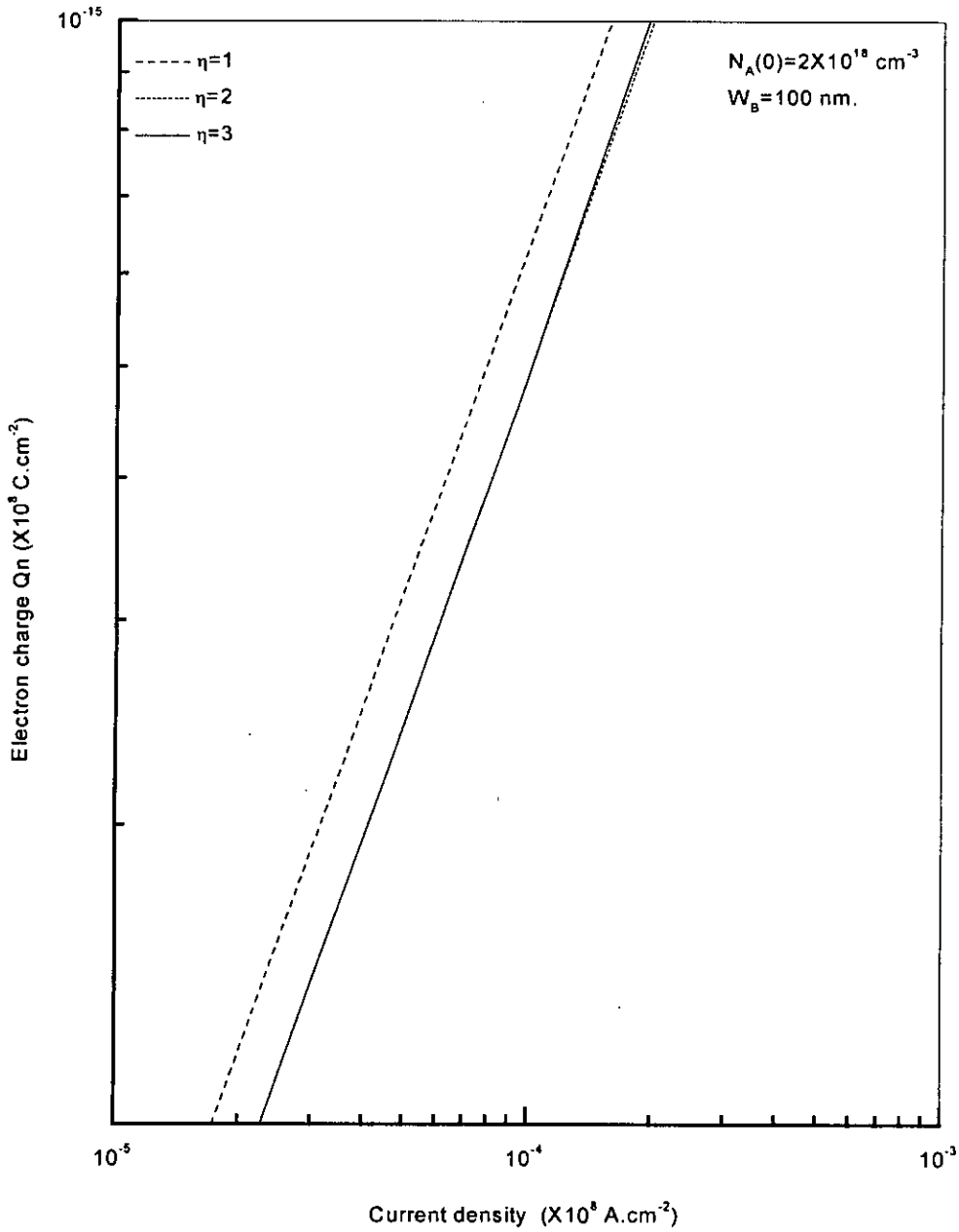

Figure 3.3(b): Variation of electron charge with current density for different slopes of base-doping.

3.5 VARIATION OF BASE TRANSIT TIME WITH BASE-EMITTER VOLTAGE

In figures 3.5-3.12 variation of base transit time (τ_B) with base-emitter voltage (V_{be}) are plotted. These curves are plotted for different peak base-doping ($N_A(0)$) and for different slope of base-doping (η). Again variation with base widths (W_B) are also plotted. So a wide range of variation of base transit time with base-emitter voltage can be inferred from these curves. As a general rule, base transit time remains independent for some values of base-emitter voltage and then it changes for some higher values of base-emitter voltage. Base transit time decreases with slope of base-doping. However, for $\eta = 2$ and 3, it can be seen that base transit time is larger for high values of base-emitter voltage (which corresponds to high levels of injection). This is due to the reduction of aiding field in the exponential base when the voltage level (i.e. the level of injection) increases. From the electric field distribution (fig.3.2) it is noted that the electric field for low voltage assists the flow of electron (minority carrier) within the base. But for high voltage levels the same field opposes the electron flow for distances $x<0.05$ μm. This decrease in electric field slows down the electron flow in the base and thereby increases the base transit time. However, the increase in aiding electric field for distances $x>0.05$ μm in the base affects the base transit time less, because the electrons in that region are already approaching the collector-base junction. As velocity saturation is considered to be active in that region, electrons will be swept toward the collector-base junction by the reverse-biased collector-base region. As base width increases, electrons have to spend more time within base and so base transit time also increases.

The dependence of base transit time upon peak base-doping concentration can also be seen from figures 3.5-3.12 . As can be seen, base transit time increases with peak base concentration. This is due to the dependence of carrier mobility on the peak base-doping as is evident from eqn.(2.2.6). That relationship shows that electron mobility in the base decreases with peak base-doping. So with the increase in the peak base-doping the base transit time increases.

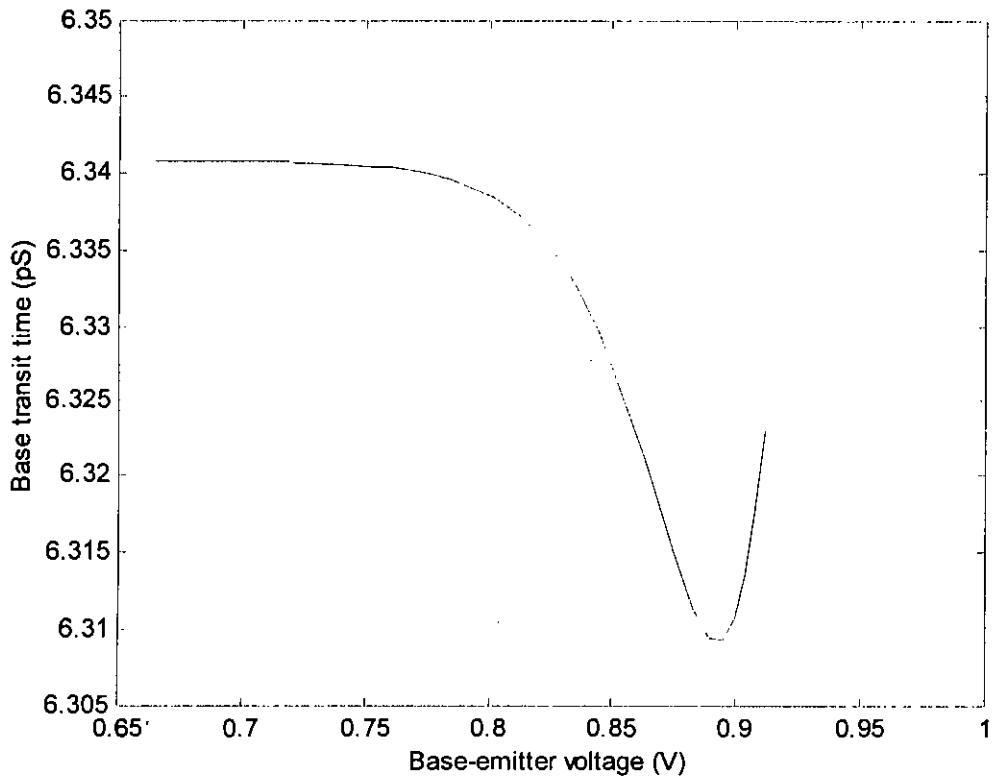

Figure 3.4(a): Variation of base transit time with base-emitter voltage for W_B = 100nm, $N_A(0)=2\times10^{18}$cm-3, $\eta=1$.

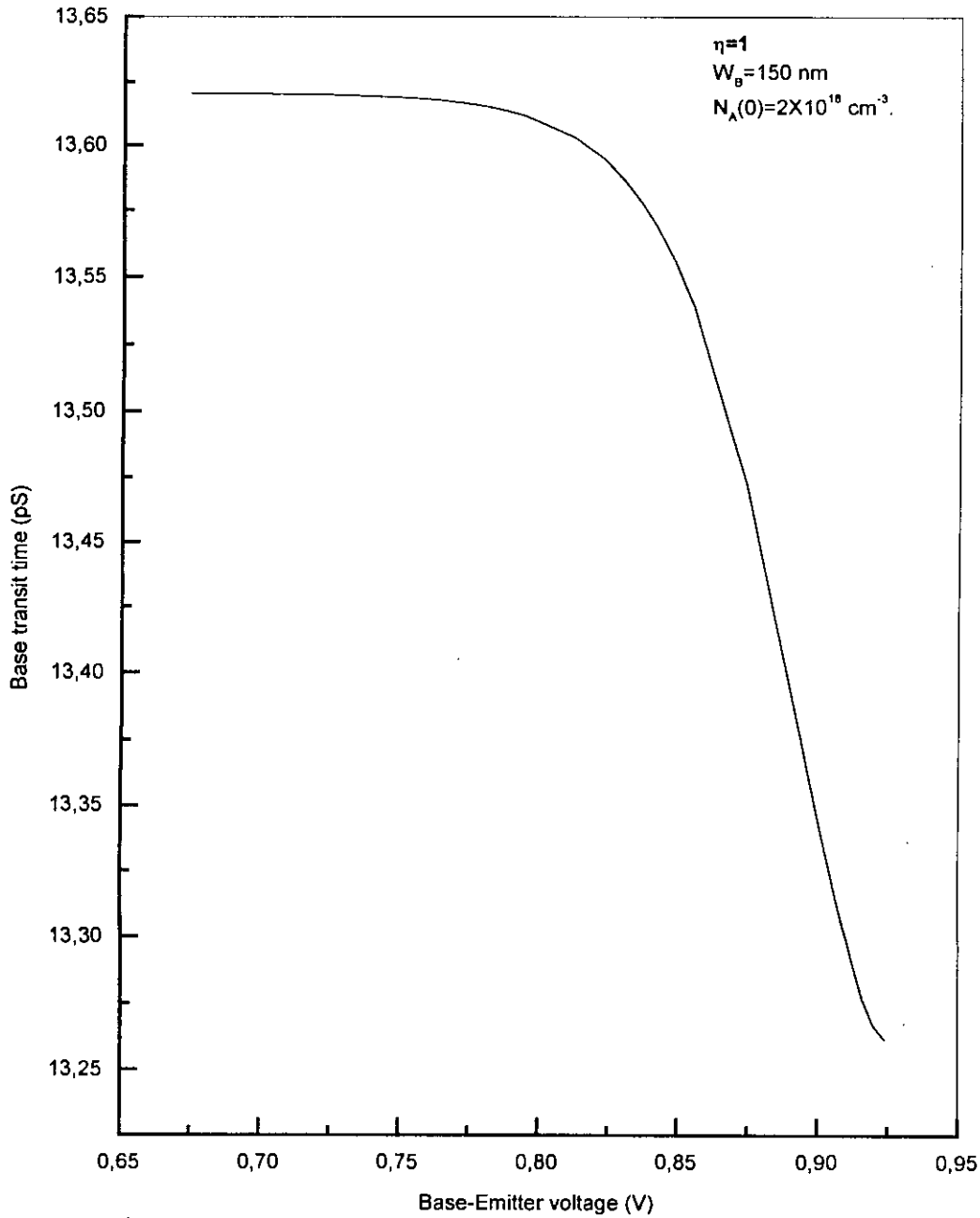

Figure 3.4(b): Variation of base transit time with base-emitter voltage for W_B = 150nm, $N_A(0)=2\times10^{18}cm^{-3}$, $\eta=1$.

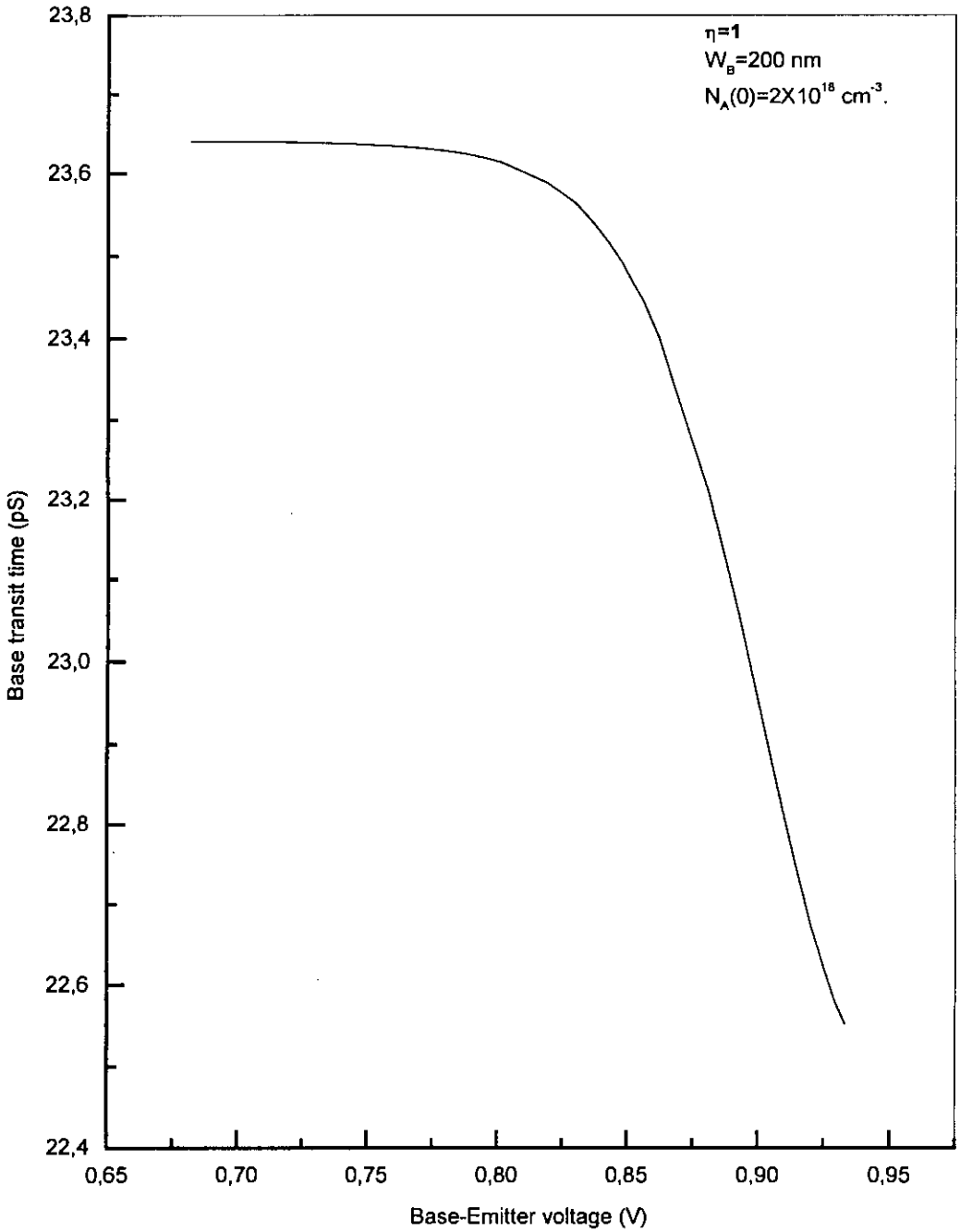

Figure 3.4(c): Variation of base transit time with base-emitter voltage for W_B = 200nm, $N_A(0)=2\times10^{18}$cm-3, $\eta=1$.

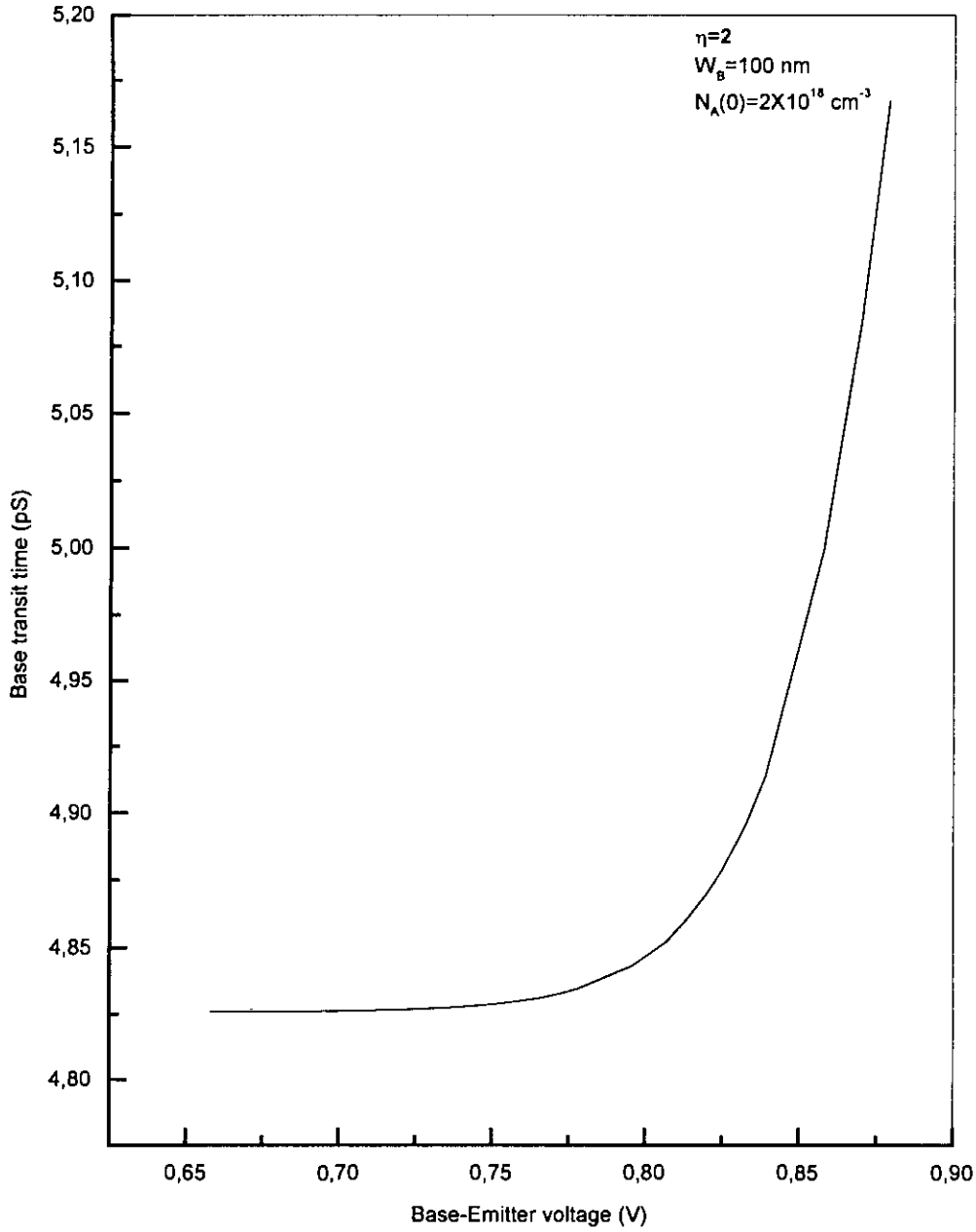

Figure 3.5(a): Variation of base transit time with base-emitter voltage for W_B = 100nm, $N_A(0)=2\times10^{18}cm^{-3}$, η =2.

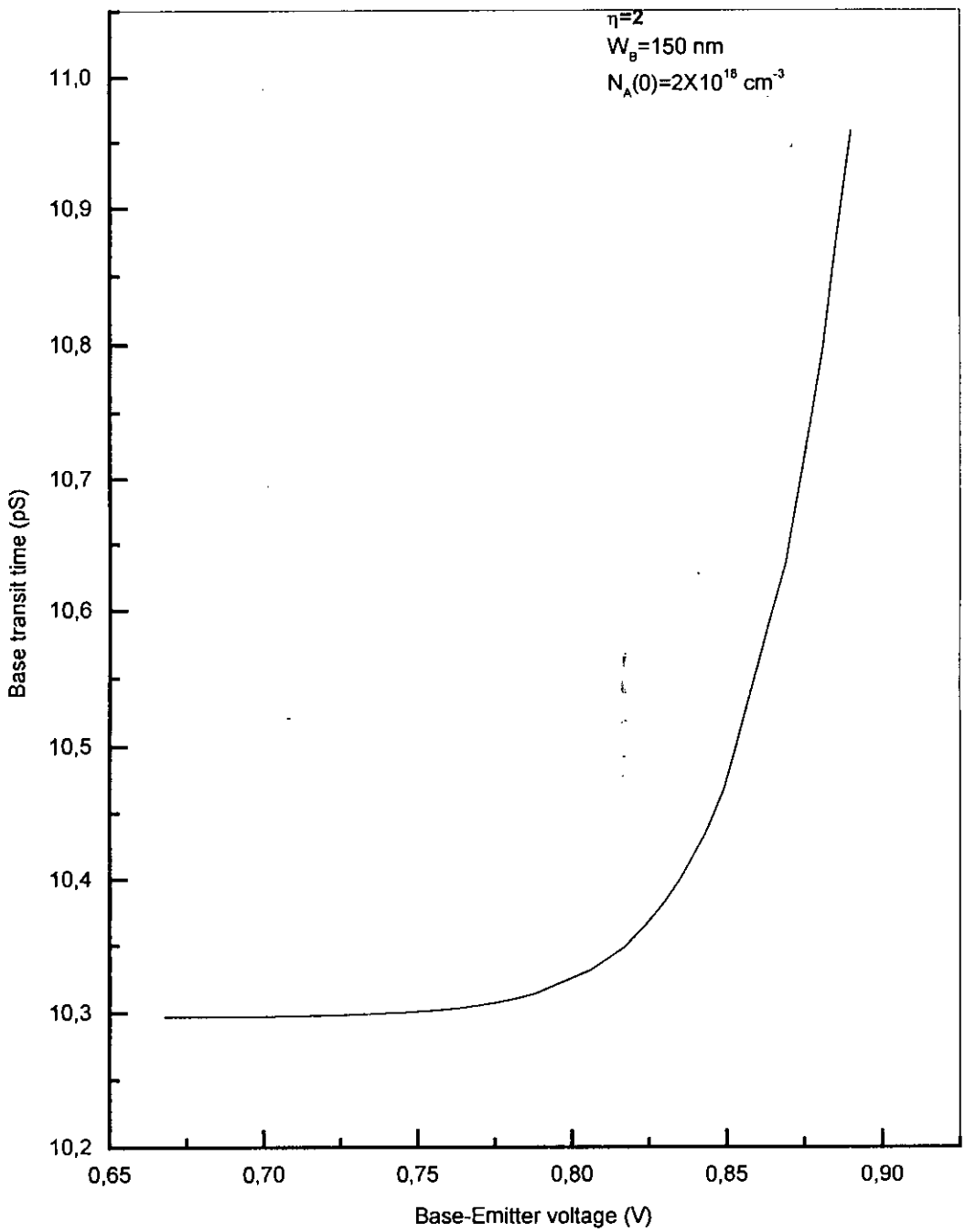

Figure 3.5(b): Variation of base transit time with base-emitter voltage for W_B = 150nm, $N_A(0)=2\times10^{18}cm^{-3}$, $\eta=2$.

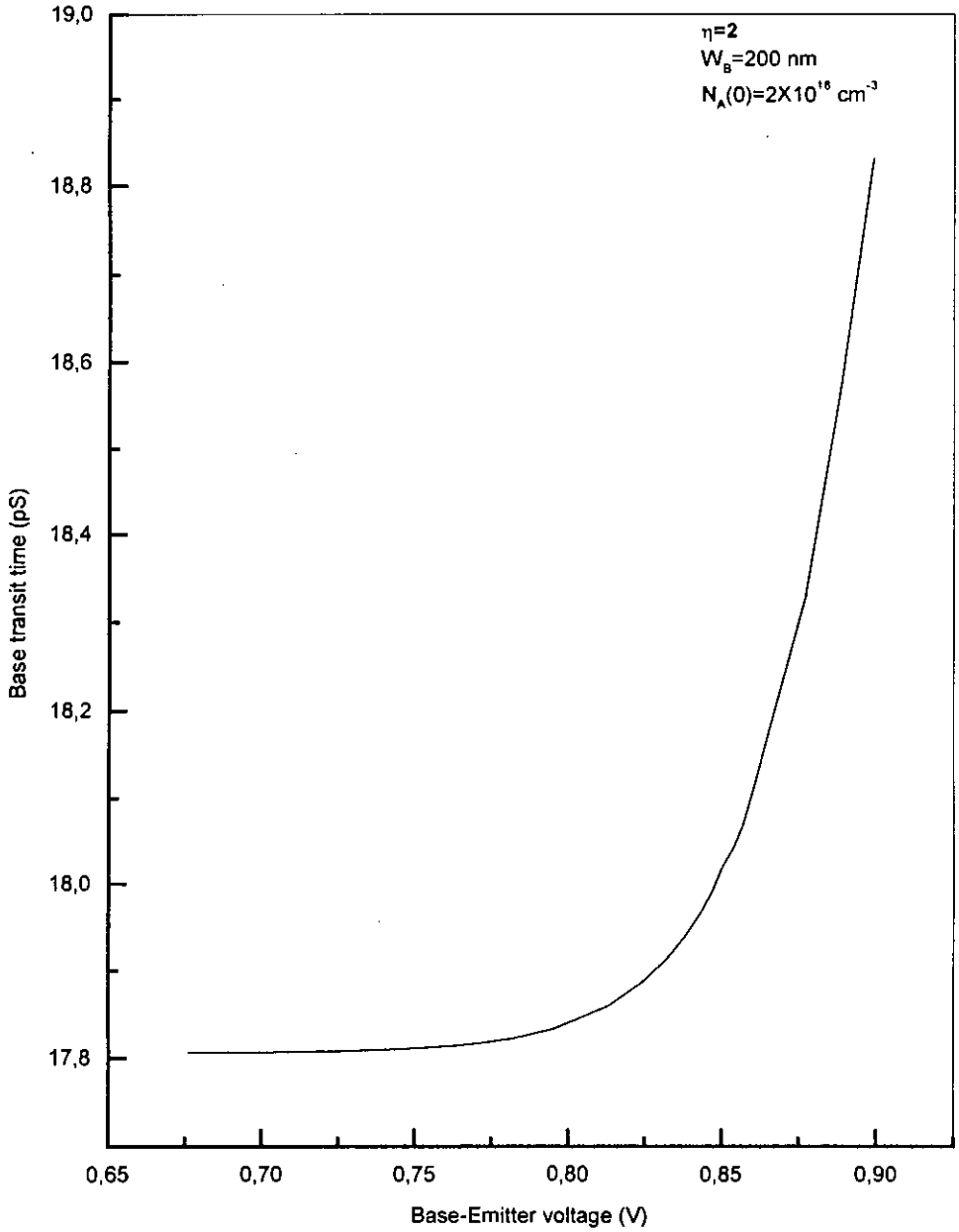

Figure 3.5(c): Variation of base transit time with base-emitter voltage for W_B = 200nm, $N_A(0)=2\times10^{18}cm^{-3}$, η =2.

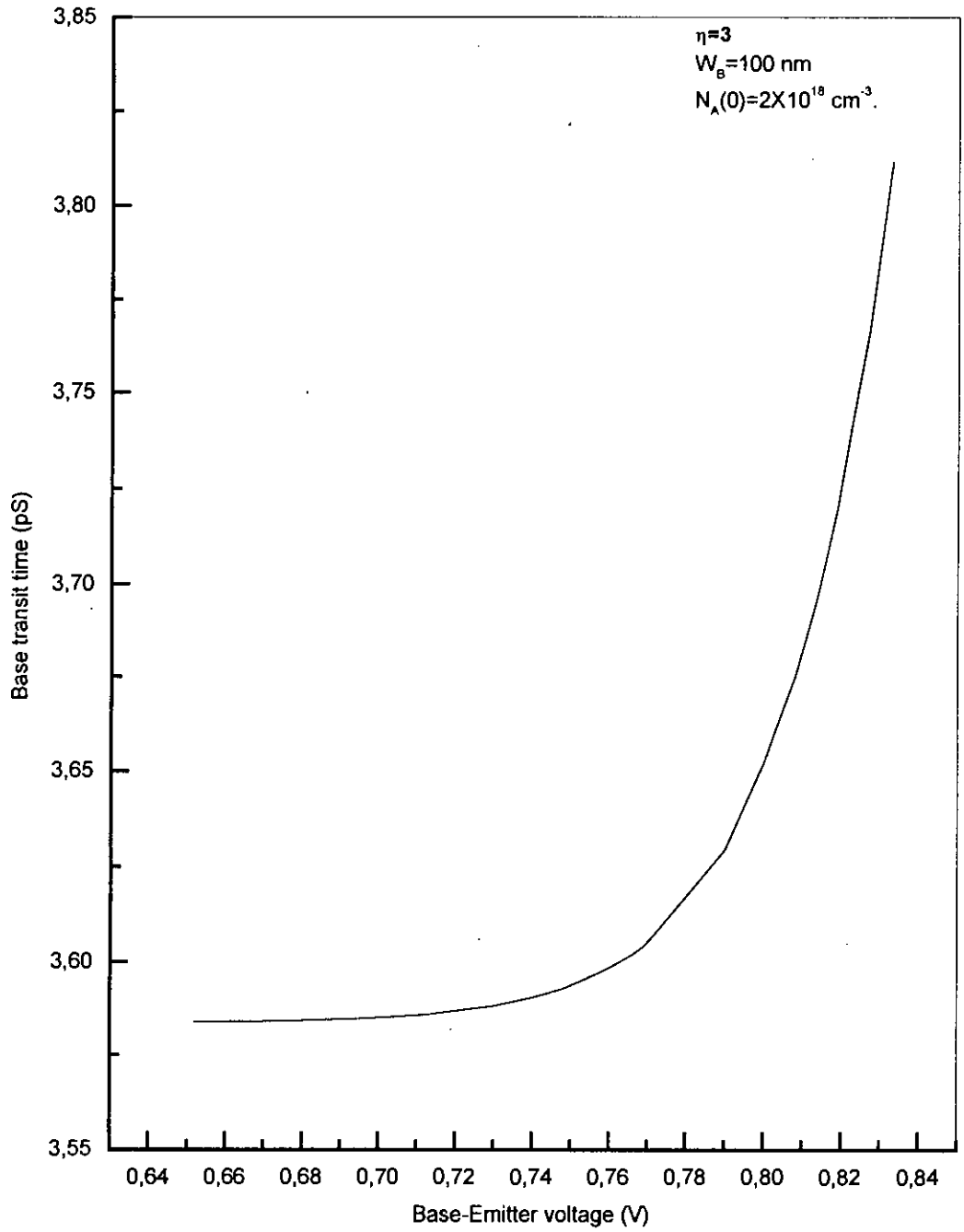

Figure 3.6(a): Variation of base transit time with base-emitter voltage for $W_B = 100\text{nm}$, $N_A(0)=2\times10^{18}\text{cm}^{-3}$, $\eta = 3$.

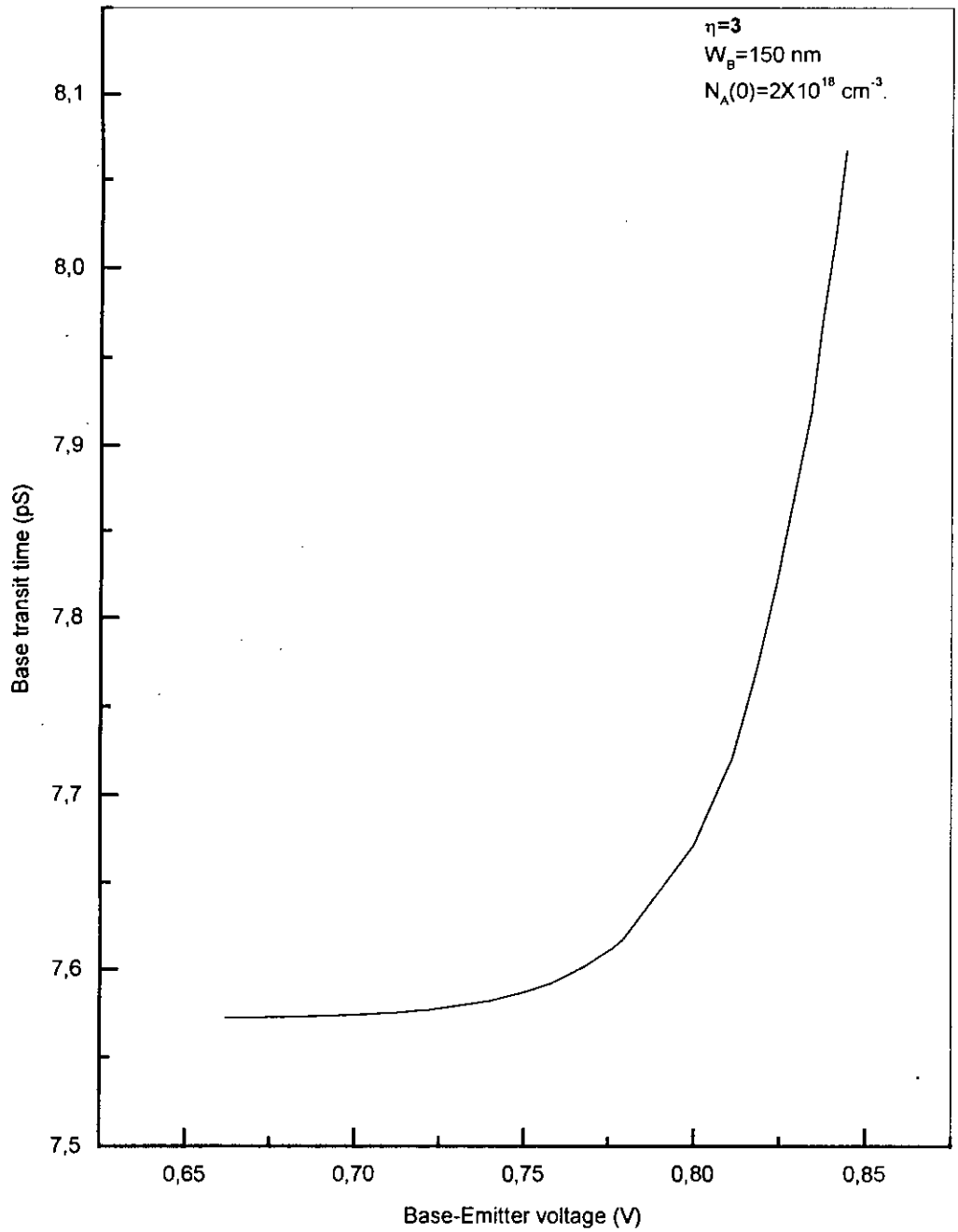

Figure 3.6(b): Variation of base transit time with base-emitter voltage for $W_B = 150\text{nm}$, $N_A(0)=2\times10^{18}\text{cm}^{-3}$, $\eta = 3$.

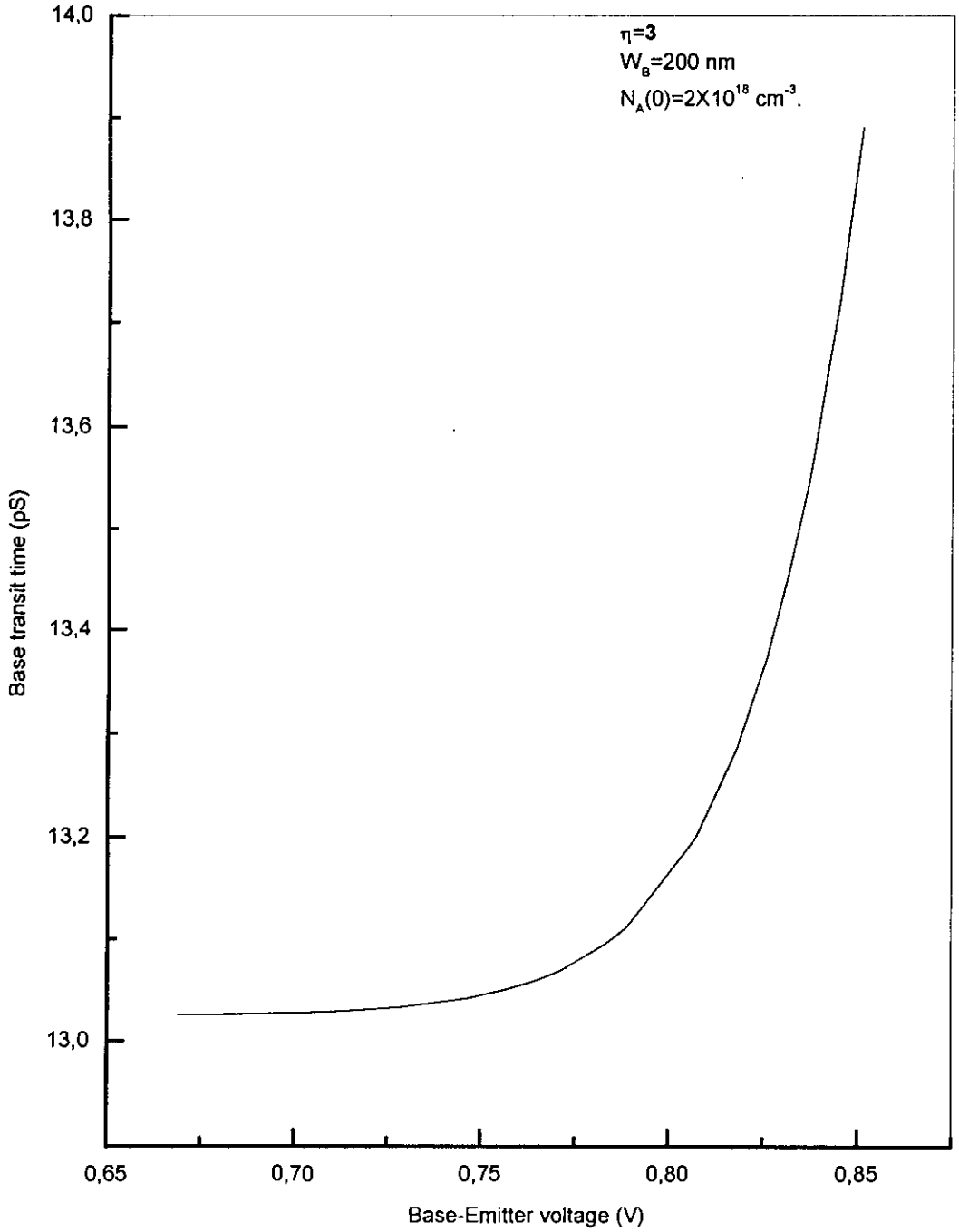

Figure 3.6(c): Variation of base transit time with base-emitter voltage for W_B = 200nm, $N_A(0)=2\times10^{18}cm^{-3}$, $\eta = 3$.

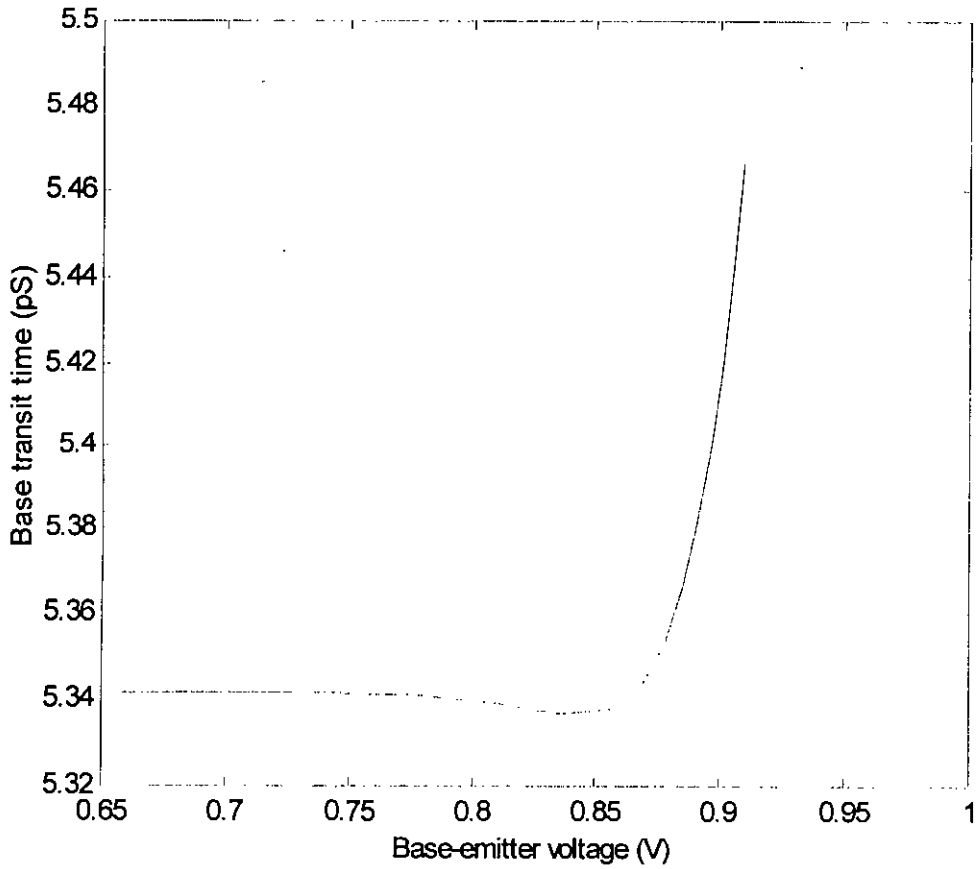

Figure 3.7(a): Variation of base transit time with base-emitter voltage for W_B = 100nm, $N_A(0)=1\times10^{18}cm^{-3}$, $\eta = 1$.

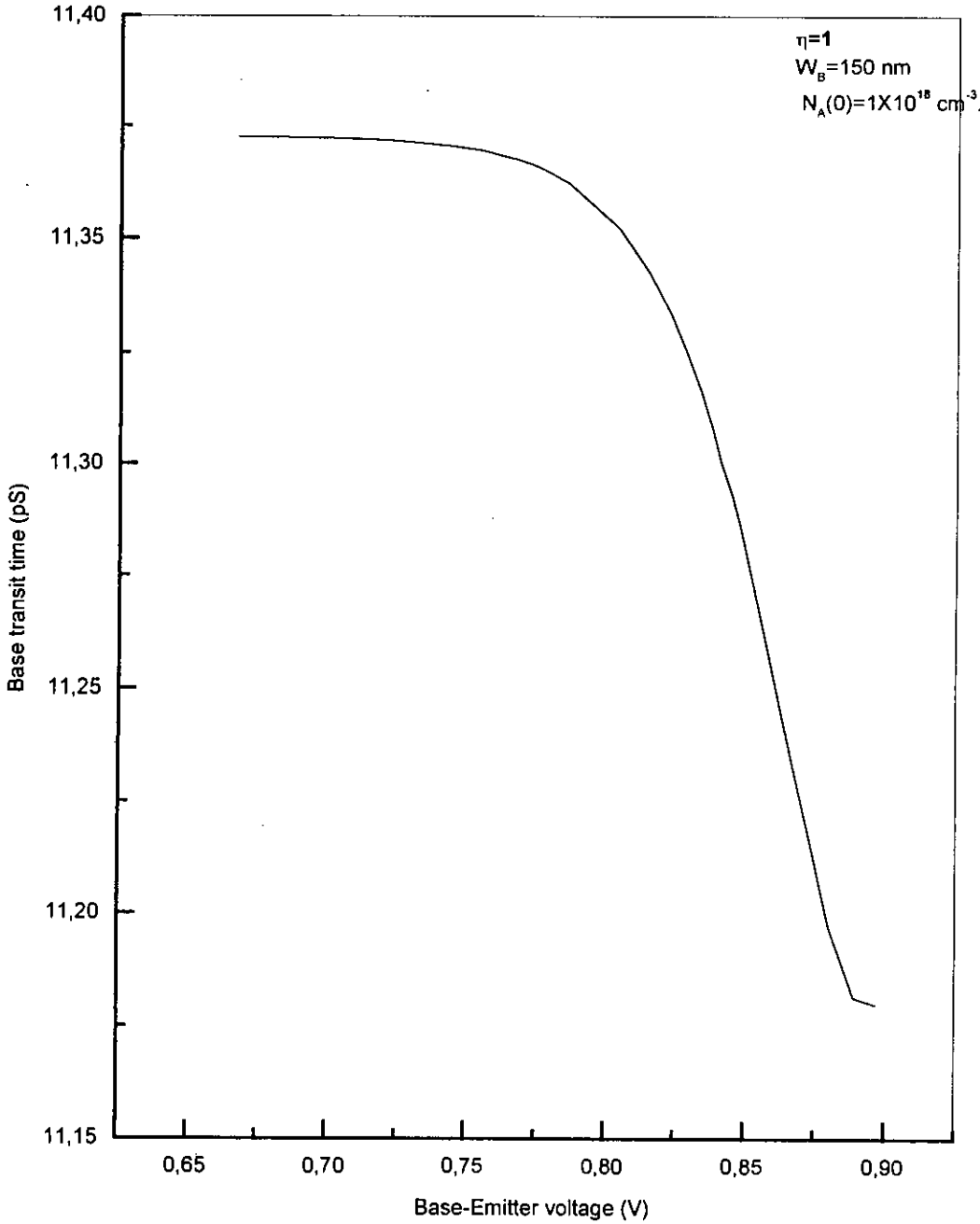

Figure 3.7(b): Variation of base transit time with base-emitter voltage for W_B = 150nm, $N_A(0)=1\times10^{18}cm^{-3}$, $\eta = 1$.

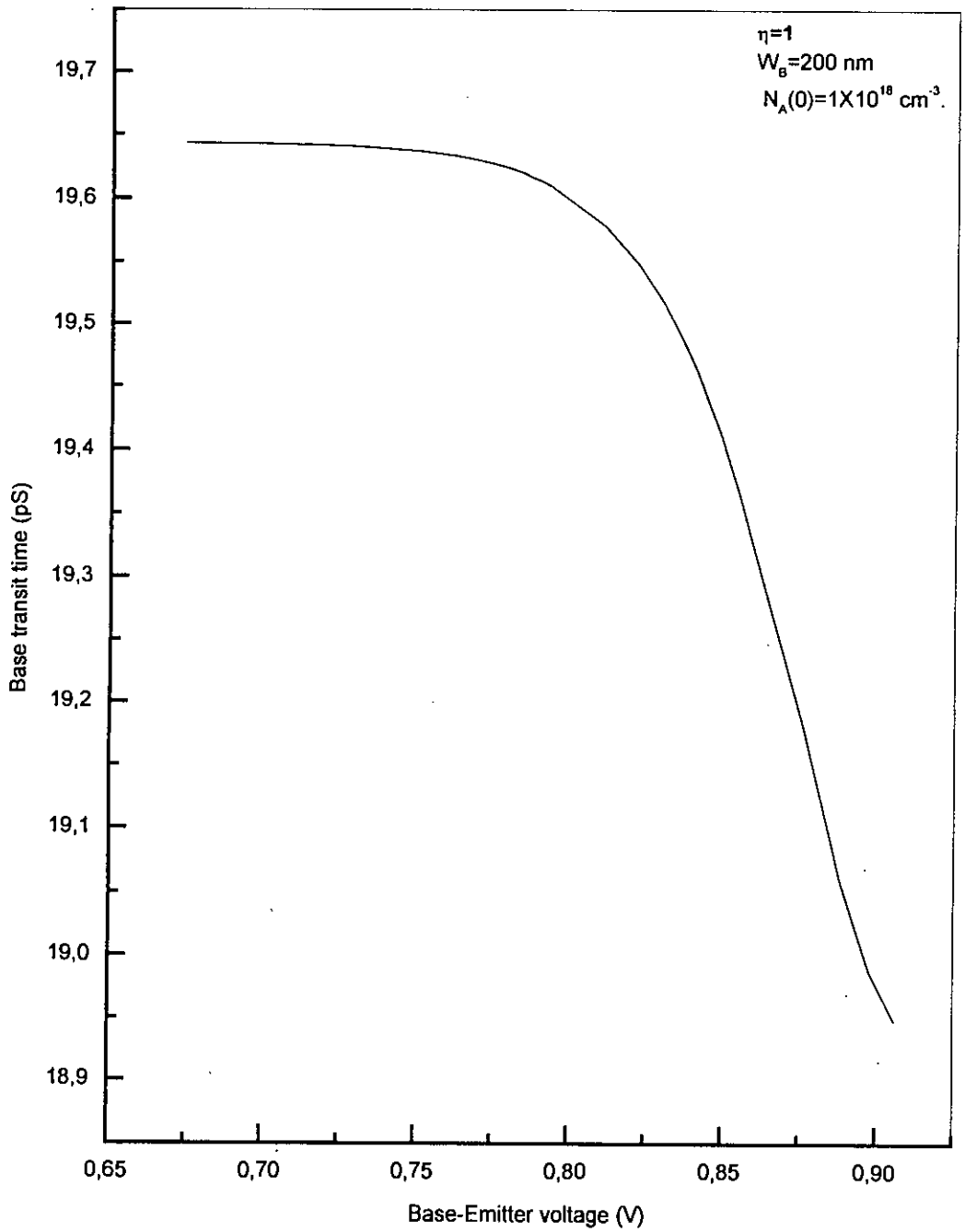

Figure 3.7(c): Variation of base transit time with base-emitter voltage for W_B = 200nm, $N_A(0)=1\times10^{18}cm^{-3}$, $\eta = 1$.

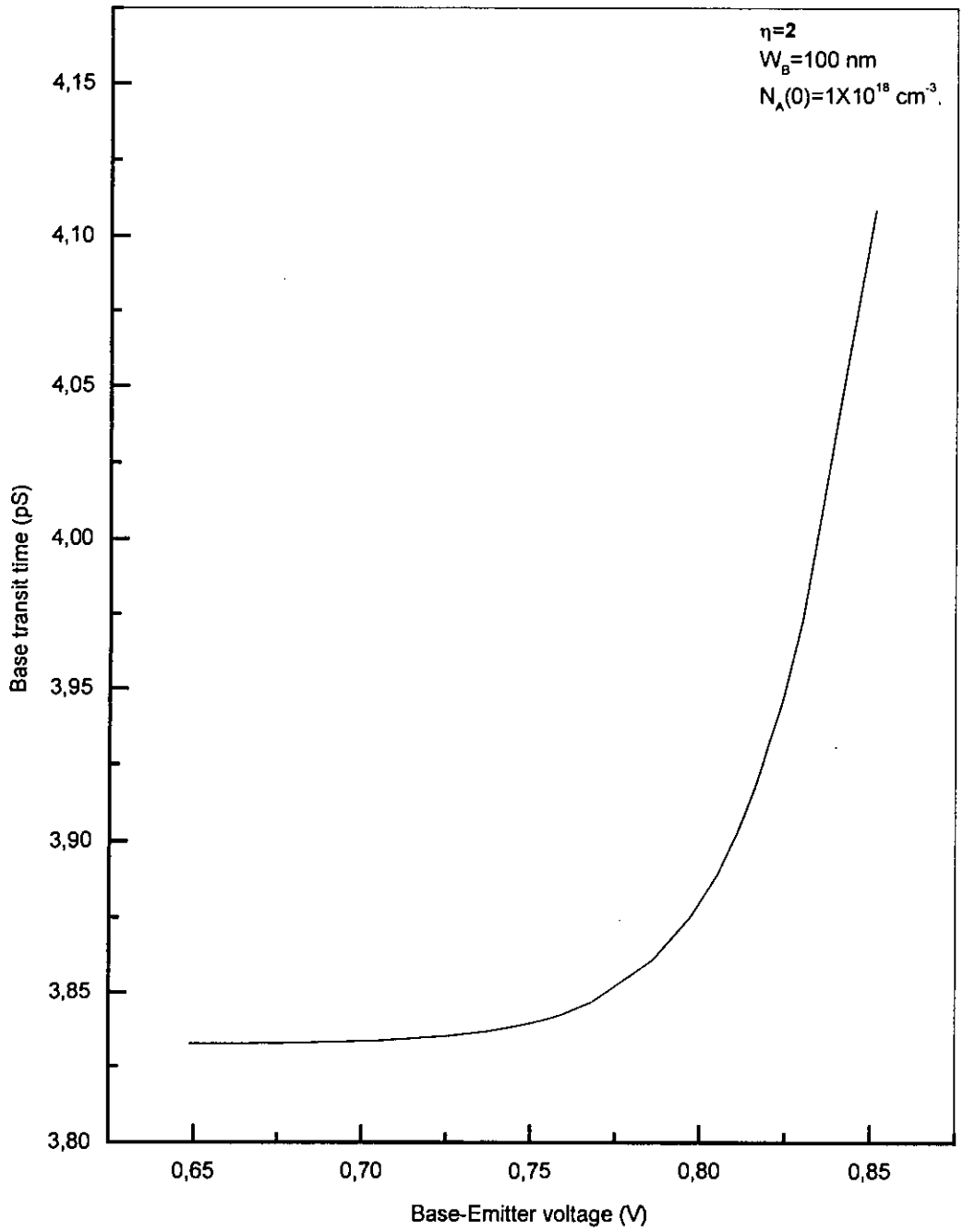

Figure 3.8(a): Variation of base transit time with base-emitter voltage for W_B = 100nm, $N_A(0)=1\times10^{18}cm^{-3}$, $\eta = 2$.

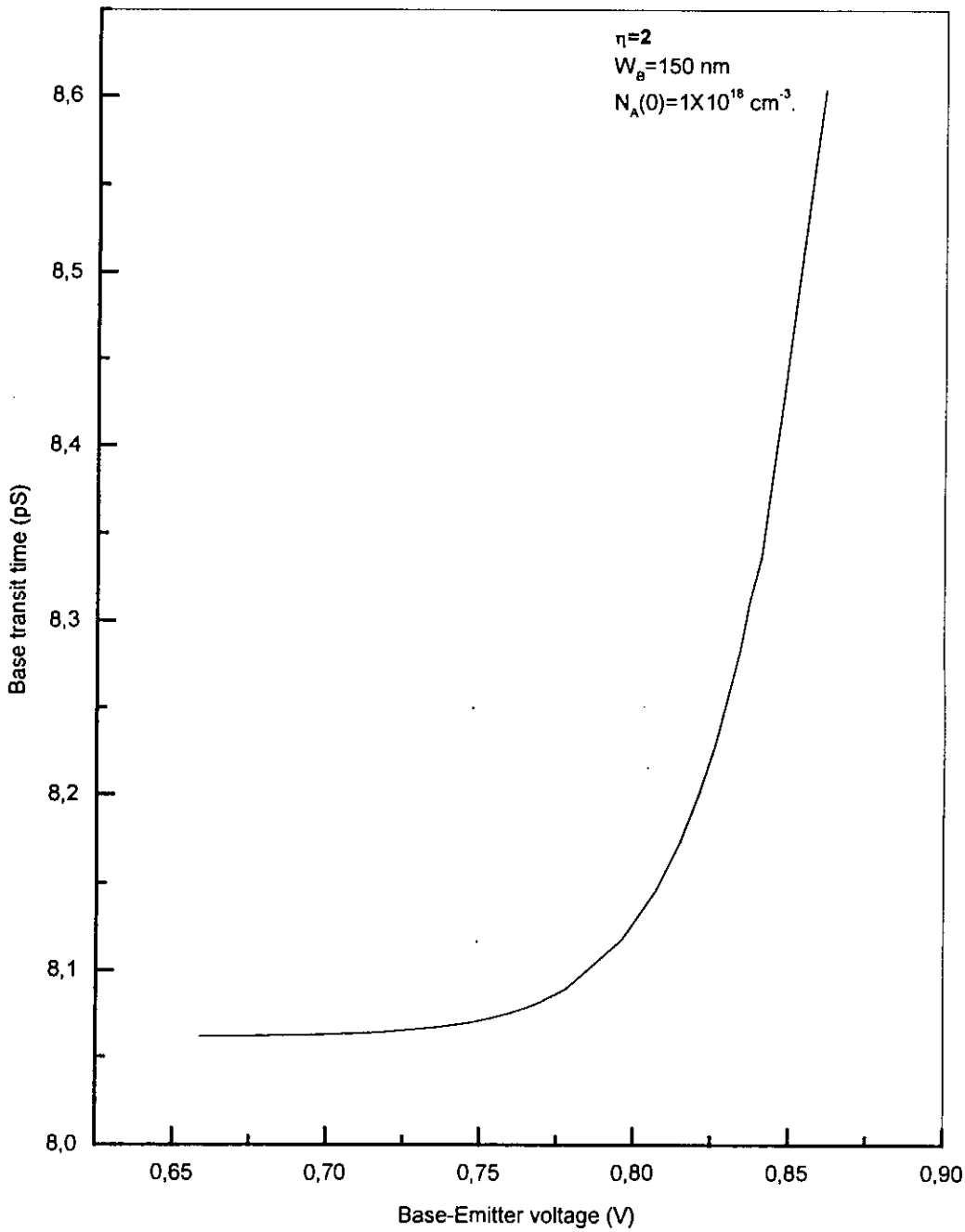

Figure 3.8(b): Variation of base transit time with base-emitter voltage for W_B = 150nm, $N_A(0)=1\times10^{18}cm^{-3}$, $\eta = 2$.

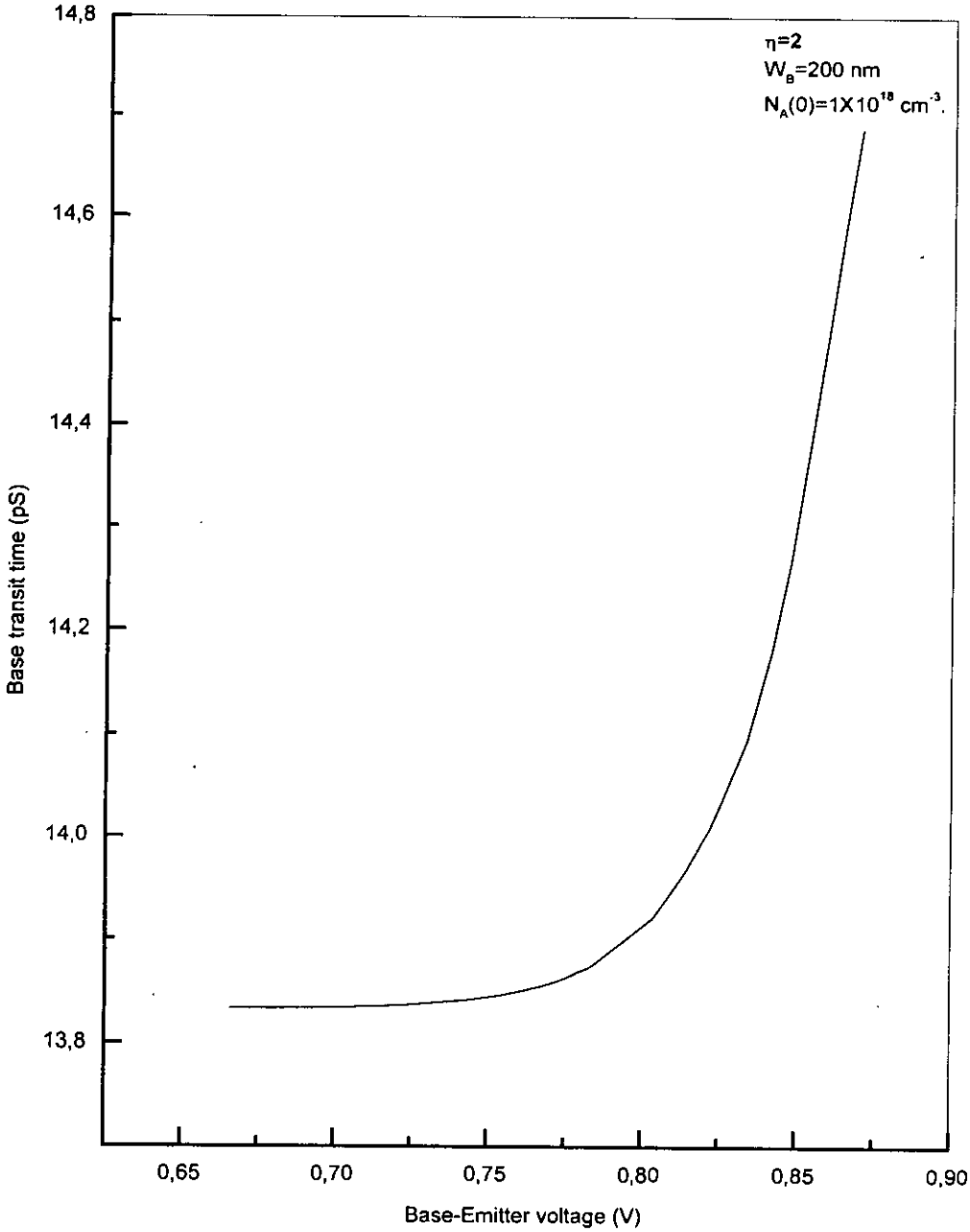

Figure 3.8(c): Variation of base transit time with base-emitter voltage for W_B = 200nm, $N_A(0)=1\times10^{18}cm^{-3}$, $\eta = 2$.

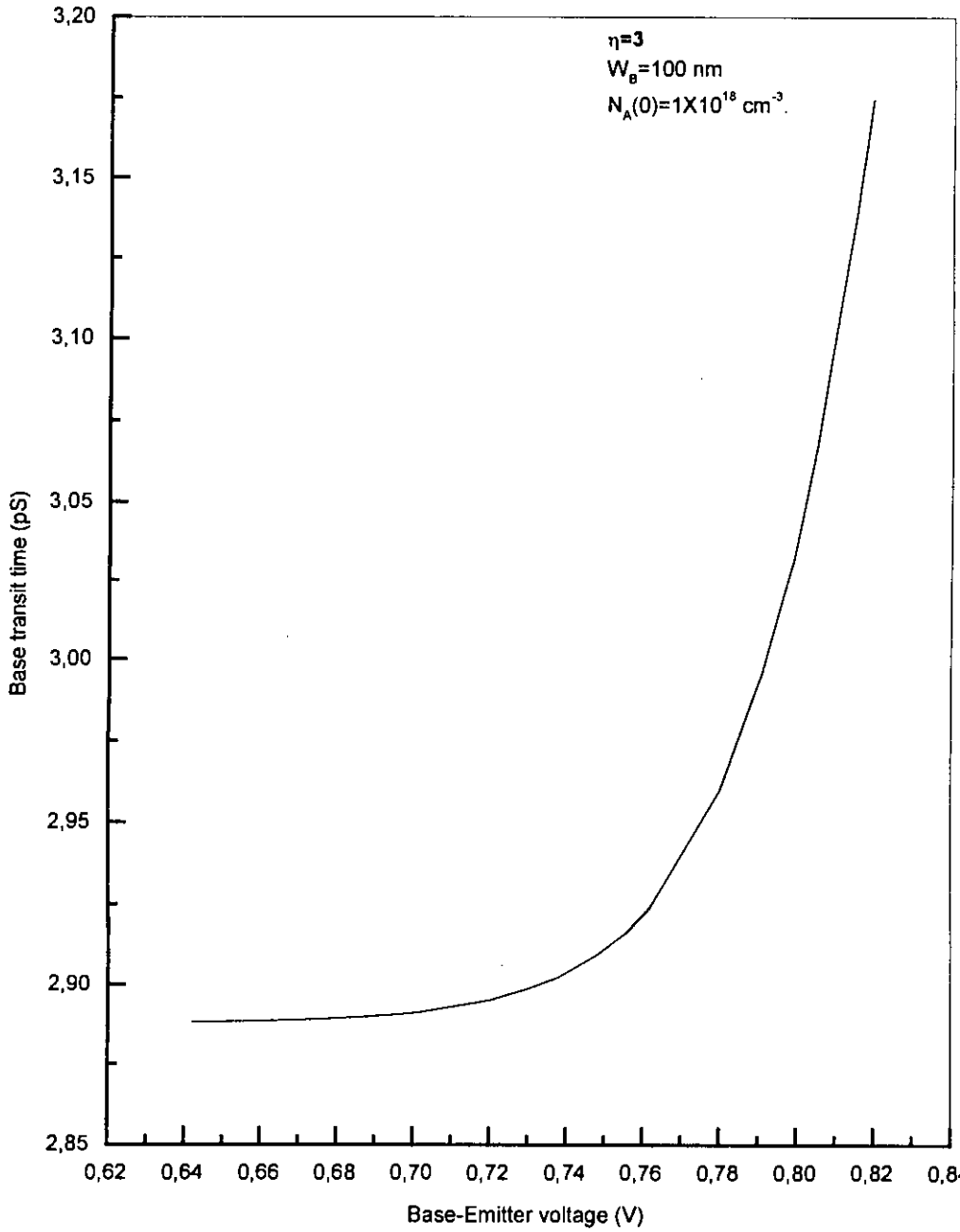

Figure 3.9(a): Variation of base transit time with base-emitter voltage for W_B = 100nm, $N_A(0)=1\times10^{18}cm^{-3}$, $\eta = 3$.

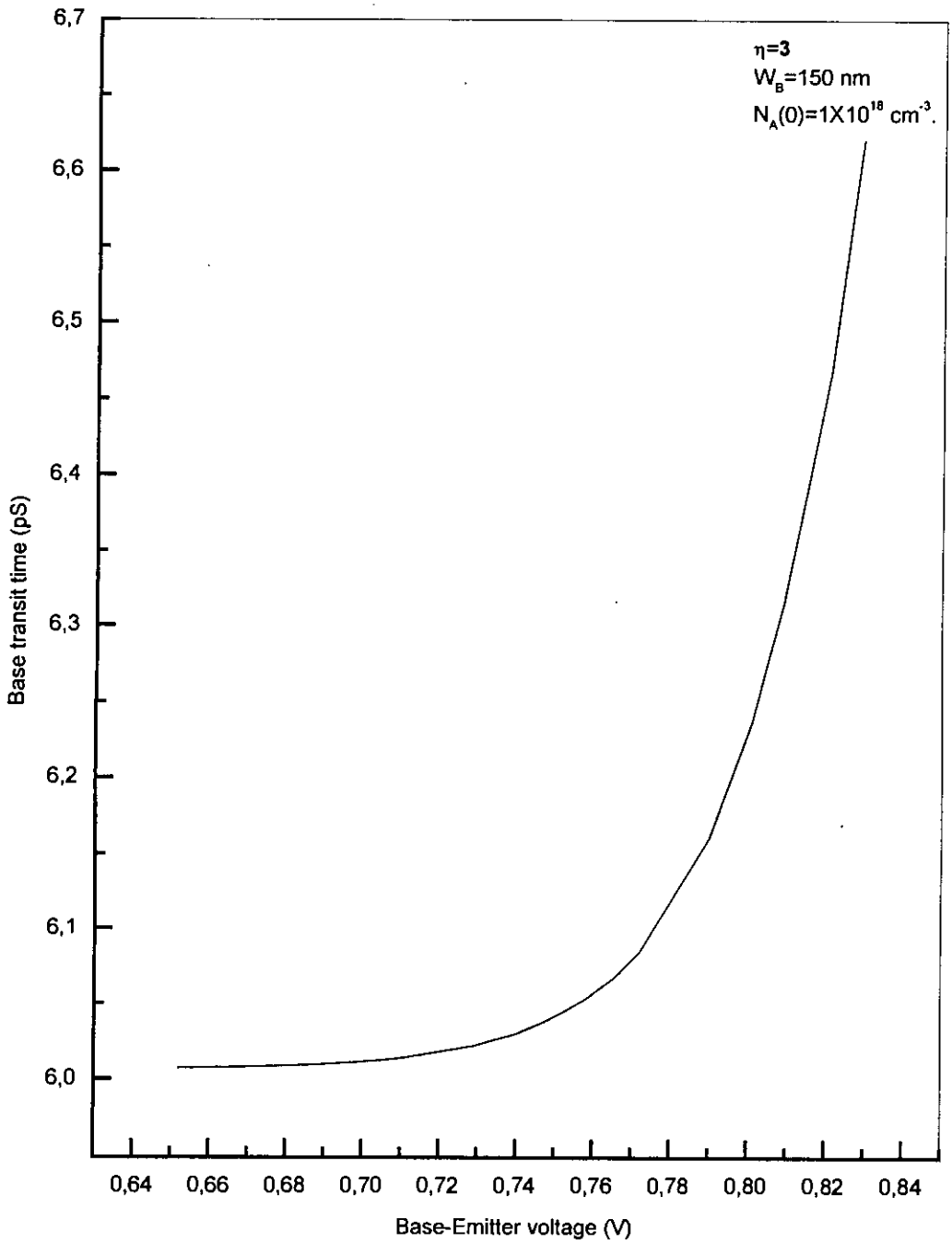

Figure 3.9(b): Variation of base transit time with base-emitter voltage for W_B = 150nm, $N_A(0)=1\times10^{18}cm^{-3}$, $\eta = 3$.

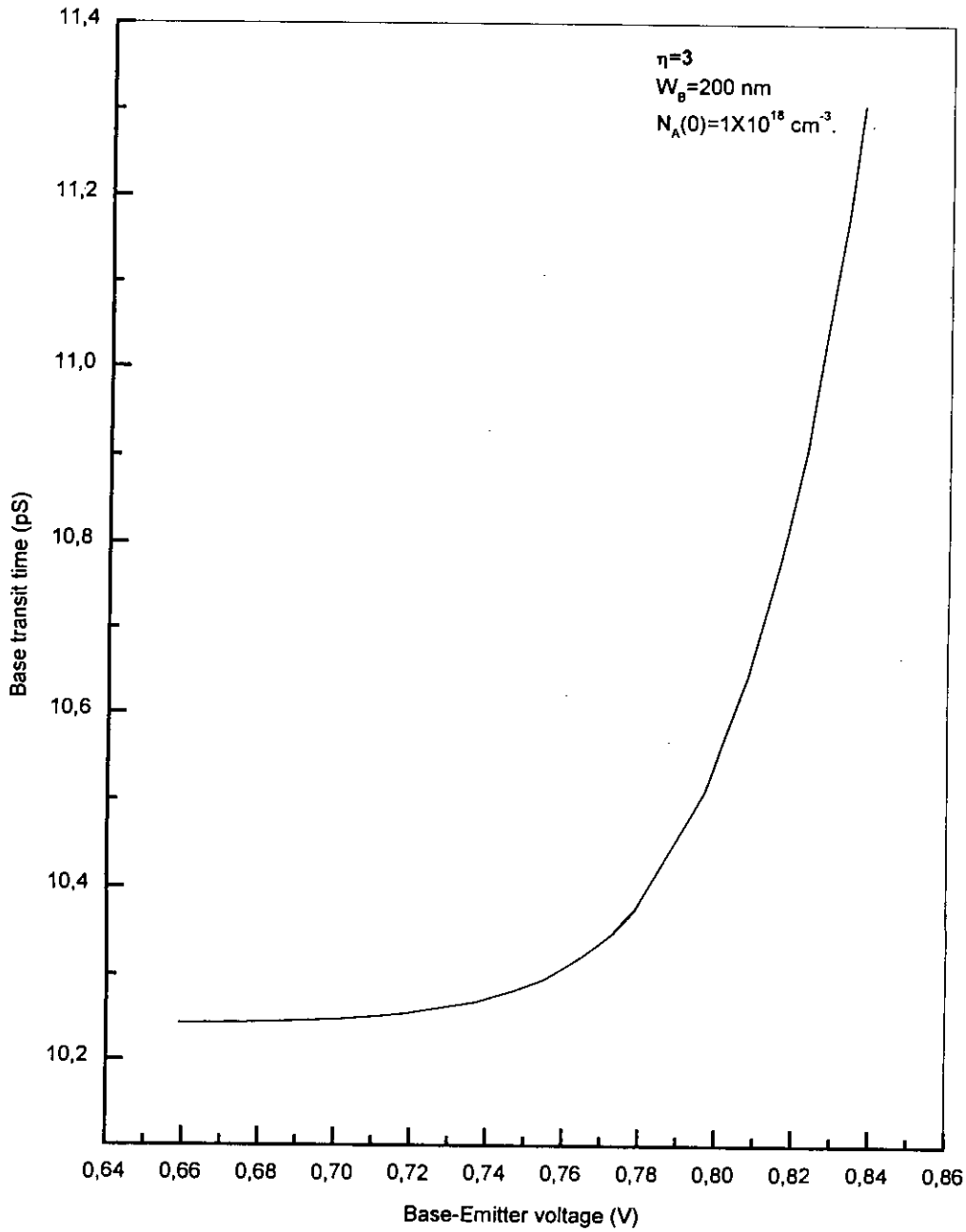

Figure3.9(c): Variation of base transit time with base-emitter voltage for W_B = 200nm, $N_A(0)=1\times10^{18}cm^{-3}$, $\eta = 3$.

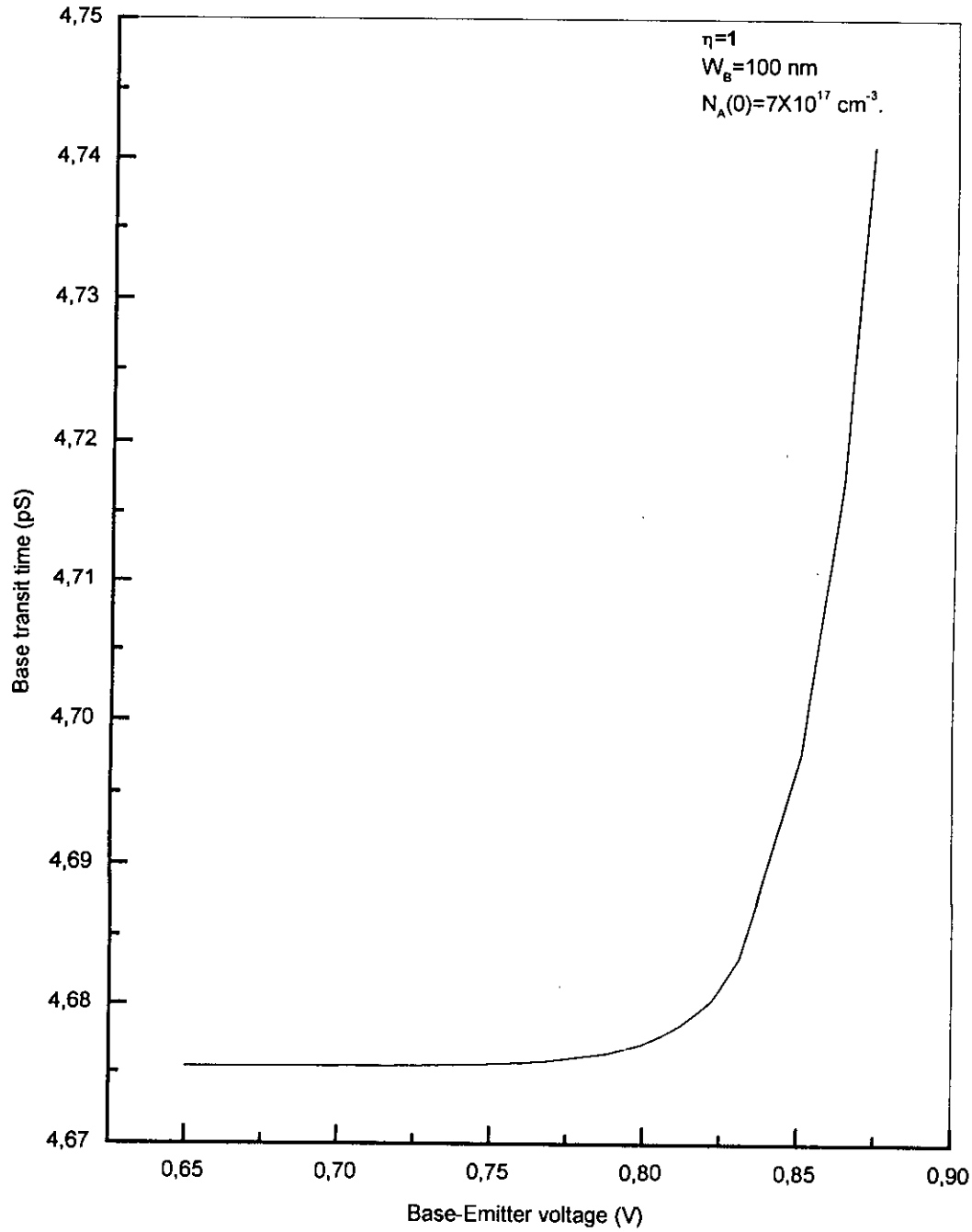

Figure 3.10(a): Variation of base transit time with base-emitter voltage for W_B = 100nm, $N_A(0)=7\times10^{17}cm^{-3}$, $\eta = 1$.

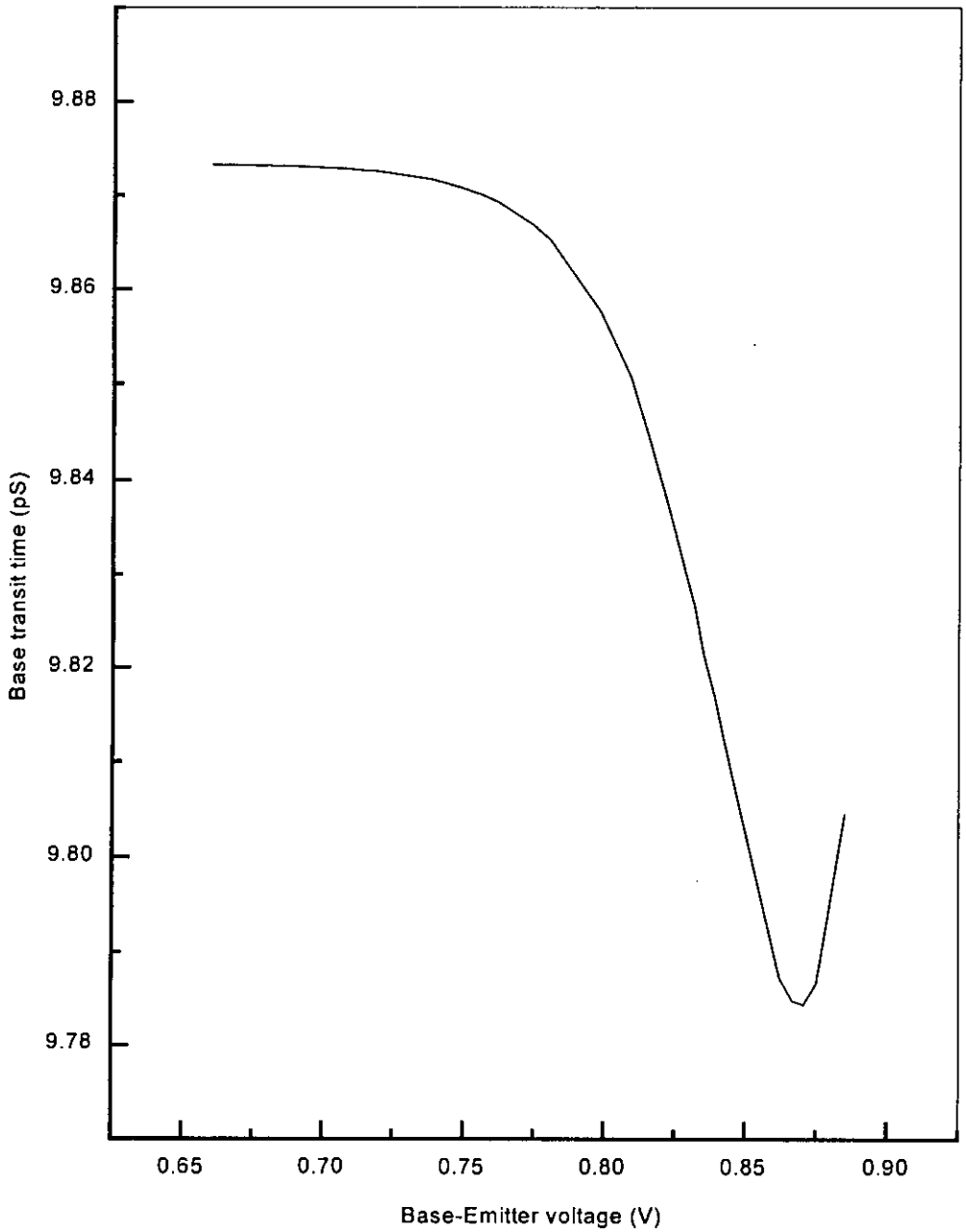

Figure 3.10(b): Variation of base transit time with base-emitter voltage for W_B = 150nm, $N_A(0)=7\times10^{17}cm^{-3}$, $\eta = 1$.

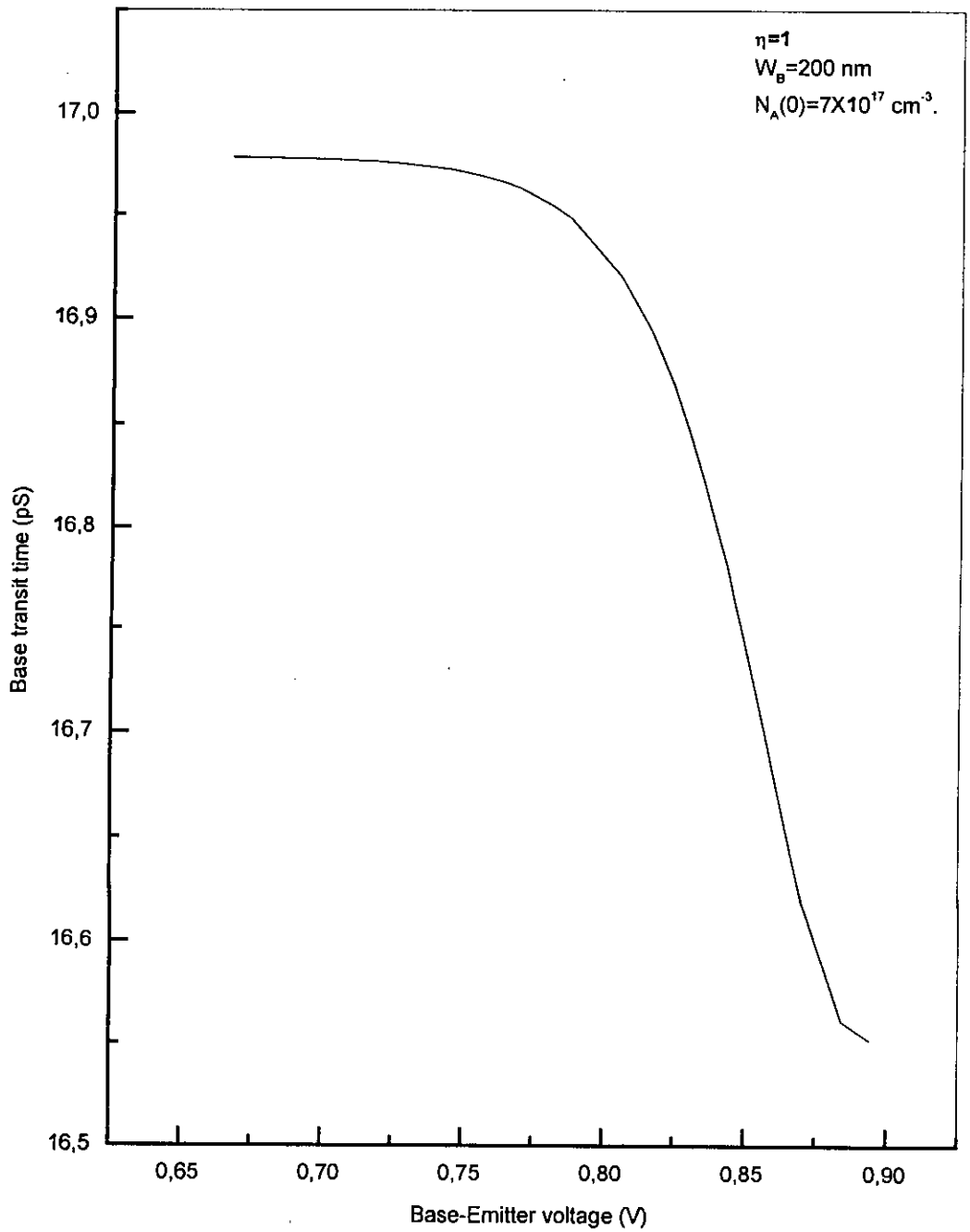

Figure 3.10(c): Variation of base transit time with base-emitter voltage for W_B = 200nm, $N_A(0)=7\times10^{17}cm^{-3}$, $\eta = 1$.

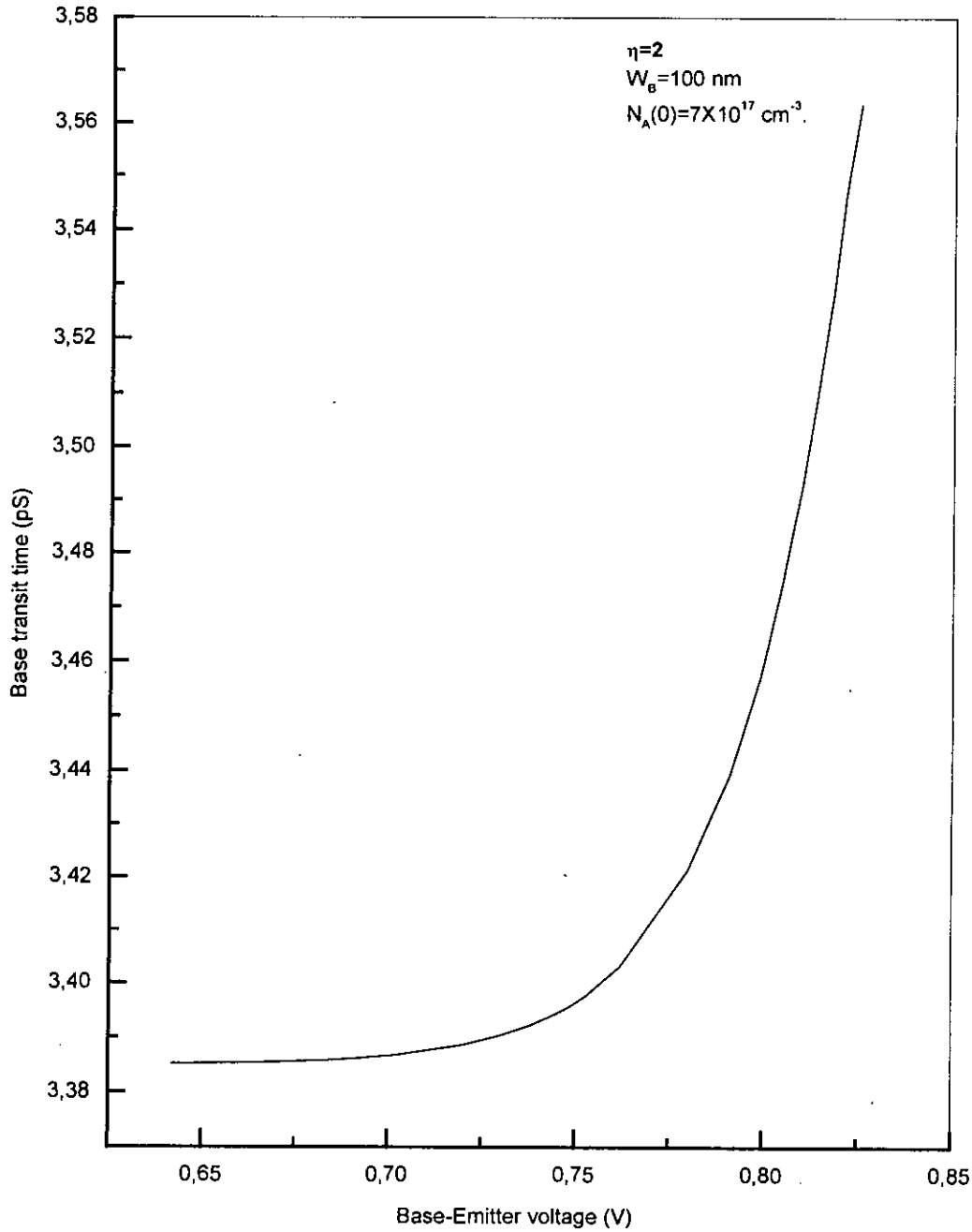

Figure 3.11(a): Variation of base transit time with base-emitter voltage for W_B = 100nm, $N_A(0)=7\times10^{17}cm^{-3}$, $\eta = 2$.

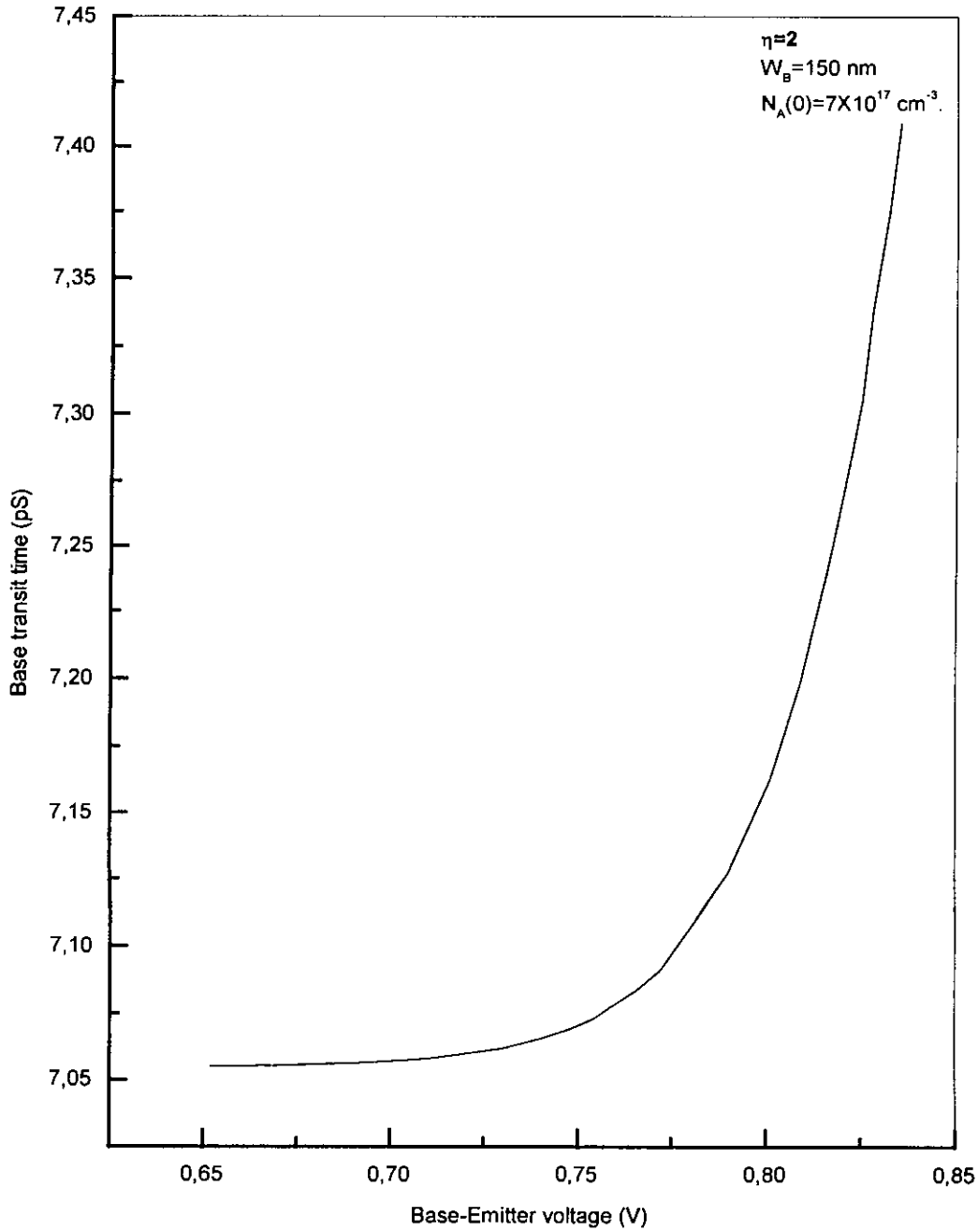

Figure 3.11(b): Variation of base transit time with base-emitter voltage for W_B = 150nm, $N_A(0)=7\times10^{17}cm^{-3}$, $\eta = 2$.

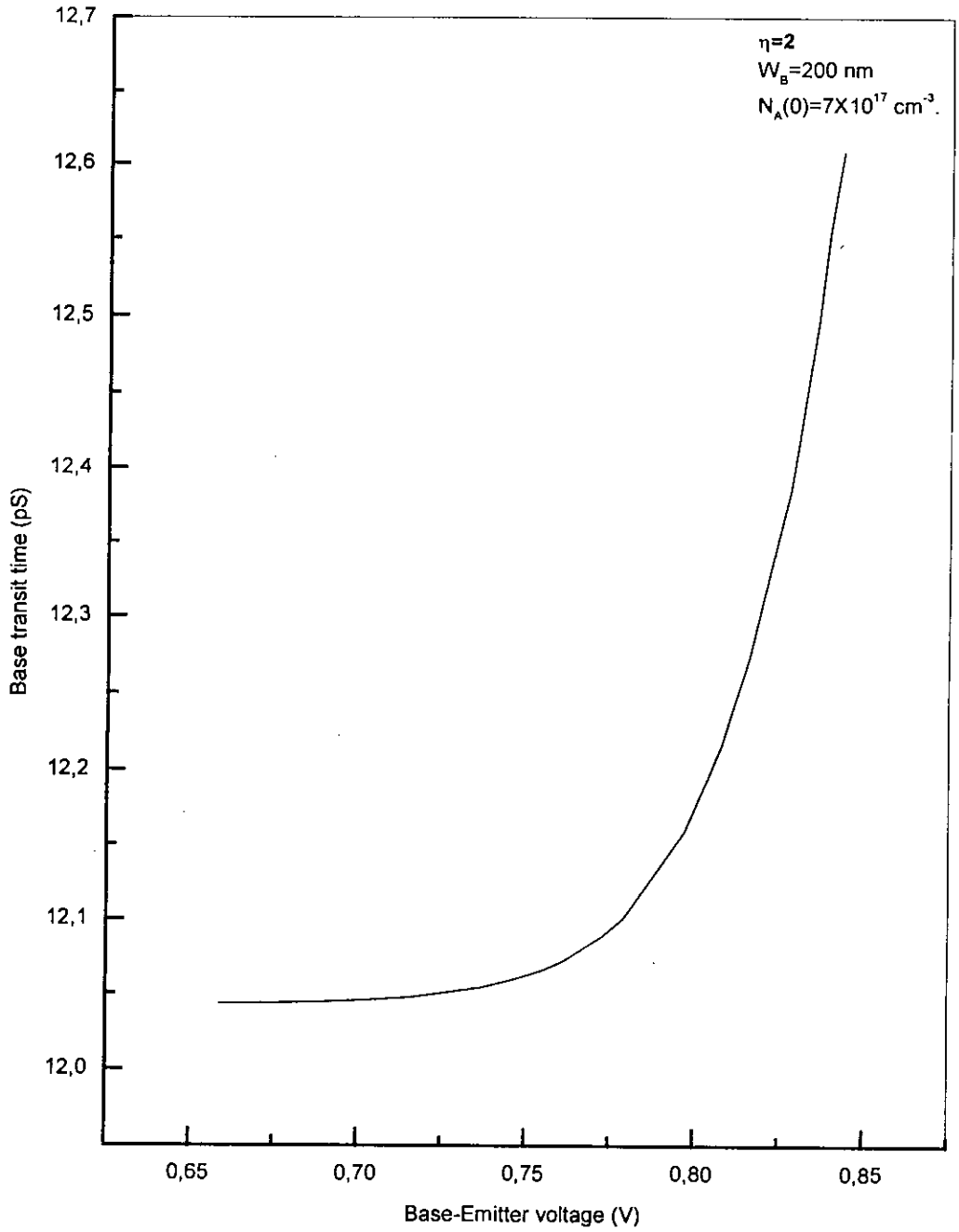

Figure 3.11(c): Variation of base transit time with base-emitter voltage for W_B = 200nm, $N_A(0)=7\times10^{17}cm^{-3}$, $\eta = 2$.

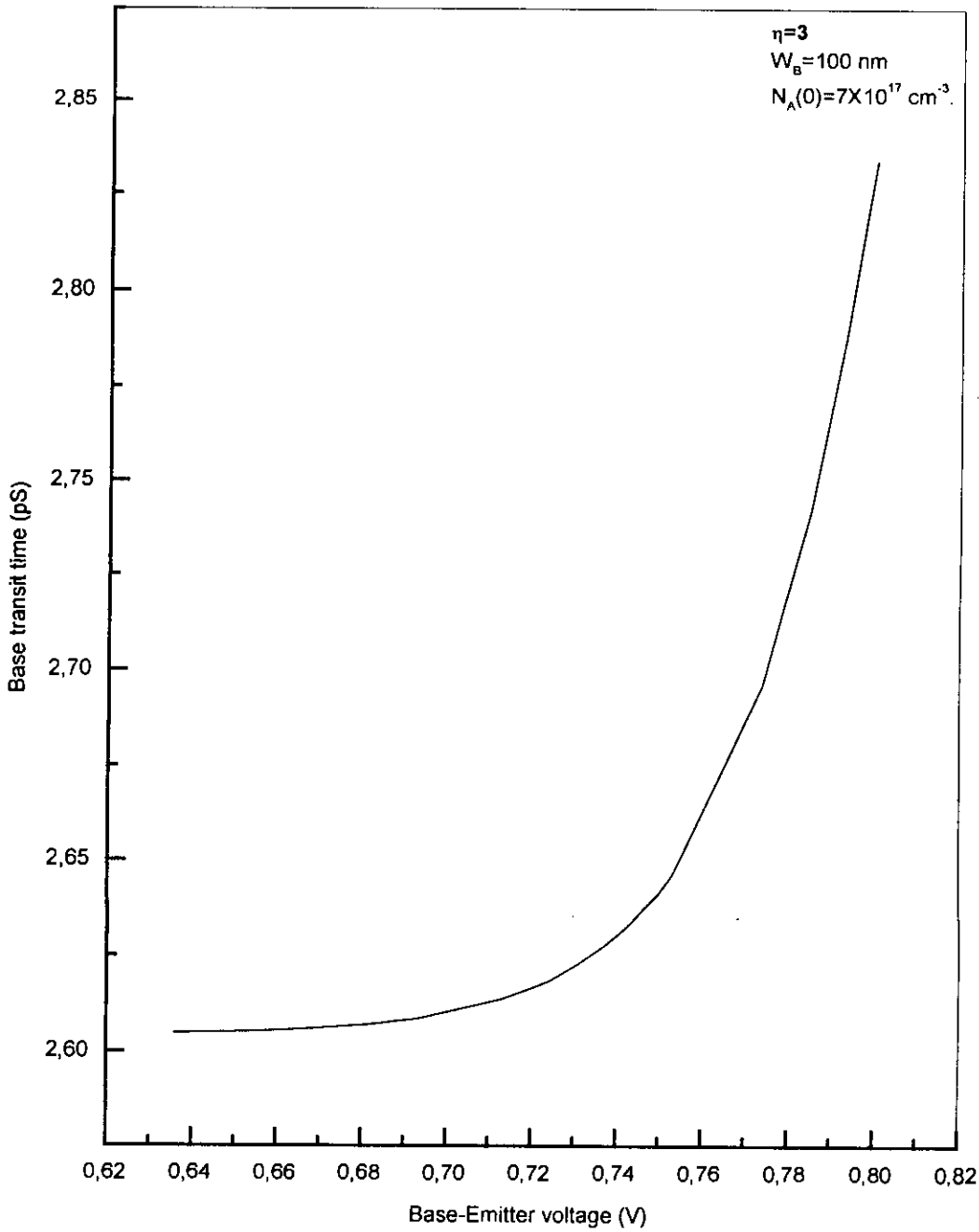

Figure 3.12(a): Variation of base transit time with base-emitter voltage for W_B = 100nm, $N_A(0)=7\times10^{17}cm^{-3}$, $\eta = 3$.

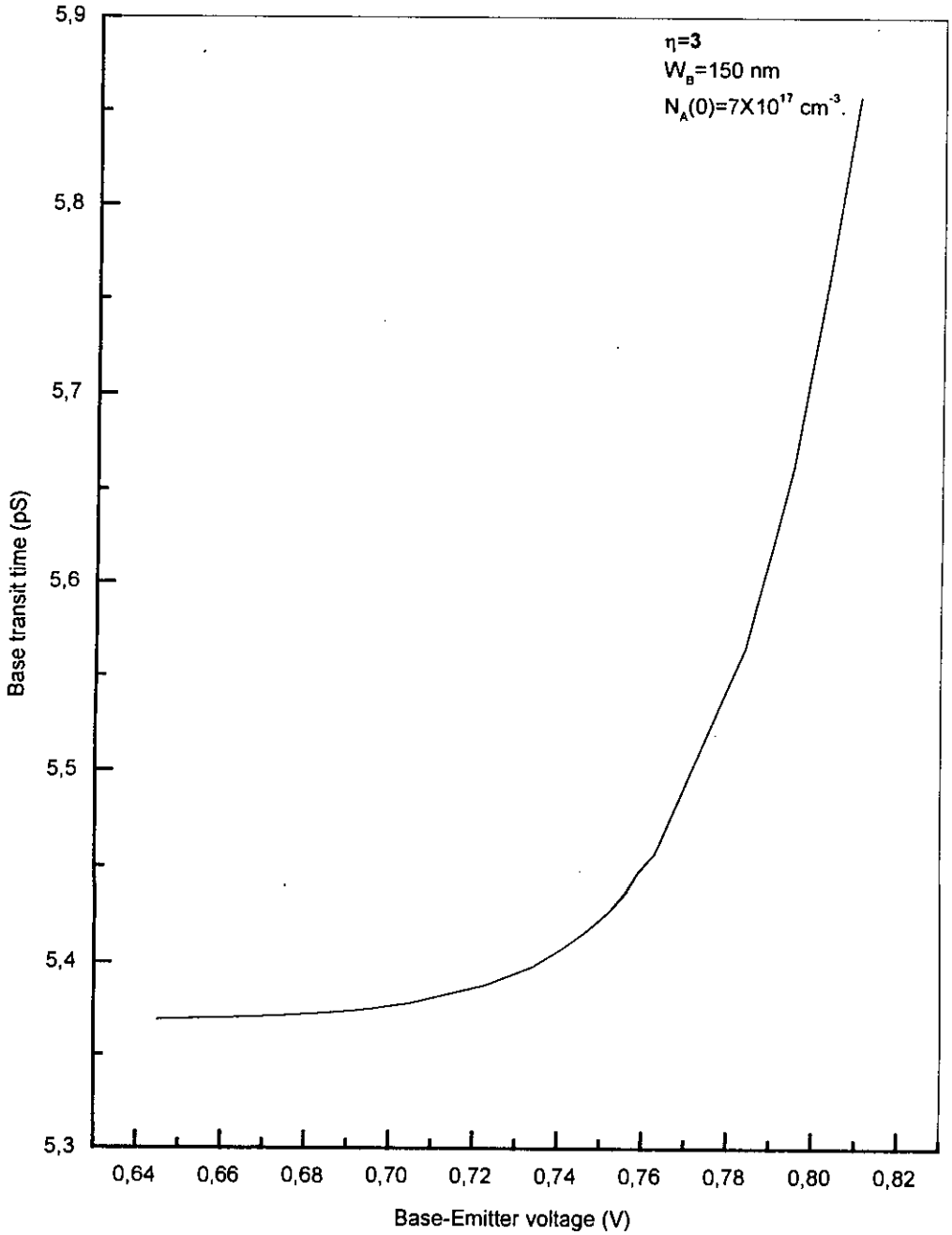

Figure 3.12(b): Variation of base transit time with base-emitter voltage for W_B = 150nm, $N_A(0)=7\times10^{17}cm^{-3}$, $\eta = 3$.

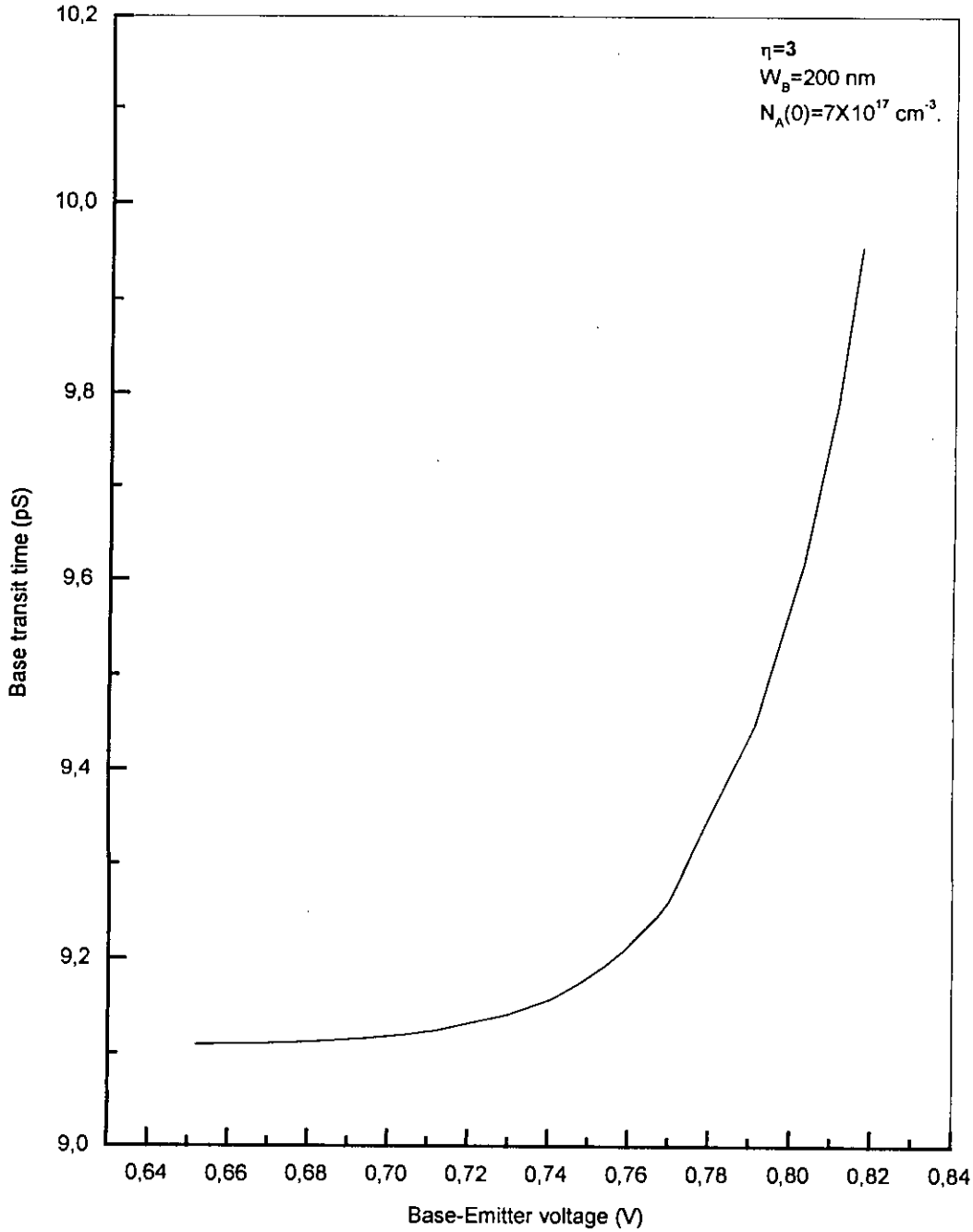

Figure 3.12(c): Variation of base transit time with base-emitter voltage for W_B = 200nm, $N_A(0)=7\times10^{17}cm^{-3}$, $\eta = 3$.

3.6 DEPENDENCE OF BASE TRANSIT TIME UPON BASE WIDTH

The dependence of base transit time upon base width for various slope of base-doping is shown in figures 3.13. It can be seen that the base transit time is an increasing function of base width. If the base width increases, more time is needed for the minority carriers to diffuse across the base. So base transit time increases with base width. These plots, along with figures 3.5-3.12, also show that base transit time is directly proportional to the base width. But as is evident from fig.3.13, the variation is not exactly linear. This is due to the reason that base transit time depends on many other factors which also depend upon the base width. So with the increase in base width, base transit time also increases but the increment is not linear.

3.7 DEPENDANCE OF BASE TRANSIT TIME UPON SLOPE OF BASE DOPING

The variation of base transit time with base-emitter voltage for different slope of base-doping is shown in figure 3.14. From this figure it is seen that the base transit time is a decreasing function of η. This is because the aiding electric field in the base increases with η. From the fig. 3.14 it is also noted that for higher values of η the base transit time for low voltage becomes smaller than that of high voltage. The reason for this becomes clear if we observe the electric field distribution within the base in fig 3.2. For low voltage, the electric field within the base increases with η for same distance. But for high voltage as η increases, the distance at which the electric field for low and high voltage are equal move towards the collector base junction. So when η is small, the aiding electric field for high voltage is larger than that of low voltage for most of the part of base width. So, for lower values of η, the base transit time is larger for low voltage. When η is high, the aiding electric field for low voltage increases. But for high η, electric field for high voltage is greater than that of low voltage only at the edge of the collector base junction. That's why, the base transit time for high voltage is larger than that of low voltage when η is high.

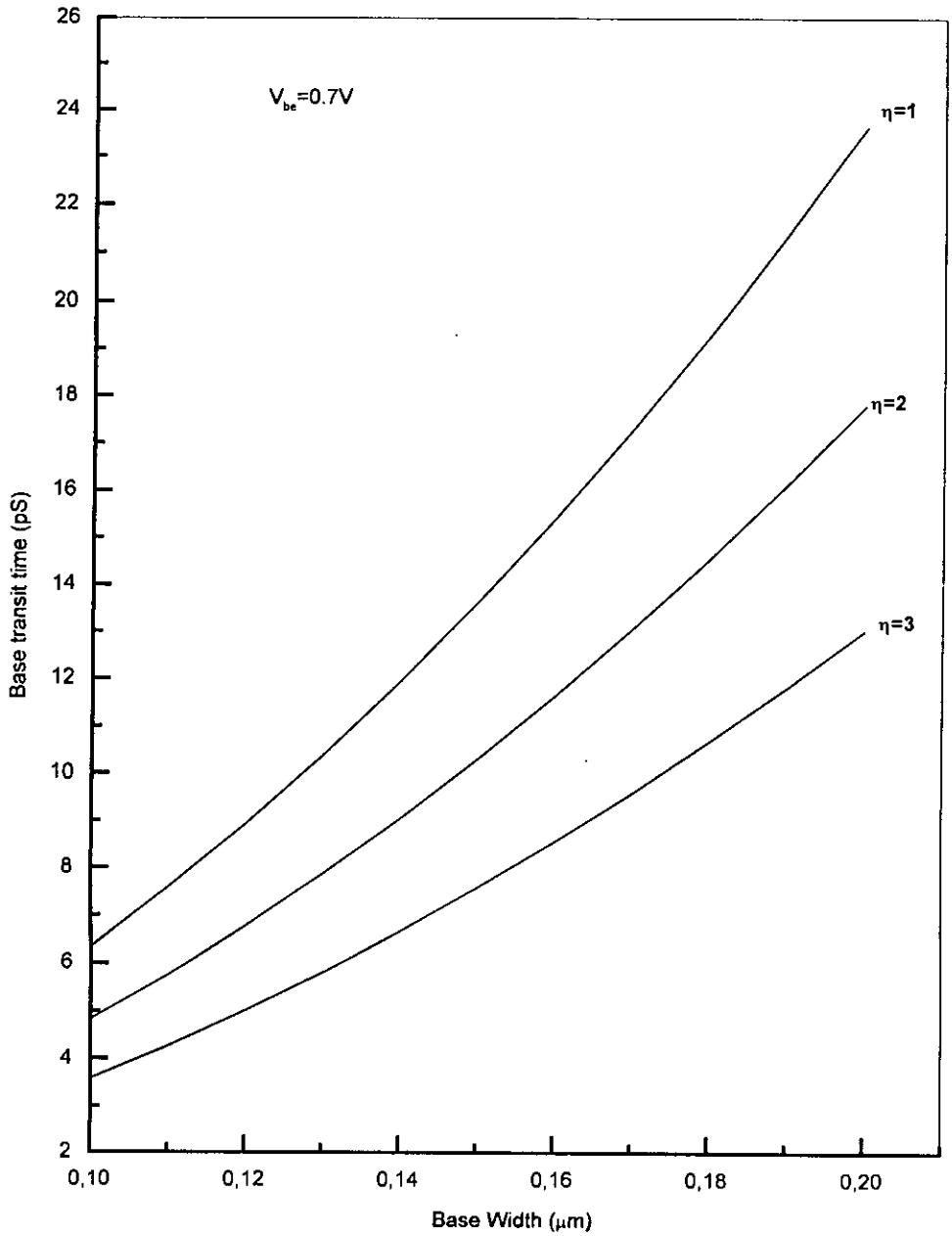

Figure 3.13: Variation of base transit time with base width for different values of slope of base-doping.

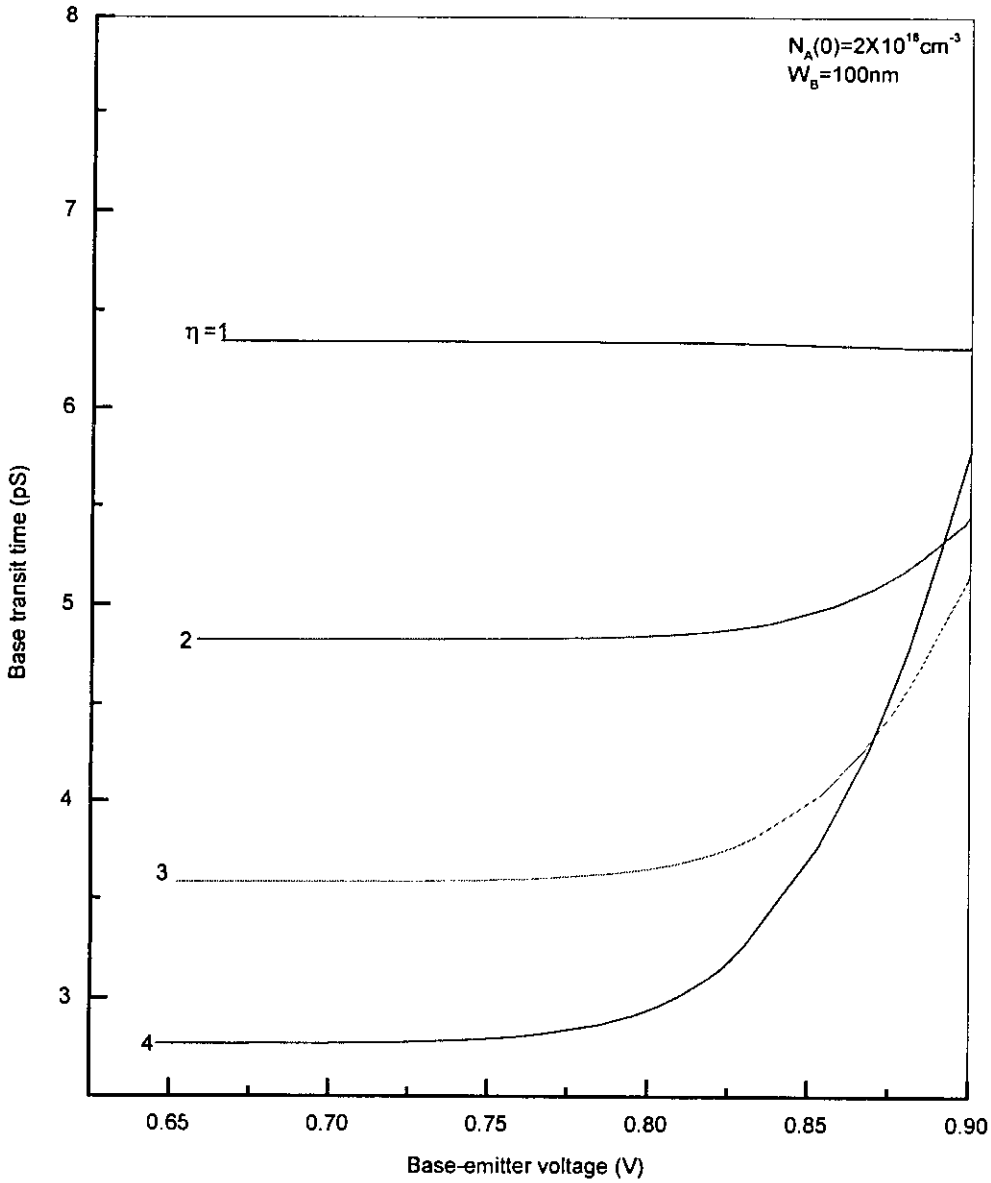

Figure 3.14: Variation of base transit time with base-emitter voltage for different values of slope of base-doping.

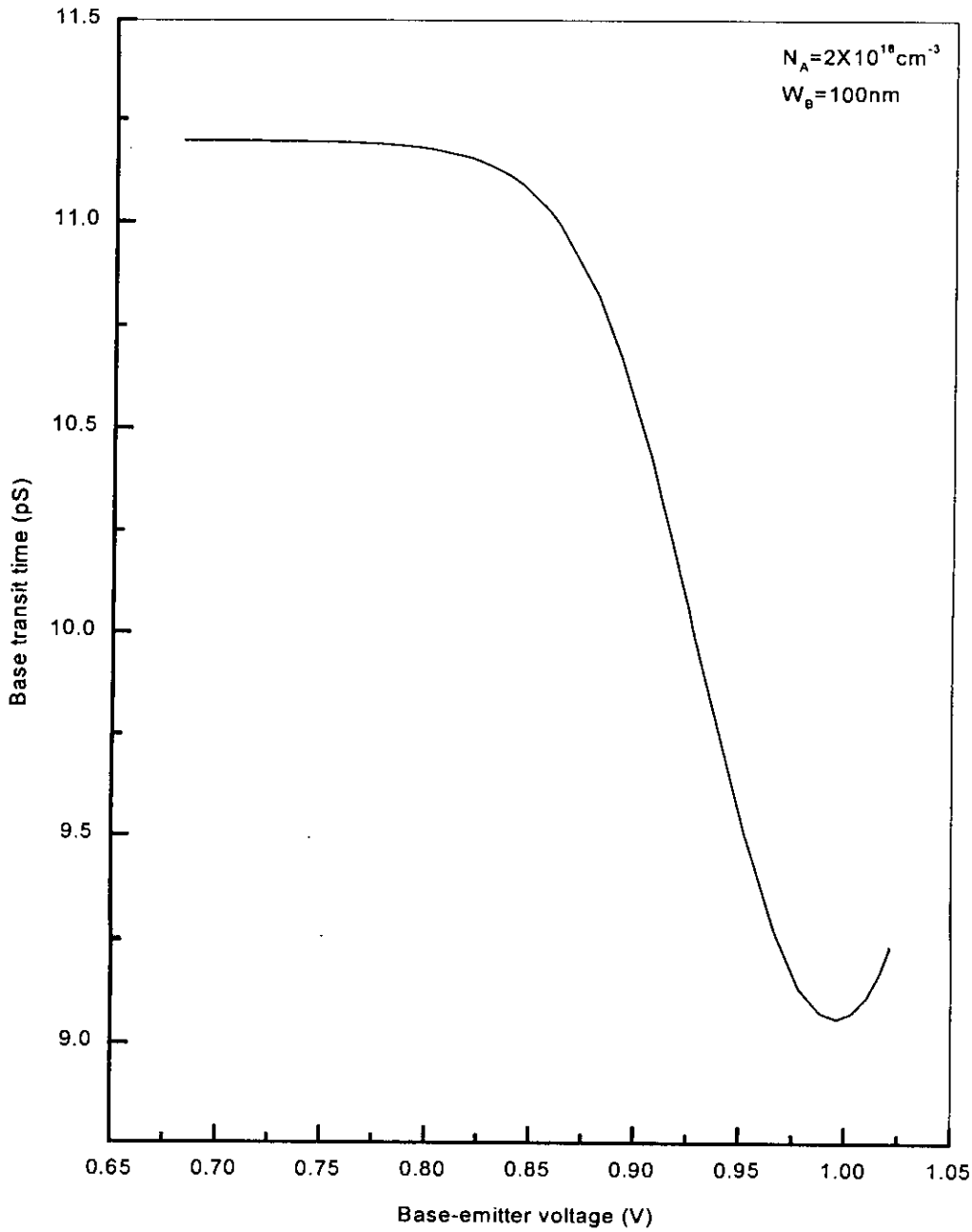

Figure 3.15: Variation of base transit time with base-emitter voltage for a uniformly doped base.

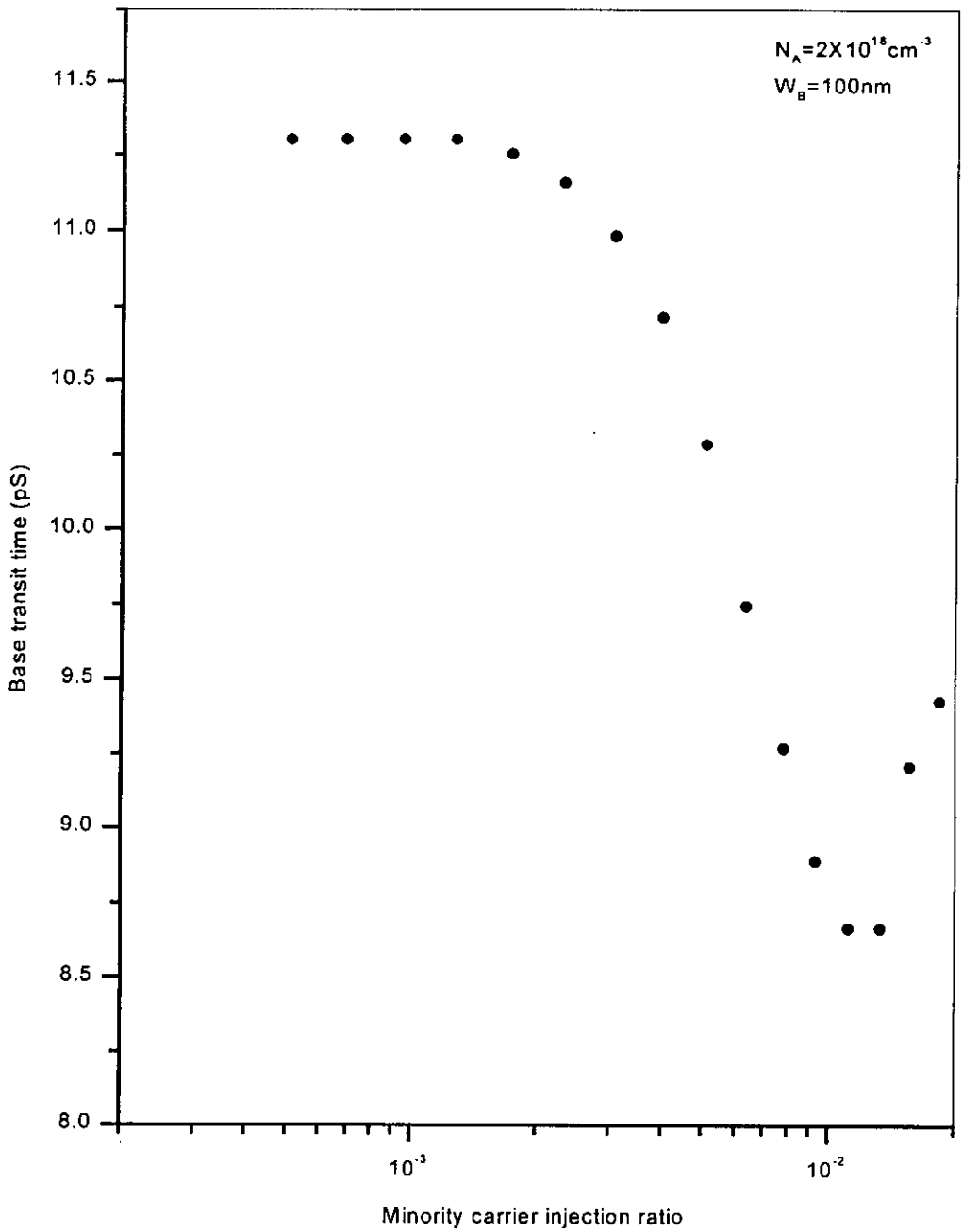

Figure 3.16: Variation of base transit time with base-emitter voltage for a uniformly doped base as in [1].

3.8 COMPARISON

The present approach is used mainly for nonuniformly doped base. But this work can successfully incorporate a uniformly doped base by putting $\eta = 0$. The plot for $\eta = 0$ is shown in figure 3.15. As can be found, for low base-emitter voltages base transit time remains constant, then at high voltages it decreses, but then it increases again, at some still higher base-emitter voltages. P. Ma *et al* [1] analysed base transit time for a uniformly doped base. The curve of [1], as shown in figure 3.16, also has similar behavior compared to fig.3.15. There difference is also small. This justifies the present novel TL modeling.

3.9 CONCLUSION

The novel TL method of calculating minority carrier concentration within base is used to obtain different performance figures of bipolar junction transistor. The ultimate objective of this work is to determine base transit time. The results presented in this chapter show that base transit time increases with base width and peak base-doping. It is also a function of base-emitter voltage. It is also found that the base transit time is a decreasing function of slope of base-doping. The results obtained are also compared with some published data. This concludes that the novel TL method is in quite good agreement with the available results. So this technique is a workable simulation technique for the BJT's .

CHAPTER 4

CONCLUSION

4.1 CONCLUSION

In the present work a novel TL model has been developed to compute minority carrier distribution within base and thereby calculate base transit time. This TL model is straightforward and conceptually easier in that it incorporates strictly distributed parameters. It regains the inherent beauty of the transmission line analysis. In the preceding chapter minority carrier distribution, electric field distribution and variation of base transit time with different parameters (such as, base-emitter voltage, base width, peak base-doping and slope of base-doping) were plotted. It can be inferred from the plots that base transit time increases with base width and peak doping but decreases with slope of base-doping. It is found that the base transit time is a strong function of base width than the other two.

4.2 SUGGESTIONS FOR FUTURE WORK

The present work used a novel TL model within the base region to calculate minority carrier distribution and hence base transit time. The present work was limited to only dc (or steady-state) analysis. However a time-dependent analysis (including the effects of L/C of transmission line) can be done in future. Also the effect of a changing base width due to changing base-emitter voltage can also be incorporated in this TL model. Again this model predicts device behavior before the onset of Kirk effect. It remains to be seen how the present TL method incorporates this effect.

REFERENCES

[1] P. Ma , L. Zhang, Y. Wang, "Analytical model of collector current density and base transit time based on iteration method," *Solid-State Electronics,* Vol. 39, No. 11, pp. 1686-1686, 1996.

[2] M.M. Shahidul Hassan, A.H. Khandoker, "New expression for base transit time in a bipolar junction transistor for all level of injection," *Microelectronics Reliability,* Vol-41, pp 137-140, 2001.

[3] J.J.H. Van Den Biesen, "A Simple Analysis of transit times in bipolar transistors," *Solid-State Electronics,* Vol. 29, No. 5, pp 529-534, 1986.

[4] J.S. Yuan , "Effects of base profile on the base transit time of the bipolar transistor for all levels of injection," *IEEE Trans. Electron Devices*, Vol. 41. No. 2, pp 212-216, Feb 1994.

[5] K. Suzuki, "Analytical base transit time model of uniformly-doped base bipolar transistors for high-injection regions," *Solid-State Electronics,* Vol. 36, No.1, pp-109-110, 1993.

[6] P. Ma, L. Zhang, Y. Wang, "Analytical relation pertaining to collector current density and base transit time in bipolar junction transistor," *Solid-State Electronics,* Vol. 39, No. 1, pp 173-175, 1996.

[7] David Rosenfeld and Samuel A. Alterovitz, "Carrier transit time through a base with dopant dependent mobility," *IEEE Trans. Electron devices*, Vol. 41. No. 5, pp 848-849, May 1994.

[8] Alan H. Marshak, "Transport equations for highly doped devices and heterostructures," *Solid-State Electronics,* Vol. 30, No. 11, pp. 1089-1093, 1987.

[9] Yih-Feng Chyan, C.Y. Chang, S.M. Sze, M.J. Lin, K. Liao and R. Reif, "Analytical modeling of polycrystalline silicon emitter bipolar transistors under high-level injection," *Solid-State Electronics,* Vol. 37, No. 8, pp. 1521-1529, 1994.

[10] Ziaur Rahman, "Base transit time of a bipolar junction transistor for nonuniformly doped base" *MSc Thesis* submitted to Dept. of EEE, Bangladesh University of Engineering and Technology, 2002.

[11] C.T. Sah, "The equivalent circuit model in solid-state electronics-III: Conduction and displacement currents," *Solid-State Electronics,* Vol. 13, pp.1547-1575, 1970.

[12] M.A. Green, V.A.K. Temple & J. Shewchun, "A simplified computational treatment of recombination centers in the transmission line equivalent circuit model of a semiconductor," *Solid-State Electronics,* Vol. 15, pp. 1027-1029, 1972.

[13] C.F. Smiley, L.D. Yau and C.T. Sah, "Application of the transmission line equivalent circuit model to the analysis of the pn-junction admittance under d.c. bias," *Solid-State Electronics,* Vol. 16, pp.895-901, 1973.

[14] J.P. Karamarković, N.D. Janković and B.D. Milovanović, "Periodical steady-state analysis of minority carrier diffusion including momentum relaxation time," *Electronics Letters*, Vol.29, No. 15, pp. 1316-1317, 1993.

[15] J. P. Karamarković, N. D. Janković and D. B. Glozić, "Transmission-line equivalent circuit model of minority carrier transient current in quasi-neutral silicon layers including inductive effects," *International Journal of Numerical Modeling: Electronic Networks, Devices and Fields*, Vol. 29, No. 15, pp. 341-356, 1995.

[16] N.D. Janković, T.V. Pesić and J.P. Karamarković, "Transmission line model of arbitrary doped base including all injection levels and Kirk effect," *CAS'98. Proceedings – 1998 International Semiconductor Conference –21st Edition*, Sinaia, Romania, Vol. 2, pp. 383-386, 1998.

[17] J. P. Karamarković, T. V. Pesić and N. D. Janković, "An analytical approach to Kirk effect modelling," *IEEE Trans. Electron Devices*, Vol. 47, No. 6, pp.-311-314, 2000.

[18] N.D. Janković, T.R. Ilić and J.P. Karamarković, "Non-quasi-static bipolar transistor models for circuit simulators," *Proceedings - 20th International Conference on Microelectronics (MIEL'95)*, Niš, Serbia, Vol. 2, pp. 681-684, 1995.

[19] Michael Shur, *Introduction to Electronic Devices*, John Wiley & Sons, Inc. N.Y., pp. 149-153, 1996.

[20] C.T. Sah, *Fundamentals of Solid-State Electronics*, World Scientific, Singapore, 1991.

[21] C. Hilsum (Editor), *Handbook on Semiconductors*, Vol.-4, "Light Emitting Diodes,"- M. H. Pilkuhn, pp. 557-559, 1981.

[22] S.M. Sze, *Physics of Semiconductor Devices*, 2nd Ed., Wiley Eastern Ltd., pp. 51-52, 1981.

[23] David M. Pozar, *Microwave Engineering*, 2nd Ed., John Wiley & Sons, Inc. N.Y., pp. 56-94, 1984.

[24] Samuel Y. Liao, *Microwave Devices and Circuits*, 3rd Ed., Prentice-Hall of India, p. 64, 1990.